EFFECT OF COOLING ON GAS TURBINE BLADE MATERIALS

Submitted in Partial Fulfillment of the Requirement for

The Award of the Degree of

DOCTOR OF PHILOSOPHY

IN

Mechanical Engineering

BY

Abdurazag Mohamed . M . Gadmor

(ID. NO:13PHME203)

FACULTY OF ENGINEERING AND TECHNOLOGY

VAUGH INSTITUTE OF AGRICULTURAL ENGINEERING & TECHNOLOGY

SAM HIGGINBOTOM UNIVERSITY OF AGRICULTURE, TECHNOLOGY AND SCIENES

(FORMERLY ALLAHABAD AGRICULTURAL INSTITUTE)

NAINI, ALLAHABAD – 211007

2019

CERTIFICATE OF ORIGINAL WORK

This is to certify that the study conducted by **Mr. Abdurazag Mohamed. M. Gadmor, ID. NO.13PHME203** reported in the present thesis was under my guidance and supervision. The results reported by him are genuine and the candidate himself has written the script of the thesis. The thesis entitled **"EFFECT OF COOLING ON GAS TURBINE BLADE MATERIALS"** is therefore, being forwarded for acceptance in partial fulfillment of the requirement for the award of degree of **Doctor of Philosophy in the Department of Mechanical Engineering**, Vaugh Institute of Engineering & Technology, Sam Higginbottom University of Agriculture, Technology & Sciences, Allahabad -211007, U.P, India.

Place: Allahabad

Date:30/05/2018

Dr. Mohd .Tariq

(Advisor)

Assistant Professor

Department of Mechanical Engineering

VIAET, SHUATS, Allahabad

SELF ATTESTATION

This is to certify that I have personally worked on this research entitled **"Effect of cooling on gas turbine blade materials"** under the guidance of **Dr. M. Tariq** (Assistant Professor, Department of Mechanical Engineering). The date presented in this thesis were obtained during the work and are genuine. Data/ information obtained from the other agencies has been duly acknowledged. None of the findings pertaining to the work has been concealed. The results embodied in this research project has not been submitted to any other university or institution for the award of the degree or diploma.

Place: Allahabad **Abdurazag Mohamed .M. Gadmor**

Date: 30/05/2018

(ID.NO.13PHME203)

ACKNOWLEDGEMENT

First and foremost, praises and thank to the ALLAH, the Almighty, for his showers of blessings throughout my research work to complete the research successfully.

I'd like to thank my supervisor and mentor Dr. Mohammad Tariq for his guidance throughout both my postgraduate and doctoral studies. Similarly, thanks go to Prof (Dr.) Mohammad Imtiyaz, Chairman, DIET for his role of indefatigable problem solver since my initial involvement with the SHUATS University. The research presented in this thesis simply would not have been possible without the efforts of these two.

I am indebted to Hon'ble Vice Chancellor, The Most Rev. Prof (Dr.) R. B Lal, Sam Higginbottom University of Agricultural Technology & Sciences, for providing higher studies under doctoral programme in the university.

I express my sincere gratitude to Dr. A. K. Lawrence, Professor and Dean, Faculty of Engineering & Technology.

I am thankful to Prof (Dr.) Anshuka Srivastava, Department of Mechanical Engineering for providing facility and advice needed to complete the work. I am also thankful to all the staff members of Department of Mechanical Engineering for providing the necessary help and encouragement during the work.

I am grateful to my member Dr. L. P Singh, SHUATS for his invaluable guidance, constant encouragement, moral support, and wholehearted co-operation during this research work.

My wife and children Abdurrahman, Tameem, Asil and Yasin. deserves recognition for providing an academic role model. Thanks also go to my parents for always supporting me, even when the world seemed to be falling apart. You are the strongest and bravest people that I know, and this thesis is dedicated to you. They have been in the unusual (and arguably unenviable) position of being able to offer me both technical and emotional support, and have provided this in abundance over the last few years.

I thankfully acknowledge the help and continual support by Dr. Rajiv Ranjan throughout my research and all the fellow friends for their direct and indirect help at various stages of this research work.

Finally, my thanks goes to all the people who have supported me to complete the research work.

Abdurazag Mohamed. M. Gadmor

Abstract

Gas turbines are broadly utilized and its outline changes as load and working conditions are changed. Warm productivity of gas turbine enhances by expanding turbine rotor gulf temperature. In the course of recent years, the gas turbine has obviously profit by critical advancements in materials innovation which is one of the elements influencing the huge changes in execution and proficiency; the early nickel base combination improvements, columnar grained amalgams, single precious stone compounds, warm obstruction coatings, earthenware production, clay framework composites and added substance fabricating. Common basic cycle motor efficiencies have enhanced altogether, profiting from the expanding temperature ability of the high quality combinations. The present rotor delta temperature in cutting edge gas turbine is for over the softening purpose of edge material. An advanced cooling plan must be produced for persistent safe activity of gas turbines with elite.

Gas turbines are cooled remotely and inside. A few strategies have been recommended for the cooling of edges and vanes. The strategy that includes the cooling of cutting edges and vanes by utilizing cooling techniques is to have outspread gaps to pass high speed cooling air along the sharp edge traverse. In this theory, a turbine cutting edge is planned and displayed in CATIA programming. The turbine edges are outlined utilizing cooling gaps. The turbine sharp edge is composed with 4 gaps with 2 examples of introduction straight forward on camber line and other is crisscross example. CFD examination is done to decide the weight conveyance, speed, temperature circulation and warmth exchange rate by applying the channel weight figured as compressor outlet weight and temperature.

Warm examination is additionally done to decide the warmth exchange rates of the cutting edges of two kinds of compressors pressure proportion 20 and 30 utilizing ANSYS FLUENT 15.0. The materials utilized for cooling of turbine cutting edge are steel and titanium. Edge material and best example for each weight proportion and both the materials are seen from the investigation.

TABLE OF CONTENTS

LIST OF TABLES

LIST OF FIGURES

LIST OF SYMBOLS

P_a	Atmospheric Pressure in (bar)
T_a	Atmospheric Temperature in K
C	Velocity (m/s), aspect ratio.
c	Cord length (m)
C_p	specific heat at constant pressure
m	Mass flow
M	Molecular weight, Mach number
n	Polytrophic index
p	Absolute pressure (bar)
Q	Heat transfer per unit mass flow
R, R	Specific, molar (universal), gas constant, R r/r m as well as pressure ratio and gas constant
r	Radius (m), Pressure ratio
s	Specific entropy
T	Absolute temperature
t	Temperature ratio
η	Efficiency
ρ	Density
h	Blade height, specific enthalpy
n	Number of blades
s/c	pitch/chord ratio
λ	work-done factor
$\wedge$	degree of reaction ($\Delta T_{rotor}/ \Delta T_{stage}$)
ϕ	Flow coefficient (Ca/U)
ψ	Temperature coefficient (CpΔTos/U2)
U	Circumferential velocity

SUFFIXES

0	Stagnation Property
1, 2, 3	Reference Plane
f	Fuel
a, w	Axial, whirl component
b	Blade row
m	Mean, Vector mean
s	Stage
r	Root radius, radial component
t	Tip radius
′	Isentropic property

INTRODUCTION

Gas turbine is a kind of combustion engine also called an ignition turbine; it has an upstream pivoting compressor coupled to a downstream turbine, and a combustion chamber in the middle section. Gas turbines are some of the time alluded to as turbine engines. Most of the parts of such engines include an inlet, fan, compressor, combustor and exhaust nozzle (jet propulsion or air craft engines).

1.1 GAS TURBINE ENGINE

The gas turbine engine was first developed a century ago. A virtual revolution has been underway to improve their performance. The goal has been to reduce the fuel burn, improve safety and reliability, and reduce the environmental impact of harmful emissions and noise. In recent years, the gas turbine has become the prime power unit in many diverse applications including military, commercial, land transport and marine propulsion systems.

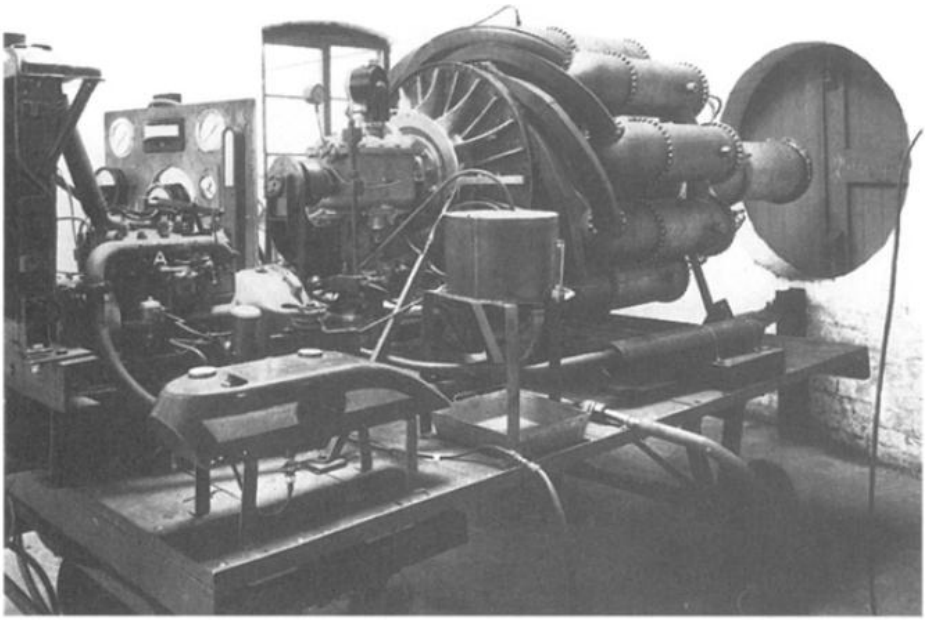

Fig. 1.1 Whittle's first experimental engine after second reconstruction in 1938 [39]

It is believed that further advancement in cooling technology of turbine blades for aircraft gas turbine engine as well as commercial turbine engines will continue for another 25-30 years, at which point the gas turbine revolution will culminate with the development of what NASA calls

“intelligent engines”. These engines will be self thinking, self adjusting (without human intervention), and able to operate at optimum conditions to achieve pre-specified customer requirements during the entire operation. A Whittle's first experimental engine after second reconstruction in 1938 has been shown in figure 1.1

A simple gas turbine is comprised of three main sections: compressor, combustor and turbine as shown in the figure 1.2. The gas turbine operates on the principle of the Brayton cycle where compressed air is mixed with fuel and burned under constant pressure conditions. The resulting hot gas is expanded through a turbine to perform work.

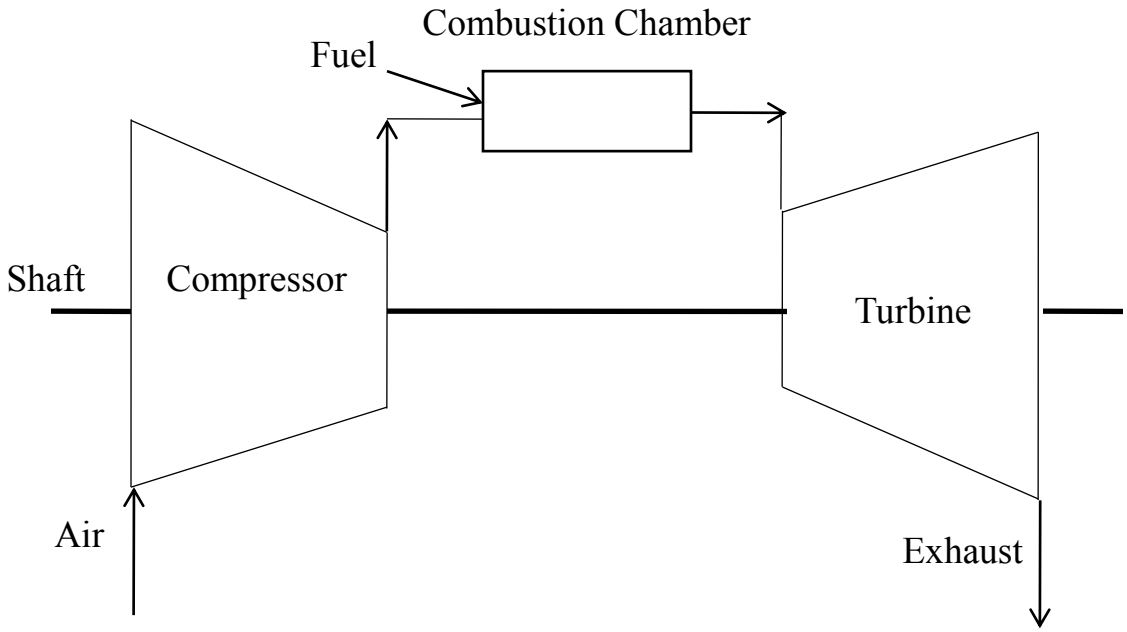

Fig. 1.2 Gas Turbine Engine [68]

A compressor is a mechanical device that expands the pressure of a compressible liquid by decreasing its volume and for incompressible pressurized the flow. Compressors are like pumps: both increase the pressure of fluid and both can convey the liquid through a pipe. As gases are compressible, the compressor likewise diminishes the volume of a gas. A combustion chamber is the part of an engine in which fuel is burned. Energy is added to the gas stream in the combustor, where fuel is blended with air and ignited. In the high pressure condition of the combustor, ignition of the fuel expands the temperature. The results of the ignition are forced into the turbine

segment. A turbine is a rotational motor that concentrates vitality from a liquid stream and changes over it into valuable work. The most straightforward turbines make them move section, a rotor assembly, which is a shaft or drum with blades connected. Moving liquid follows up on the blade, or the blades respond to the flow with the goal that they move and give rotational energy to the rotor.

1.1.1 Working Cycle

The Brayton cycle is a cycle that depicts the working of the gas turbine engine, premise of the air breathing jet engine. It is likewise now and then known as the Joule cycle. The Ericsson cycle is analogous yet utilizes external heat and joins the utilization of a regenerator.

The working cycle of the gas turbine engine is like four-stroke piston engine. Likewise, in the gas turbine engine, combustion takes place at a constant pressure, though in the piston engine it occurs at a constant volume. Both engine cycles demonstrate that in each occurrence there is induction, compression, combustion and exhaust. These procedures are irregular on account of the piston engine while they happen consistently in the gas turbine. In the piston engine just a single stroke is used in the creation of energy, the others being associated with the charging, compressing and debilitating of the working liquid. Conversely, the turbine engine takes out the three 'idle' strokes, in this manner empowering more fuel to be scorched in a shorter time; thus it delivers a more noteworthy power output for a given size of engine.

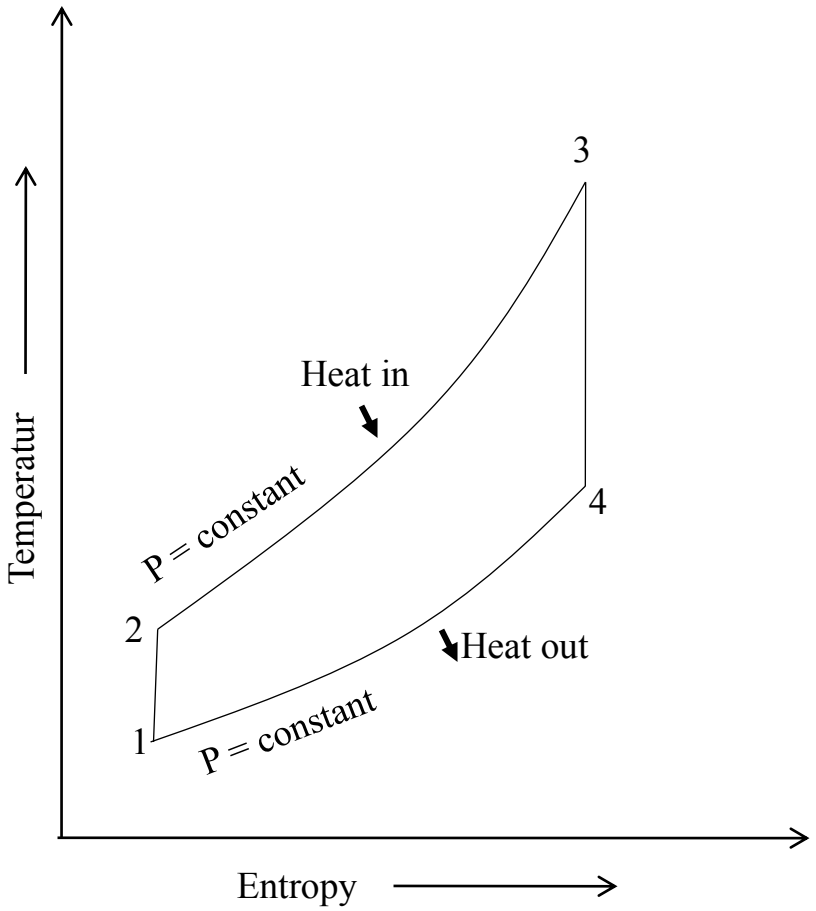

Fig. 1.3 T-s representation of Brayton Cycle [69]

Because of the constant activity of the turbine engine and the way that the combustion chamber is not an encased space, the pressure of the air does not rise, similar to that of the piston engine; during combustion however its volume increases. This procedure is known as heating at constant pressure. Under these conditions there is no peak or fluctuating pressures to be withstood, just like the case with the piston engine with its peak pressures more than 70 bar. This peak pressure makes it important for the piston engine to utilize barrels of overwhelming development and to utilize high energizes, as opposed to the low energy fills and the light manufactured combustion chambers utilized on the turbine engine.

The working cycle of gas turbine engine, represented by the temperature entropy diagram is shown in fig. 1.3. Point 1 represents air at atmospheric pressure that is compressed along the line 1-2. From 2 to 3, heat is added to the air by burning fuel at consistent pressure, in this way impressively expanding the volume of gas. Pressure misfortunes in the combustion chambers are not demonstrated but rather there will be some losses. From 3 to 4 the gases coming about

because of ignition extend through the turbine and jet pipe back to atmosphere. Amid this part of the cycle, a portion of the vitality in the extending gases is transformed into mechanical power by the turbine; discharge to atmosphere gives a propulsive jet.

Since the turbojet engine is a heat engine, the higher the temperature of combustion the more prominent is the extension of the gases. The combustion temperature, in any case, must not surpass an esteem that gives a turbine gas entry temperature reasonable for the design and materials of the turbine assembly. The upgrades of the gas turbine cycle have generally been aiming for expanding the efficiency, bringing down the venture cost, and lessening environmental emissions. To expand efficiencies, turbine architects have attempted to build terminating temperatures without harming the turbines. Be that as it may, terminating turbines past the limit temperatures of their parts debilitate their integrity and reliability. Improvement of cooling methods and enhancing materials are two noteworthy techniques of tackling this issue. The upgrades of the individual efficiencies of the primary gas turbine segments like the compressor and turbine have likewise helped in expanding the gas turbine proficiency. What's more, enhanced efficiency can be accomplished by changes to the original cycle. Energy can be extricated as shaft power, compacted air or thrust or any combination of these and used to control power aircraft, trains, boats, generators, or even tanks.

In a gas turbine engine, a turbine area is comprised of a disc or hub that holds numerous turbine blades. That turbine segment is associated with a compressor segment by means of spool, and that compressor segment can either be axial or centrifugal. Air is compressed, raising the pressure and temperature, through the compressor stages of the engine. The pressure and temperature are then significantly expanded by burning of fuel inside the combustor, which sits between the compressor stages and the turbine stages. The high temperature and high pressure deplete gases at that point go through the turbine stages. The turbine stages extract energy from this flow, bringing down the pressure and temperature of the air, and transfers the kinetic energy to the compressor stages along the spool. This procedure is fundamentally the same as how a axial compressor functions just in turn around. There, the high speed and volume of the gas stream is coordinated through a nozzle over the turbine's blades, turning the turbine which controls the compressor and, for a few turbines, drives their mechanical output. The energy

offered up to the turbine originates from the scattering in the temperature and pressure of the exhaust gas.

1.2 GAS TURBINE ENGINE COMPONENTS

1.2.1 Inlet

The air inlet duct must provide sifted and unhampered airflow to the engine. Clean and undisturbed inlet airflow extends engine life by averting erosion, corrosion, and foreign object damage (FOD). Thought of environmental conditions such as pollution, foreign objects and icing conditions must be made when designing the inlet system. Fairings ought to ensure minimum airflow losses to the engine at all conditions.

1.2.2 Diffuser

Air leaves the compressor through exit guide vanes, which change over the outspread segment of the wind stream out of the compressor to straight-line stream. The air at that point enters the diffuser segment of the engine, which is a divergent duct. The essential capacity of the diffuser structure is streamlined. The different shapes of pipe, changes over the greater part of the air velocity into static pressure. Subsequently, the most noteworthy static pressure and least speed in the whole engine are at the purpose of diffuser discharge and combustor inlet [21]. Other aerodynamic design contemplations that are imperative in the diffuser area emerge from the requirement for a short flow path, uniform flow distribution, and low drag loss.

1.2.3 Compressor

The compressor is accountable for providing the compressor with all the pressurized air it needs in a competent mode. In accumulation, it must contribute this air at elevated static pressures. The compressor is implicit to contain certain stages of rotor blades and stator vanes. The overall pressure ratio (pressure at the back of the compressor compared to pressure at the front of the compressor) will characterize how much of air is getting compressed per unit time and rise in temperature from that computation at last it can be proficient to analyze power specified by engine at utmost rated angular speed. In an axial flow compressor, every stage incrementally boosts the pressure from the preceding stage. A single stage of compression consists of a set of rotor blades attached to a rotating disk, followed by stator vanes attached to a stationary ring.

The flow area between the compressor blades is considerably divergent. Flow area involving compressor vanes is also divergent, as compared to blades [39].

In general terms, the compressor rotor blades convert mechanical energy into gaseous energy. This energy conversion greatly increases total pressure. Most of the increase is in the form of velocity; with a small increase in static pressure due to the divergence of the blade flow paths. The stator vanes slow the air by means of their divergent duct shape, converting the accelerated velocity to higher static pressure. The vanes are positioned at an angle such that the exiting air is directed into the rotor blades of the next stage at the most efficient angle [16].

In addition to the stages of blades and vanes, the compressor also incorporates the inlet guide vanes and the outlet guide vanes. These vanes, located at the inlet and the outlet of the compressor, are neither divergent nor convergent. The inlet guide vanes direct air to the first stage compressor blades at the "best" angle. The outlet guide vanes "straighten" the air to provide the combustor with the proper airflow direction [4].

The efficiency of a compressor is primarily determined by the smoothness of the air flow. During design, every effort is made to minimize airflow losses due to friction and turbulence. This task is a difficult one, since the air is forced to flow into ever-higher pressure zones. Air has the natural tendency to flow toward low-pressure zones. If air were allowed to flow "backward" into the lower pressure zones, the efficiency of the compressor would decrease tremendously as the energy used to increase the pressure of the air was wasted. To prevent this from occurring, seals are incorporated at the base of each row of vanes to prevent air leakage. In addition, the tip clearances of the rotating blades are also kept at a minimum by the use of coating on the inner surface of the compressor case.

Most of the components in the compressor designed as airfoil or streamed shapes to reduce the turbulence and to increase the uniformity of the flow, air angles need to find out from traditional velocity triangles for each section of the blade for each stage it will maintained stream lined flow according to Reynolds number from root to tip of the blade and efficiency will maximized.

1.2.4 Combustor

Once the air flows through the diffuser, it enters the combustion section, also called the combustor. The combustion section has the difficult task of controlling the burning of large amounts of fuel and air. It must release the heat in a manner that the air is expanded and accelerated to give a smooth and stable stream of uniformly-heated gas at all starting and operating conditions. This task must be accomplished with minimum pressure loss and maximum heat release. Their many types of combustion chamber in gas engine let's say engine in this example uses a can-annular combustion section. Combustion liners (cans) are positioned within an annulus created by inner and outer combustion cases.

The remaining air, referred to as secondary or dilution air, is admitted into the liners in a controlled manner. The secondary air controls the flame pattern, cools the liner walls, dilutes the temperature of the core gasses, and provides mass. This cooling air is critical, as the flame temperature is above 1930^0C, which is higher than the metals in the engine can endure. It is important that the fuel nozzles and combustion liners control the burning and mixing of fuel and air under all conditions to avoid excess temperatures reaching the turbine or combustion cases. Maximum combustion section outlet temperature (turbine inlet temperature) in this engine is about 1070^0C [6].

The rear third of the combustion liners is the transition section. The transition section has a very convergent duct shape, which begins accelerating the gas stream and reducing the static pressure in preparation for entrance to the turbine section [12, 13].

1.2.5 Turbine

The turbine converts the gaseous energy of the air/burned fuel mixture out of the combustor into mechanical energy to drive the compressor. Turbine converts gaseous energy into mechanical energy by expanding the hot, high-pressure gases to a lower temperature and pressure. Each stage of the turbine consists of a row of stationary vanes followed by a row of rotating blades. This is the reverse of the order in the compressor. In the compressor, energy is added to the gas by the rotor blades, and then converted to static pressure by the stator vanes. In the turbine, the stator vanes increase gas velocity, and then the rotor blades extract energy [29].

Once again blade and vanes are designed with airfoil sections. As the airstream enters the turbine section from the combustion section, it is accelerated through the first stage stator vanes. The stator vanes (also called nozzles) form convergent ducts that convert the gaseous heat and pressure energy into higher velocity gas flow. In addition to accelerating the gas, the vanes "turn" the flow to direct it into the rotor blades at the optimum angle. As the mass of the high velocity gas flows across the turbine blades, the gaseous energy is converted to mechanical energy. Velocity, temperature, and pressure of the gas are sacrificed in order to rotate the turbine to generate shaft power. The efficiency of the turbine is determined by how well it extracts mechanical energy from the hot, high-velocity gasses. Since air flows from a high-pressure zone to a low pressure zone, this task is accomplished fairly easily. The use of properly positioned airfoils allows a smooth flow and expansion of gases through the blades and vanes of the turbine [15].

1.2.6 Exhaust

After the gas has passed through the turbine, it is discharged through the exhaust. Though, the most of the gaseous energy is converted to mechanical energy by the turbine. A significant amount of power remains in the exhaust gas. This gas energy is accelerated through the convergent duct shape of the exhaust to make it more useful as jet thrust - the principle of equal and opposite reaction means that the force of the exhausted air drives the airplane forward [21].

1.3 EFFECTS OF ATMOSPHERIC CONDITIONS

The efficiency of the gas turbine engine is dependent on the mass of air the engine is pumping. At a constant speed, the compressor pumps a constant volume of air into the engine with no regard for air mass or density. If the density of the air decreases (in summer or on hotter day), the same volume of air will contain less mass, so less power is produced. If air density increases (on a cold day), power output also increases as the air mass flow increases for the same volume of air. At high altitude, air density is decreased, resulting in a decrease of output shaft power [2].

1.4 PERFORMANCE AND EFFICIENCY

Mainly determined by the amount of shaft horsepower (S.H.P.) the engine produces for a given conditions. The bulk of aircraft gas turbine engines are evaluated at standard day states of 32.78^0C and 1.0132075 bar [39]. This gives a pattern to which gas turbine engines of numerous kinds can be analyzed. The requirement for high proficiency in the engine turns out to be more imperative as fuel turn out to be more expensive. Engine efficiency is principally characterized by the specific fuel consumption (S.F.C.) of the engine at a given arrangement of conditions.

Numerous factors affect both the efficiency and performance of the engine. The mass flow rate of air through the engine will govern engine performance. Any impedance acting against the smooth flow of air through the engine will confine the engine's efficiency. The pressure ratio of the compressor, the engine turbine inlet temperature, and the entity section efficiencies will also manipulate both the performance and the efficiency of the overall engine. Every one of these elements is considered amid the plan of the engine. An optimum pressure ratio, turbine inlet temperature, and air mass flow rate are selected to obtain the required performance in the most efficient manner. In addition, individual engine mechanism is deliberate to curtail flow losses to capitalize on section efficiencies.

1.5 TURBINE BLADES

Turbine blade alone important part of gas turbine section, profile of cross-section is obvious airfoil so smoothness of this shape is very difficult to create and retain, in this particular environment of high temperature the blade should sustain, we should approach to super alloy or thermal barrier coatings. It will be very challenging task to produce the blades which can perform well in variable velocities and sudden change in temperature.

The number of turbine stages varies in different types of engines, with high bypass ratio engines tending to have the most turbine stages. The number of turbine stages can have a great effect on how the turbine blades are designed for each stage [9]. Many gas turbine engines are twin spool designs, meaning that there is a high pressure spool and a low pressure spool. Other gas turbines use three spools, adding an intermediate pressure spool between the high and low pressure spool

[39]. The high pressure turbine is exposed to the hottest, highest pressure air, and the low pressure turbine is subjected to cooler, lower pressure air. That difference in conditions leads the design of high pressure and low pressure turbine blades to be significantly different in material and cooling choices even though the aerodynamic and thermodynamic principles are the same [20].

1.5.1 Environment and Failure Modes

Turbine blades are subjected to very strenuous environments inside a gas turbine. They face high temperatures, high stresses, and a potentially high vibration environment [6]. All three of these factors can lead to blade failures, which can destroy the engine, and turbine blades are carefully designed to resist those conditions. They are also subjected to stress from centrifugal force (turbine stages can rotate at tens of thousands of revolutions per minute (RPM)) and fluid forces that can cause fracture, yielding, or creep failures [9]. Additionally, the first stage (the stage directly following the combustor) of a modern turbine faces temperatures around $1{,}370^0$C, up from temperatures around 820^0C in early gas turbines. Modern military jet engines, like the Snecma M88, can see turbine temperatures of $1{,}590^0$C. Those high temperatures weaken the blades and make them more susceptible to creep failures. The high temperatures can also make the blades susceptible to corrosion failures. Finally, vibrations from the engine and the turbine itself (see blade pass frequency) can cause fatigue failures [14].

1.6 COOLING OF GAS TURBINE BLADES

Cooling of parts can be accomplished via air or liquid cooling. Liquid cooling is by all accounts more alluring as a result of high specific heat capacity and odds of evaporative cooling however there can be issue of leakage, corrosion, choking, and so forth which conflicts with this method. On the other hand, air cooling permits the released air into main flow with no issue. Amount of air required for this object is 1- 3% of main flow and blade temperature can be lessened by 200^0C-300^0C [8]. Cooling technique may be classified as inward and outward flow cooling. While all strategies have their disparities, they all work by utilizing cooler air to expel heat from the turbine blades [5].

1.6.1 Methods of Cooling

For cooling purpose there are two mode of blade cooling i.e. of liquid cooling and air cooling. In liquid cooling, there is a possibility of liquid getting choked, getting leaked and corrosion of blades. On the other hand, air may be used and exhausted very easily but specific heat capacity is lower as compare to liquids but air will give more advantages such as low maintenance cost, easy presence of air [1]. There are many types of cooling used in gas turbine blades; convection, film, transpiration cooling, cooling effusion, pin fin cooling etc. which fall under the categories of internal and external cooling. While all methods have their differences, they all work by using cooler air (often bled from the compressor) to remove heat from the turbine blades [11, 12].

1.6.2 INTERNAL COOLING

1.6.2.1 Convection cooling

It works by passing cooling air through passages internal to the blade. Heat is transferred by conduction through the blade, and then by convection into the air flowing inside of the blade.

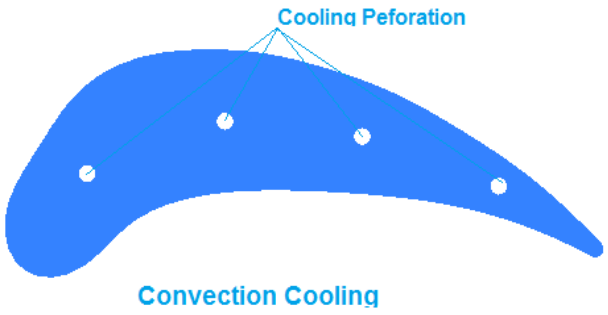

Fig. 1.4 Blade cooling by convection [56]

A large internal surface area is desirable for this method, so the cooling paths tend to be serpentine and full of small fins. The internal passages in the blade may be circular or elliptical in shape. Cooling is achieved by passing the air through these passages from hub towards the blade tip. This cooling air comes from an air compressor. In case of gas turbine the fluid outside is relatively hot which passes through the cooling passage and mixes with the main stream at the blade tip [17, 56]. Fig. 1.4 shows the blade cooling by technique by convection.

1.6.2.2 Impingement cooling

A variation of convection cooling, impingement cooling, works by hitting the inner surface of the blade with high velocity air. This allows more heat to be transferred by convection than regular convection cooling does. Impingement cooling is used in the regions of greatest heat loads. In case of turbine blades, the leading edge has maximum temperature and thus heat load. Impingement cooling is also used in mid chord of the vane. Blades are hollow with a core. There are internal cooling passages. Cooling air enters from the leading edge region and turns towards the trailing edge [18]. Fig.1.5 shows the blade cooling by Impingement technique.

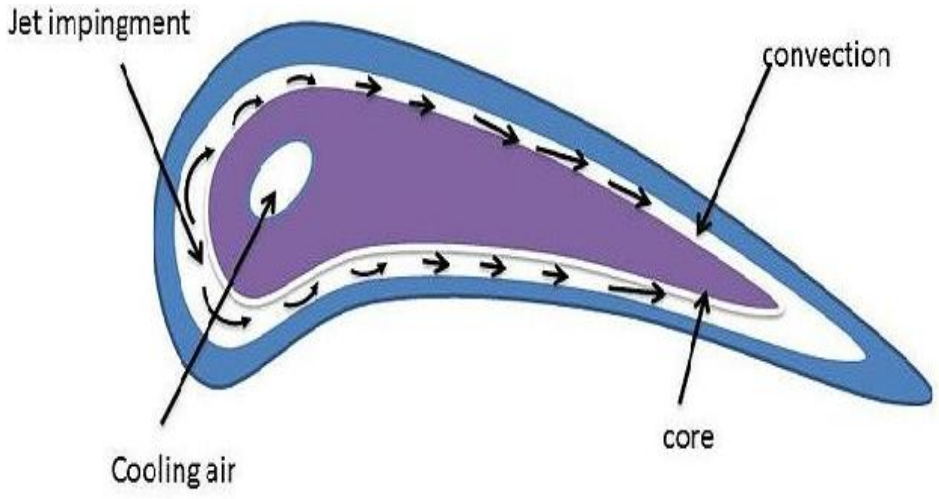

Fig.1.5 Blade cooling by Impingement [18]

1.6.2.3 Pin fin cooling

In the narrow trailing edge film cooling is used to enhance heat transfer from the blade. There is an array of pin fins on the blade surface. Heat transfer takes place from this array and through the side walls. As the coolant flows across the fins with high velocity, the flow separates and wakes are formed.

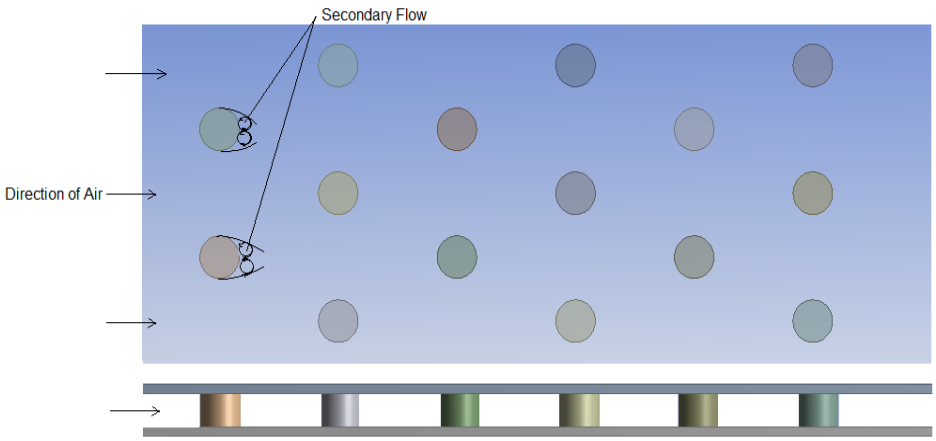

Fig. 1.6 Typical Test Model and Secondary Flow for Pin-Fin Cooling [19]

Many factors contribute towards heat transfer rate among which the type of pin fin and the spacing between fins are the most significant. Figure 1.6 represents the test model of pin-fin cooling [19].

1.6.3 EXTERNAL COOLING

1.6.3.1 Film cooling

Film cooling (also called thin film cooling) is a major type of cooling which works by pumping cool air out of the blade through small holes in the blade. This air creates a thin layer (the film) of cool air on the surface of the blade, protecting it from the high temperature air. The air holes can be in many different blade locations, but they are most often along the leading edge [25]. A United State Air Force program in the early 1970s funded the development of a turbine blade that was both film and convection cooled, and that method has become common in modern turbine blades. There are orifices on the surface through which the cool air flows on the surface and makes a film on the surface which acts as a barrier to heating and provides effective cooling. Besides cooling blade surface it decreases heat transfer from metal surface to the hot fluid [26].

Fig. 1.7 Turbine blade with cooling holes for film cooling [33]

One consideration with film cooling is that injecting the cooler bleed into the flow reduces turbine efficiency. That drop in efficiency also increases as the amount of cooling flow increases. The drop in efficiency, however, is usually mitigated by the increase in overall performance produced by the higher turbine temperature [33]. Figure 1.7 shows the turbine blade with cooling holes.

1.6.3.2 Cooling effusion

Blade surface is made of porous material which means having a large number of small orifices on the surface. Cooling air is forced through these porous holes which form a film or cooler boundary layer. Besides this, uniform cooling is caused by effusion of the coolant over the entire blade surface [31]. Fig. 1.8 shows the cooling technique by effusion.

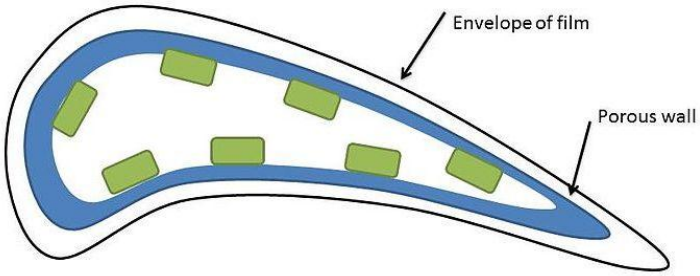

Fig. 1.8 cooling by effusion [31]

1.6.3.3 Transpiration cooling

It makes a thin film of cooling air on the blade, however it is distinctive in that air is "spilled" through a permeable shell instead of infused through holes. This kind of cooling is viable at high temperatures as it consistently covers the whole blade with cool air [11]. Transpiration-cooled generally comprise of a rigid strut with a porous shell. Air flows through inside channels of the strut and after that go through the effectiveness, in this manner that reduction must be adjusted with enhanced temperature execution. Figure 1.9 represents a model for transpiration cooling [52].

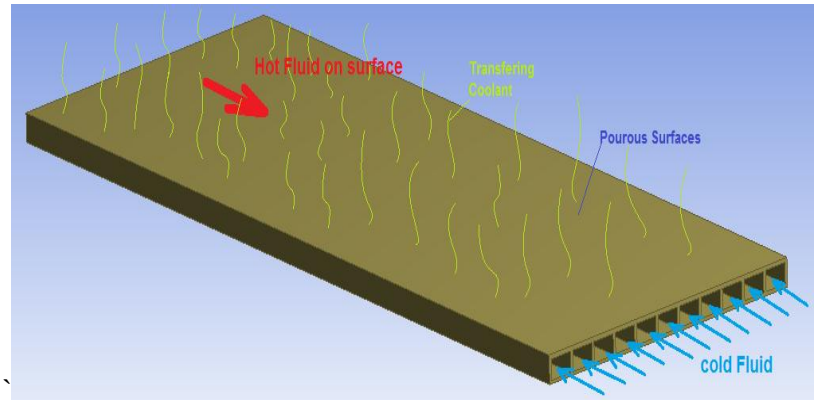

Fig. 1.9 Transpiration cooling model [52]

1.6.3.4 Rib Turbulated cooling

Rib turbulators are the most frequently used method to enhance the heat transfer in the internal serpentine cooling passages. The rib turbulence promoters are typically cast on two opposite walls of the cooling passage. Heat that conducts from the pressure and suction surfaces through the blade walls is transferred to the coolant passing internally through the blade. The heat transfer performance of the ribbed channel depends on the channel aspect ratio, the rib configurations, and the Reynolds number of the coolant flow [37]. Fig. 1.10 represents typical test model for turbulated cooling studies with rib induced secondary flow.

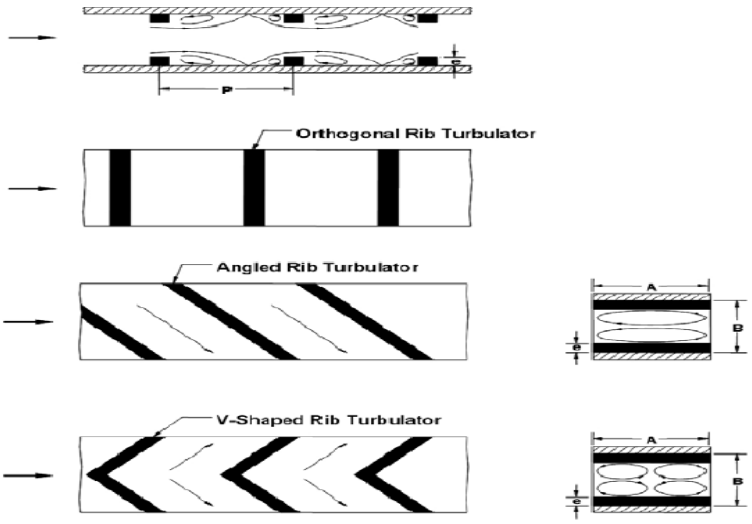

Fig. 1.10 Typical Test Model for Turbulated Cooling Studies with Rib Induced Secondary Flow [37]

1.6.3.5 Dimple Cooling

A typical test section for dimple cooling studies is shown in figure 1.12, which shows the dimple induced secondary flow. These concave dimples induce flow separation and reattachment with pairs of vortices. The areas of high heat transfer include the areas of flow reattachment on the flat surface immediately downstream of the dimple. The heat transfer in the dimpled channel is typically 2 to 2.5 times greater than the heat transfer in a smooth channel with a pressure loss penalty of 2 to 4 times that of a smooth channel.

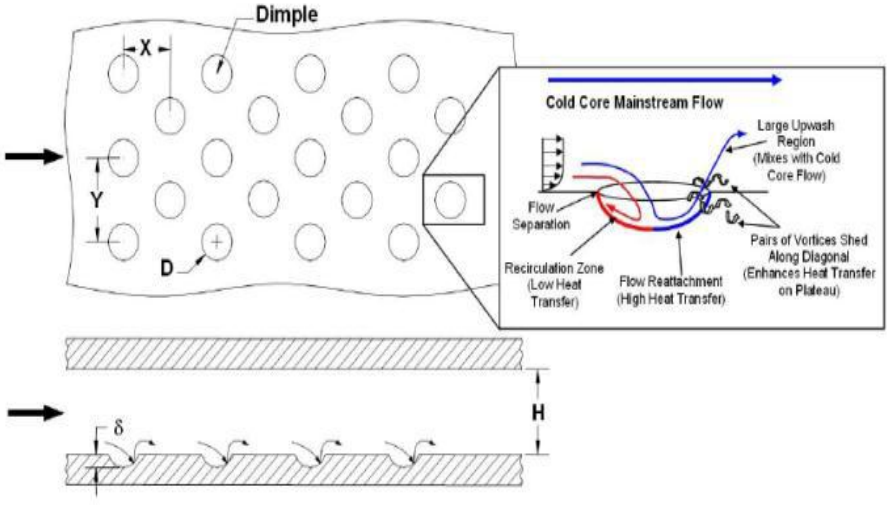

Fig. 1.11 Typical Test Model for Dimple Cooling [50]

These values show little dependence on Reynolds number and channel aspect ratio. However, the dimple size, dimple depth (depth-to-print diameter ratio = 0.1 to 0.3), distribution, and shape (cylindrical, hemispheric, teardrop) each effect the heat transfer distribution in the channel. The heat transfer is further enhanced on a surface that is concavely shaped (compared to a flat surface); however, a convexly curved surface with a dimple decreases the level of heat transfer enhancement [50].

1.7 Objectives

The present study is proposed to investigate the cooling of gas turbine blades with the following specific objectives.

1. To design and analyze the performance of gas turbine for different blade materials using ANSYS.
2. To calculate the performance of gas turbine of cycle for various operating conditions.
3. To optimize the quality of blade material.

REVIEW OF LITERATURE

El-Masri and Mattingly have suggested to Rolls Royce during their research for better cooling techniques in gas turbine should be adopted to increase the turbine blade life. Thermodynamics of gas turbine cycles in three parts- The first part deals with combined cycles which will be dealt separately. Part 2 deals with the development of a model for expansion in cooled turbine. A general albeit approximate model is presented to quantify those cooling losses for different types of cooling techniques. It is based upon representing the turbine as an expansion path with continuous, rather than discrete work extraction. The formulation shows the key factor in determining the cooling losses is the parameter scaling the ratio of heat to work fluxes loading the machine surfaces. Solutions are given for three cases:-

a) Internal air cooling
b) Transpiration cooling
c) Internal liquid cooling

The first and second cases represent lower and upper bounds respectively for the performance of film-cooled machines, irreversibilities arising from flow path friction, heat transfer, cooling air throttling and mixing of coolant with mainstream are quantified and compared. Sample results presented show air-cooled cycles peaking at about 40% for simple cycles for conditions thought to represent state of art [70].

Joseph L. Steger et. al (1988) calculated formulation for solving the boundary-layer equations in general body-fitted curvilinear coordinates while retaining the innovative Cartesian reliant variables to authenticate the approach. The arrangement methodology does not required any of the directions be orthogonal, and a great part of the product was created for some, Navier-Stokes plans which can be promptly utilized for limit conditions.[27]

M. Y. Jabbari et. al (1996) investigated the film cooling performance for injection through discrete openings in the endwall of a turbine blade. The effectiveness was anticipated at 60 locations in the region secured by injection. Three insignificant blowing rates, two thickness proportions, and two approaching flow Reynolds numbers were inspected. The analysis revealed that even 60 locations are lacking for the assurance of the field of film cooling effectiveness with its solid local varieties. Representation of the traces of the coolant jets on the endwall surface, utilizing ammonium-diazo-paper, gives helpful subjective data to the translation of the

estimations, uncovering the ways and connection of the jets, which changes with blowing rate and density ratio.[34]

S. Friedrichs et. al(1997) portrays the aerodynamic parts of endwall film-cooling in which the flow field downstream of an expansive scale low-speed linear turbine course was estimated for the integrated losses and of secondary flow features with and without end wall film-cooling. Determination for variety of both the coolant supply pressure and injection area together with past estimations of adiabatic film-cooling effectiveness and surface-flow perception was likewise explored. The outcomes uncovered the idea of the interaction between the ejected coolant and the flow in the blade section estimated hole mass flows and a consistent static pressure combining investigation with the deliberate misfortunes permitted the decomposition losses into three particular entropy generation instruments misfortune age inside the opening. Loss generation due to the mixing of the coolant with the mainstream and change in secondary loss generation within the coolant holes is substantial and that ejection into regions of low static pressure increases the lose per unit coolant mass flow. Discharge upstream of the three-dimensional separate lines on the outcomes demonstrated that it is important to consider the three dimensional nature of the endwall stream in the outline of endwall film-cooling configurations.[56]

Ronald S. Bunker and Jeremy C. Bailey (1999) performed a collective trial and computational study to examine the comprehensive circulation of convective heat transfer coefficients on the first stage blade tip surface for a geometry distinctive of large power generation turbines (>100MW). It showed concerned with the design and execution of the experimental segment of the study, which represents the first reported investigation to obtain nearly full surface information on heat transfer coefficients within an environment which develops an appropriate pressure distribution about an airtbil blade tip and shroud model. A stationary blade cascade trial was performed consisting of three airtbils, the center airtbil having inconsistent tip gap consent. The airfoil models the aerodynamic tip section of a high pressure turbine blade with inlet Mach number of 0.30, exit Mach number of 0.75, pressure ratio of 1.45, exit Reynolds number based on axial chord of 2.57.10 and total turning of about 110 degrees. A hue recognition based liquid crystal method was induced to achieve the thorough heat transfer coefficient distribution on the blade tip surface for flat, smooth tip surfaces with both sharp and rounded edges. The cascade

inlet turbulence intensity level took on values of either 5% or 9%. The cascade also models the casing recess in the shroud surface ahead of the blade. Investigational results shows the pressure distribution measurements on the airfoil near the tip gap, on the blade tip surface and on the opposite shroud surface. Tip surface heat transfer coefficient distributions were found for sharp-edge and rounded-edge tip geometries at each of the inlet turbulence intensity levels.[54]

M. Mirzaei and R. Karimi (2001) examined the pressure investigation and life evaluation of a first-stage air-cooled sharp edge made of the super alloy IN738LC. Three-dimensional finite element thermal and stress analyses of the sharp edge were done for the consistent state full-load operation. The consequences of these examinations were utilized for assurance of the areas where the blend of high temperature and high tensile stress was adequate for creep-fatigue crack growth. Similarly, a basic point at the main edge of the airfoil, close to the root, was chosen for crack modeling. With the supposition of event of small scale creep and thermal fatigue amid each begin stop cycle, the relevant crack tip parameters were ascertained utilizing the vitality area basic strategy. An incremental crack growth conspire was viewed as and the aggregate life for the development of a 0.5mm surface break to a 5mm through-thickness split was computed.[33]

R. Jones et. al (2005) presented a new model (the v f- kω 2 model), which is based on ω as the relevant length scale, and provides predictive accuracy that is comparable to or better than the v f-kε 2 , but with considerably enhanced numerical stability. The model was tested on a film cooling flow application, and computations were compared with detailed flow and cooling effectiveness measurements. It showed that the v f-kω 2 model provides enhanced flow predictions over other turbulence models, but that a variable Prandtl number formulation is necessary for improved cooling effectiveness predictions. A Prandtl number articulation was proposed which yielded enhanced predictions. Film-cooling flows are characterized by a row of jets injected at an angle from the blade surface or end walls into the heated cross flow. The resulting flow field is quite complex, and accurate predictions of the flow and heat transfer have been difficult to obtain using traditional two-equation turbulence models employed with Reynolds Averaged Navier-Stokes (RANS) solvers.[48]

Hildebrandt T. et al. (2006) used present day business turbo-apparatus arranged CFD-techniques for the demonstrating of film cooling openings that can be accomplished by different

numerical strategies for various intricacy. The CFD strategies to each advanced high-pressure turbine require a profoundly complex cooling framework. The most of the time utilized cooling technique for to date is film cooling, portrayed by a high level of connection between the main stream and the cooling stream. In this manner the impacts of film cooling must be considered in the aerodynamic design of film cooled high-pressure turbines. The alleged source term modeling is quick and simple to apply, however can't give exceptionally point by point stream data. Interestingly, the discretization of each and every cooling gap speaks to an exceptionally complex approach, however gives more inside and out data about the cooling design. The endeavors of full-scale modeling should be adjusted against the more thorough and precise outcomes. Notwithstanding the intricate geometries of film cooled turbines, the stream wonders are profoundly flimsy, along these lines requiring a CPU escalated time subordinate numerical approach. The analysis gives itemized investigation of the unsteady flow field in a film cooled high-pressure turbine stage. An unsteady 3D Navier-Stokes estimation is connected to the whole stage setup including a full discretization of all the cooling holes.[22]

Carlos A Estrada M. (2007) discussed and exhibited the new innovations for increasing the execution, dependability and emanations in gas turbines due changes materials. After the world word II, gas turbines turned into a vital innovation for its applications in flight and industrial processes. Toward the starting materials utilized for the engine development and all the more unequivocally; materials utilized as a part of compressor and turbine blade materials, couldn't survive in excess of a couple of hundred hours at then generally unassuming temperatures and low power settings; then again, reliability and thermodynamic effectiveness were moderately low, creating a few mishaps making harm gear and harms to people.[6]

Gregory M. Laskowski and Frederic N. Felten (2010) assessed RANS and URANS for anticipating the downstream momentum and thermal wake evolution. There is a consistently expanding interest for higher performance higher efficiency gas-turbines. The first stage of the high-pressure turbine is subjected to high temperatures subsequently. Expand cooling techniques are required to guarantee the life of the stator and rotor with insignificant effect to efficiency. The trailing edges of the vanes and sharp edges that constitute the stator and rotor are especially helpless and coolant flow is ejected out the trailing edge to ensure life. This coolant flow interfaces with the unsteady trailing edge wake that sustains the downstream sharp edge lines.

Recreation comes about for three diverse trailing edge coolant flow rates were approved against accessible trial information. Great understanding in vane stacking and momentum deficiencies were noted. The URANS simulations catch Kelvin-Helmholtz actuated vortex shedding because of the shear layers that frame downstream of the suction-side and pressure side surfaces. Settling the subsequent vortex shedding is appeared to be less affect to the wake development. It demonstrated that the momentum and warm wakes developed in various areas that are credited to compressibility, shock formation and coolant ejection location.[18]

Robert Yancey et al. (2011) applied computational improvement techniques to propose lighter and more effective structures for numerous aviation structures. Turbine blades have inward sections that give cooling amid activity in a high temperature engine. The design of the cooling sections is basic to accomplish close uniform temperature of the blade amid activity. The temperature of the blade is reliant on the thermal properties of the blade material and additionally the fluid dynamics of the air circling in the cooling entries. An expansion of these systems is presently connected to directing the thermal design of a turbine blade by planning the ideal cooling entry design. Enhancement techniques was connected to decide the optimal pattern of the cooling sections and afterward to streamline the extent of the individual cooling entries. The objective was to deliver an all the more thermally effective turbine blade design that will create blades with longer lives and better performance.[53]

G. Narendranath and S. Suresh (2012) examined the first stage rotor cutting edge off the gas turbine utilizing ANSYS 9.0 for the mechanical and radial elongations from the tangential, axial and centrifugal forces. The gas forces namely tangential, axial were determined by constructing velocity triangles at inlet and exist of rotor blades. The material of the edge was indicated as N155. This material is an iron based super amalgam and structural and thermal properties at gas room and room temperatures. The turbine blade along the groove blade is demonstrated with the 3D-Solid Brick component. The geometric model of the cutting edge profile is produced with splines and barred to get a strong model in CATIAV5R15. The first stage rotor blade of a two stage gas turbine has been analyzed for structural, thermal and modal analysis utilizing ANSYS 9.0 finite element analysis programming. The gas turbine rotor blade model is coincided in HYPERMESH 7.0. The thermal boundary condition, for example, convection and working

temperatures on the rotor blade is acquired by hypothetical displaying. An expository approach is utilized to gauge the tangential, radial and centrifugal forces.[13]

Josin George and Titus R. (2014) composed a strong model of the turbine blade on CATIA V5 with the assistance of the spline and expel alternatives. Gas turbine blades subjects to high tangential, axial and centrifugal forces amid their working conditions. While withstanding these powers gas turbine blades may subject to elongation. A few techniques have been proposed for the better improvement of the mechanical properties of blade to withstand these outrageous conditions. It compresses the design, analysis and modification of the cooling section in the gas turbine blade design. ANSYS 14.0 software was utilized for the investigation of finite element model created by finite element model generated by meshing of the blade by applying boundary conditions. Better material for first stage turbine blade is expressed from the analysis. After that by utilizing the better material properties the cooling entry of the turbine blade is adjusted into serpentine model and changing the quantity of holes.[28]

V. Naga BhushanaRao et al. (2014) presented the failure breakdown made on HPT turbine blades of 100 MW gas turbine used in marine applications. As high pressure temperature (HPT) turbine blade is the most significant module of the gas turbine and failures in this turbine blade can have striking effect on the security and performance of the gas turbine engine. The gas turbine blade was made of Nickel based super alloys and was manufactured by outlay casting method. The gas turbine blade under assessment was operated at elevated temperatures in corrosive environmental attack such as oxidation, hot corrosion and sulphidation etc. The analysis on gas turbine blade incorporated the behavior like visual inspection, determination of material composition, microscopic examination and metallurgical analysis. Metallurgical examination revealed that there was no micro-structural damage due to blade operation at high temperatures. It indicated that the gas turbine was operated within the designed temperature conditions. It was also observed that the blade might have suffered both corrosion (including HTHC & LTHC) and erosion. Low temperature hot corrosion (LTHC) was major at the root of the blade while the regions near the tip of the blade were affected by the high temperature hot corrosion (HTHC). It could be concluded that the turbine blade malfunction might be caused by numerous failure mechanisms such as hot corrosion, erosion and fatigue. Hot corrosion could have reduced the thickness of the blade material and thus destabilized the blade. This reduction

of the blade thickness decreases the fatigue strength which eventually led to the malfunction of the turbine blade.[59]

L.Umamaheswararao and K. Mallikarjunarao (2014) analyzed the first stage rotor blade of a gas turbine for structural, thermal analysis using ANSYS (Finite Element Analysis Software). The material considered for the blade was specified as INCONEL 718. The thermal boundary conditions on the rotor blade are taken from the reference. The temperature distribution across the blade was obtained. The maximum stress up to which the blade can survive was identified and the stress distributions across the blade were obtained consequently. The concluded outcomes were compared with N-155, Mild Steel and the most suitable material was discussed. Finally, the actual fir tree model blade root was compared with I-section model blade root. The results accomplished that stress distribution was less in fir tree model as compared to the I-section model.[32]

Amjed Ahmed Jasim AL-Luhaibi and Mohammad Tariq (2014) investigated the film cooling strategy which was produced to cool gases in the underlying phases of the turbine blade, where temperature is high (>1122 K). It was discovered that the thermal efficiency of a cooled gas turbine is less as contrast with the uncooled gas turbine for a similar info conditions. The reason is that the temperature at the gulf of the turbine is diminished because of cooling and the work delivered by the turbine is somewhat diminished. It was additionally discovered that the power utilization of the cool inlet air is of considerable concern since it diminishes the net power yield of gas turbine. Moreover, net power diminishes on expanding the overall pressure ratio. As the performance of a gas turbine is for the most part subject to different parameters e.g. surrounding temperature, compressor weight proportion, turbine inlet temperature etc. The most essential parameter to build the life of the turbine blade is the cooling of the edge, which is important subsequent to achieving a specific temperature of the gases going through the blades.[2]

K. Vijaya Krishna Varma and M.V BabuTanneru (2016) built up an advanced cooling plan for constant safe operation of gas turbines with high performance. The procedures that required to cool the blades and vanes by utilizing cooling strategies is to have radial holes to pass high speed cooling air along the blade span. The turbine cutting edge was composed with different holes i.e., 5 holes, 9 holes, 13 holes. CFD analysis was done to conclude the pressure

distribution, velocity, temperature distribution and heat transfer rate by applying the inlet velocities. Thermal analysis was additionally done to decide the heat transfer rates of the blade. The material used for turbine blade was chromium steel and Inconel 718.[30]

Deepak Kumar Patel et. al (2016) explored the three dimensional CFD simulations to investigate the heat transfer and fluid flow characteristics of artificially roughened rectangular channel using Ansys-CFX. Heat transfer characteristics of the rectangular channel were investigated for Reynolds numbers ranging from 8000 to 18000. Model geometry was deliberated in CATIA V5 R20, and then meshed, analyzed, and post-processed using Ansys-CFX software. Fluid flow and heat transfer characteristics of various roughness configurations were replicated and then results were compared using turbulent flow model (k-omega model). Rectangular channel had an aspect ratio of 5, while the domain length for statistical study was kept 550 mm long the hydrodynamic diameter (Dh) of duct is 66 mm the relative roughness height (e/Dh) is 0.030, relative roughness pitch (p/e) is 10. Total three models of rectangular channel was created with base portion of the channel, provided with aluminium plate and this plate was roughened by three different ribs shape in such a way that the cross-section area of every shape is same, the ribs attack angle is taken as 45o .The another surface of the aluminium plate is kept at constant heat flux 1000 W/m2. Realistic variation was found between the heat transfer simulation data for different roughness configurations. It was also found that there is a momentous change in heat transfer rate, friction factor, Nusselt Number ratio, friction factor ratio and thermal performance factor, and it was concluded that the change in rib shape in rectangular channel can boost the heat transfer rate.[11]

Priyanka Singh and O P Shukla (2016) recommended a few strategies for the cooling of blades and one such procedure is to have radial holes to pass high velocity cooling air along the blade span. CFD examination is utilized to inspect the heat transfer investigation of gas turbine with six unique models comprising of 5, 9 and13 inline one row of holes and contrasted with 9 and 13 demonstrate in stunned gaps masterminded in the three lines and built up another model with 14 gaps in the amazed course of action. The expectations were regularly utilized as a part of CFD programming FLUENT (a turbulence feasible k-e display with upgraded wall treatment) on assessing the contour plot of the pressure, velocity and velocity vector. It was discovered that the temperature appropriation on the 13 amazed openings, consistently conveyed along the blade

area, when contrasted with 13 inline holes. The heat transfer likewise increments in the 13 and 14 staggered holes arrangements.[45]

A.B. Moskalenko and A.I. Kozhevnikov(2016) evaluated one of the most thermally stressed gas turbine elements, first stage power turbine blades, cooling efficiency. The calculations were implemented using a numerical simulation based on the Finite Element Method. The volume average temperature of the blade and the coefficient of heat transfer from the cooling medium to the cooling channel wall were chosen as the cooling efficiency criteria. A comparison of steam and air used as coolants was done, and the calculations were performed using ANSYS Fluent software.[1]

Harsha D A and Yogananda A (2017) have built up a complex cooling plan for continuous safe activity of gas turbines with high performance. Gas turbines are cooled outwardly and within. A few strategies were proposed for the cooling of blades and vanes. The procedures that included cooling the blades and vanes was by utilizing cooling techniques with radial holes to pass high speed cooling air along the blade span. They outlined a turbine blade and demonstrated in CATIA v5 and ICEM CFD programming. The turbine blades were composed utilizing cooling gaps. The turbine blade was composed with 12 gaps. CFD investigation was done to decide the pressure distribution, velocity, temperature distribution and heat transfer rate by applying the inlet velocities. Thermal and structural analysis investigation was likewise done to decide the heat transfer rates and strength of the blade. The material utilized for examination of blade was chromium steel and Titanium aluminum alloy.[24]

Jovin Jose and V. V PrathibhaBharathi (2017) performed a relative study for various parameters like temperature, turbulent kinetic energy and heat transfer rate through cooling air to find the best model which conveys efficient cooling of the blade. Thermal efficiency of gas turbine can be enhanced by increasing turbine rotor inlet temperature. The current rotor inlet temperature in sophisticated gas turbine is for above the melting point of blade material. A few techniques have been proposed for the cooling for the cooling of blades and vanes. The strategy that depicts the cooling of blades was given by circulating sodium liquid filled inside it. The hot less dense sodium liquid schedule the bottom region of the blade and exchange heat to the high velocity air passing near it. A turbine blade demonstrated was outlined and displayed in CATIA V5. CFD examination of the model was performed for variation models.[29]

CH. S. NAGA PRASAD (2017) designed a turbine blade and modeled in 3D modeling software Pro/Engineer. The proposed model was adjusted by changing the base of the blade to enhance the cooling efficiency. Since the design of turbo machinery is intricate, and efficiency is specifically identified to material performance, material selection is of prime significance. Two materials were considered for turbine blade i.e. titanium alloy and nickel alloy. Optimization was done by varying the materials Titanium alloy and Super Alloy by performing coupled field analysis (thermal and structural) on the turbine blade for both the designs. CFD technique was utilized in the present study to examine the flow the fluid over the turbine blade and the analysis was done in ANSYS.[7]

G.Muniyandi (2017) employed strategies for the cooling of blades and one such procedure is to have radial holes to pass high speed cooling air along the blade span. The constrained convection heat transfer from the blade to the cooling air diminishes the temperature of the blade as far as possible. Finite element analysis was utilized to look at the steady state thermal & structural performance for two unique materials i.e. N155, Inconel 718 and Titanium T6. Four unique models comprising of solid blade and blades with changing number of openings (6, 9 and 12 gaps) were broke down to discover the ideal number of cooling gaps. The investigation was carried utilizing ANSYS CFD software package.[14]

Ravi Ranjan Kumar and K. M Pandey (2017) have analyzed three different blade profiles for three different materials viz. Super Alloy X, Nimonic 80A and Inconel 625 at three different speeds viz. 20000, 40000 and 60000RPM. They introduced the issues concerning cutting blade profile determination, material selection and turbine rotor blade vibration that genuinely affect the prompted stress deformation and auxiliary working of formative gas turbine engine. For producing particular power by rotating blade at particular RPM, blade profile and material has been chosen by static structural analysis. Gas turbine rotating blade RPM is chosen by Modal analysis so that the natural frequency of blade ought not to coordinate with the excitation frequency. The blade profile has been displayed in SOLIDWORKS and investigation has been done in ANSYS WORKBENCH 14. Existing NACA6409 profile is chosen as base model and after that it is adjusted by bending it through 72.5 and 145. It is discovered that the material Inconel 625 gives the best outcome as blade material Inconel 625 indicated 72.5 bowed profile which is thought to be the best combination for all RPM.[52]

MATERIALS AND METHODS

In this chapter, theoretical calculation of various parameters to develop a particular blade profile has been discussed. "CATIA V" is being used to develop three section of blade namely; hub, mean and tip of blade and projected airfoil section are produced. Two different designs for cooling of blades have been considered. Standard design and zigzag design are taken for blade cooling. In standard design, holes are arranges along with the contour of the blade profile while in zigzag design pattern, the holes are shifted little outer from eccentric line but on the same section. Four numbers of holes have been taken for each design.

Table 3.1: Chemical composition and other properties of AISI 4140 alloy steel [42].

Element	**Contents / values**
Chemical Composition	
Chromium, Cr	0.80 - 1.10
Manganese, Mn	0.75 - 1.0
Carbon, C	0.380 - 0.430
Silicon, Si	0.15 - 0.30
Molybdenum, Mo	0.15 - 0.25
Sulfur, S	0.040
Phosphorous, P	0.035
Iron, Fe	Balance
Physical Properties	
Density	7.85 g/cm^3
Melting point	1416^0C-1470^0C
Mechanical Properties	
Tensile strength	655 MPa
Yield strength	415 MPa
Bulk modulus (typical for steel)	140 GPa
Shear modulus (typical for steel)	80 GPa
Elastic modulus	190 - 210 GPa
Poisson's ratio	0.27
Elongation at break (in 50 mm)	0.30

Hardness, Brinell	25.70%
Hardness, Knoop (converted from Brinell hardness)	197
Hardness, Rockwell B (converted from Brinell hardness)	219
Hardness, Rockwell C (converted from Brinell hardness.	92
Value below normal HRC range, for comparison purposes only)	13
Hardness, Vickers (converted from Brinell hardness)	207
Machinability (based on AISI 1212 as 100 machinability)	65
Thermal Properties	
Thermal expansion coefficient (@ 0100°C)	12.2 μm/m^{0}C
Thermal conductivity (@ 100°C)	42.6 W/mK

Table 3.2: Chemical composition and other properties of Titanium (Ti) alloy [42].

Element	**Contents / Values**
Chemical Properties	
Thermal neutron cross section	5.6 barns/atom
Electrode potential	0.20 V
Ionic radius	0.680 Å
Electro negativity	1.54
Xray absorption edge	2.497 Å
Electrochemical equivalent	0.4468 g/A/h
Physical Properties	
Density	4.50 g/cm^3
Melting point	1650 - 1670°C
Boiling point	3287 °C
Mechanical Properties	
Tensile strength	220 MPa
Modulus of elasticity	116 GPa
Shear modulus	43.0 GPa
Hardness, Brinell	70
Hardness, Vickers	60

Elongation at Break	54%
Poisson's Ratio	0.34
Thermal Properties	
Thermal expansion coefficient (@100°C)	8.90 μm/m°C
Thermal conductivity	17 W/mK

Table 3.1 and 3.2 listed the properties of steel alloy and titanium alloy respectively.

3.1 Design Calculation and Modeling

3.1.1 Design for pressure ratio 20

Researchers have suggested that there is a need for a low cost turbojet with a takeoff thrust of about 12000 N, preliminary studies show that a single-spool axial flow arrangement is satisfactory, using a pressure ratio 20 and 30 and a modest/high turbine inlet temperature to keep the cost optimum. For that purpose, cycle calculations for a suitable design point under sea-level static conditions (P_{atm}= 1·01 bar and T_{atm}=300 K) may discuss as follows.

Table 3.3 Input data for the present analysis [72]

Parameters	Values
Pressure Ratio	20
Turbine Inlet Temperature(K)	1200
Compressor Inlet Pressure (bar)	1.01325
Compressor Inlet temperature(K) T01	300
C_{pa}	1.005
C_{pg}	1.15
Ambient Pressure (bar)	1.01
R	0.296
γ	1.4
λ	0.05
Air Mass Flow Rate(Kg/s)	60
Axial Inlet Velocity (m/s)	175
ϕ	0.2

Calculation for Gas turbine compressor which is required for some input parameters of turbine blade calculation:

$C_1 = C_{\alpha 1} = 150 m/s$ (1)

$T_1 = T_{01} - \left(\frac{V^2}{2C_p}\right)$ (2)

$300 - \left(\frac{175 \times 175}{2 \times 1.005 \times 1000}\right) = 284.76$ K

$T_1 = 284.76$ K

$\frac{P_1}{P_{01}} = \left(\frac{T_1}{T_{01}}\right)^{\frac{\gamma}{\gamma-1}}$ (3)

$P_1 = 0.841575491$ bar

$\rho_1 = \frac{100 \times P_1}{R \times T_1}$

$\rho_1 = \frac{100 \times 0.841575491}{R \times 284.76}$

$\rho_1 = 1.029737629$ Kg/m^3

$r_t^2 = \left(\frac{m}{(\pi \times \rho \times C_{\alpha 1} \times)[1-(r_r/r_t)^2]}\right)$ (4)

$Y = Y1 + \frac{(X+X1)(Y2-Y1)}{X2-X1}$ …. (interpolationformula)

$r_t = 0.37004$ m (5)

Table 3.4 Revolution per unit second (angular velocity) chosen according to radii ratio

r_r/r_t	r_t (m)	N (rev/s)
0.4	0.2137	260.6
0.45	0.2194	253.9
0.5	0.2262	249.3
0.55	0.2346	237.5
0.6	0.2449	227.5

$r_r/r_t = 0.5$ has been chosen from table 3.4 for N = 250 rev/s

$U_t = 2\pi \times r_t \times N$

$U_t = 580.9683529$ m/s (6)

Calculation for Gas Turbine Blade

$T_2 = T_1 \left(\frac{P_2}{P_1}\right)^{\frac{\gamma-1}{\gamma}}$ (7)

$T_2 = 706.064$ K

Pressure after compression = 20.265 bar, $P_3 = 19.8597$ bar (compressor efficiency is 98%)

$$C_{pa}(T_2 - T_1) = C_{pg}(T_3 - T_4) \quad (8)$$

$$T_4 = 706.064 \text{ K}$$

$$P_4 = \frac{P_3 \times T_4}{T_3} \quad (9)$$

Pressure at exit of turbine = 13.98678 bar

$$\psi = \frac{2 \times C_{pg} \times \Delta T}{U^2} \quad (10)$$

Change in temperature ΔT will be 354.8646 K

$$\psi = 2.418163$$

If the rotational speed, which is assumed to be fixed by the compressor, had led to an ill-proportioned annulus, it would be necessary to rework this preliminary design. For example r_r/r_t could be increased by decreasing the axial velocity, i.e. by using a lower value of the flow coefficient ϕ. This would also decrease the nozzle efflux velocity, but it has been observed that it was comfortably subsonic and so could be decreased if necessary (table 3.4) Swirl increases the losses in the jet pipe; swirl is governed by angle α_3 equal to zero.

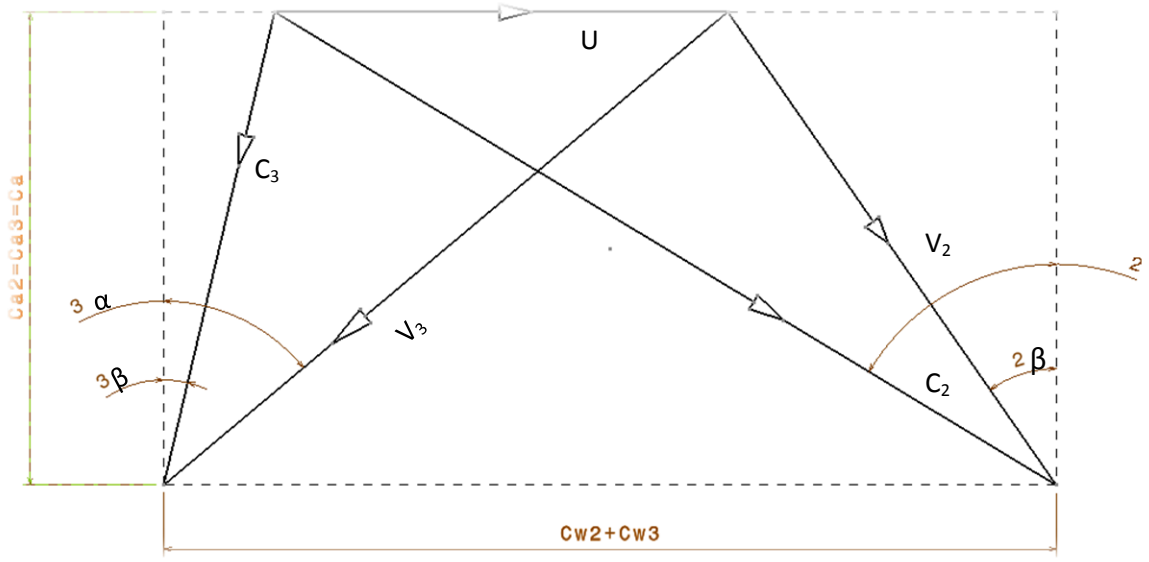

Fig. 3.1 Velocity triangle of turbine blade

$$\tan\alpha_3 = 0 = \tan\beta_3 - \frac{1}{\phi} \quad (11)$$

$$\tan\beta_3 = \frac{1}{2\phi}\left(\frac{1}{2}\psi + 2\Lambda\right) \quad (12)$$

$\Lambda = 0.395459117$ (13)

Including three-dimensional effects, the reaction should increase from root to tip of the blades, and a degree of reaction of only 0·395 at the mean diameter might mean too small value at the root. Negative values must certainly be avoided because this would imply expansion in the nozzles followed by recompression in the rotor and the losses would be large. Perhaps a modest amount of swirl will bring the reaction to a more reasonable value if α_3=10 has been taken for analysis.

$$\tan\alpha_3 = 0.1763 = \tan\beta_3 - \frac{1}{\emptyset} \quad (14)$$

$$\tan\alpha_3 = 0.1763,\ \alpha_3 = 10,\ \tan\beta_3 = 5.176326981,\ \beta_3 = 79.06589,\ \Lambda = 0.43072$$

$$\tan\beta_2 = \frac{1}{2\emptyset}\left(\frac{1}{2}\psi + 2\Lambda\right) \quad (15)$$

$$\tan\beta_2 = 0.8963,\ \beta_2 = 40.99331$$

$$\tan\alpha_2 = 5.8690818,\ \alpha_2 = 80.33055$$

$$C_{a2} = U \times \emptyset \quad (16)$$

$$C_{a2} = 580.96 \times 0.2 = 116.19\ \text{m/s}$$

$$C_2 = \frac{C_{a2}}{\cos\alpha_2} \quad (17)$$

$$C_2 = \frac{116.19}{\cos 80.33055} = 691.7781\ \text{m/s}$$

Change in the temperature at inlet of turbine rotor,

$$T_{02} - T_2 = \frac{{C_2}^2}{2C_p} \quad (18)$$

$$T_2 = 991.93\ \text{K}$$

$$T_2 - T_2' = \lambda n \frac{{C_2}^2}{2Cp} \quad (19)$$

$$T_2' = 991.93 - 0.05\frac{691.7781^2}{2Cp}$$

$$T_2' = 981.528329$$

$$\frac{P_{01}}{P_2} = \left(\frac{T_{01}}{T_2'}\right)^{\gamma/(\gamma-1)} \quad (20)$$

$$\frac{19.8597}{P_2} = \left(\frac{1200}{981.5283}\right)^{1.4/(1.4-1)}$$

$$P_2 = 9.82\ \text{bar}$$

$$\rho_2 = \frac{P_2}{R \times T_2} \quad (21)$$

$$\rho_2 = \frac{9.82\times10^2}{0.296\times991.93}$$

$$\rho_2 = 3.3475\ \text{Kg/m}^3$$

$$A_2 = \frac{m}{\rho_2\times C_{a2}} \quad (22)$$

$$\frac{60}{3.3475\times116.19} = 0.154256694\ \text{m}^2$$

$$A_{2n} = \frac{m}{\rho_2\times C_2} \quad (23)$$

$$\frac{60}{3.3475\times691.778} = 0.025909537\ \text{m}^2$$

$$C_{a1} = C_1 = C_3 = \frac{C_{a3}}{\cos\alpha_3} \quad (24)$$

$$C_{a1} = C_1 = C_3 = 612.577\ \text{m/s} \quad (25)$$

Temperature equivalent of the inlet and outlet kinetic energy is given by

$$\frac{{C_1}^2}{2\times C_p} = 163.1525\ \text{J} \quad (26)$$

$$T_1 = T_{01} - \frac{{C_1}^2}{2\times C_p} \quad (27)$$

$$T_1 = 1036.8474\ \text{K}$$

$$\frac{P_1}{P_{01}} = \left(\frac{T_1}{T_{01}}\right)^{\gamma/(\gamma-1)} \quad (28)$$

$$P_1 = 12.15106\ \text{bar}$$

$$\rho_1 = 3.9592\ \text{kg/m}^3$$

$$A_1 = 0.02473\ \text{m}^2$$

Here,

$$T_{03} = T_4 = \text{Exittemperature}$$

$$T_3 = T_{03} - \left(\frac{{C_3}^2}{2c_p}\right) \quad (29)$$

$$T_3 = 681.982\ \text{K}$$

$$P_3 = 6.60211\ \text{bar}$$

$$\rho_3 = 3.2705262\ \text{kg/m}^3$$

$$A_3 = 0.157888733\ \text{m}^2$$

Since, $U_m = 2\pi N r_m$ (30)

$$r_m = 0.37004\ \text{m}$$

Circumferential velocity of turbine, will be calculate as follows

$U_m = 2\pi N r_m$ (31)

$U_m = 2 \times \pi \times 250 \times 0.37004 = 580.9683$ m/s

$A = 2\pi N r_m h = \left(\frac{U_m h}{N}\right)$ (32)

$h = \left(\frac{NA}{U_m}\right)$ (33)

Aspect ratio mostly taken as 3 [39] to reduce the secondary losses according to this value cord length is calculated as,

$c = \frac{0.066379+0.067942}{2\times3} = 0.022387\text{m}$ (34)

Pitch distance (s) from calculated value of cord length, will be:

$s = 0.018581$ (35)

$\text{Number of blades} = \frac{2\times\pi\times r_m}{s} = 125.0665$ (36)

Angles calculation,

$r_t = r_m + \frac{h}{2}$

$r_r = r_m - \frac{h}{2}$

Table 3.5 Root, tip radii list at different planes

Sections	**2**	**3**
r_t	0.403233102	0.404015
r_r	0.336853972	0.336073

Ratio of radiuses to compare the annulus area at various sections are given in table 3.5

Table 3.6 Calculated areas and height at particular sections

Stations	**1**	**2**	**3**
A	0.024739032	0.154257	0.157889
h	0.010645602	0.066379	0.067942
r_t / r_r	1.029188366	1.197056	1.202165

$$\tan\alpha_2 = \left(\frac{r_m}{r}\right) \times \tan\alpha_{2m} \quad (37)$$

$$\tan\alpha_{2t} = 0.917691369 \times \tan 80.33055007 = 5.386$$

$$\alpha_2 = \tan^{-1}(5.386) = 79.481$$

$$\tan\beta_{2t} = \tan\alpha_2 - \left(\left(\frac{r_t}{r_m}\right) \times \frac{U_m}{C_{a2}}\right) \quad (38)$$

$$\tan\beta_{2t} = \tan 79.48187 - \left(\left(\frac{0.403233}{0.37004}\right) \times \frac{580.9683}{116.19}\right) \quad (39)$$

$$\tan\beta_{2t} = -0.0624491$$

$$\beta_{2t} = -3.57343^\circ$$

Gas angles calculation at plane 3 for tip section are calculated as

$$\tan\alpha_3 = \left(\frac{r_m}{r}\right) \times \tan\alpha_{3m} \quad (40)$$

Also, $\tan\alpha_{3t} = 0.915916 \times \tan 10 = 0.161500702$

$$\alpha_{3t} = 9.17409^\circ$$

Table 3.7 Radii ratios at respective planes

Section	2	3
r_m / r_r	1.098528049	1.101082
r_m / r_t	0.917691369	0.915916
r_r / r_m	0.910309027	0.908197
r_t / r_m	1.089690973	1.091803

Table 3.8 Angles for three sections of blade (tip, mean and root)

Angles	α_2	β_2	α_3	β_3
Mean	80.33055007	40.99331	10	79.06589
Tip	79.48187096	-3.57343	9.174098	79.91152
Root	81.18353436	62.18924	10.98731	78.07509

3.1.2 BLADE PROFILE (For pressure ratio 20)

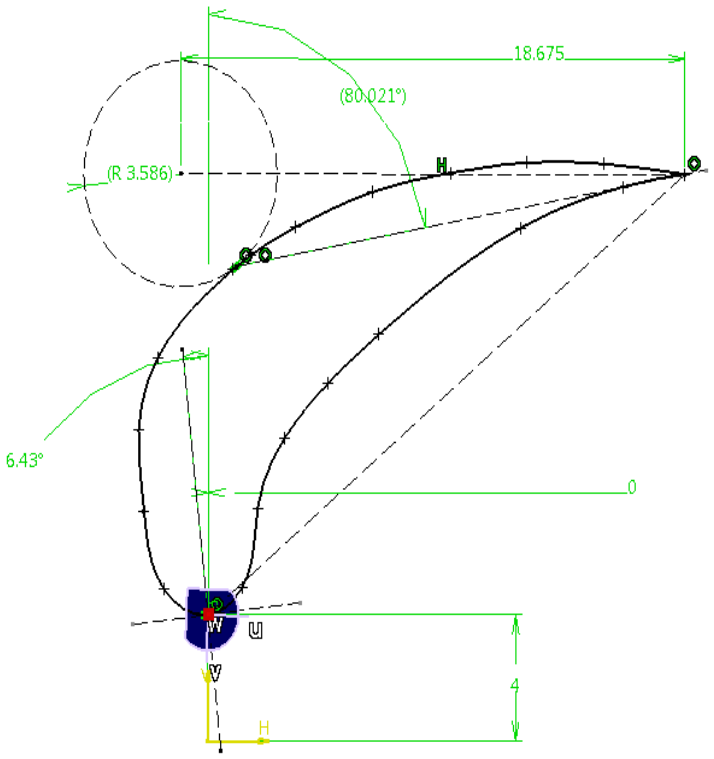

Fig. 3.2 Airfoil section with angle of orientation for mean surface

The blade profile will reduce the losses due to aerodynamic shapes. Stream-lined flow is possible from air-foils only. The above airfoil mostly used for gas turbine engine namely T-6 is shown in fig. 3.2 and its coordinates are listed below. These coordinates are feed in the form of ".xls" file to orient airfoil in particular blade angle which has already been calculated and listed in table 3.9.

Table.3.9 Co-ordinates of Airfoil section

File Edit Format View Help

20 2			
2.600000	0.000000	-17.30000	0.0000
5.850000	0.000000	-21.50000	0.0000
10.00000	0.000000	-25.00000	0.0000
14.80000	0.000000	-26.60000	0.0000
22.90000	0.000000	-25.30000	0.0000
28.00000	0.000000	-23.00000	0.0000
33.40000	0.000000	-19.50000	0.0000
38.00000	0.000000	-15.30000	0.0000
42.00000	0.000000	-10.90000	0.0000
45.40000	0.000000	-6.000000	0.0000
6.180000	0.000000	-12.40000	0.0000
11.20000	0.000000	-14.50000	0.0000
16.18000	0.000000	-15.50000	0.0000
21.10000	0.000000	-14.90000	0.0000
26.00000	0.000000	-13.60000	0.0000
38.20000	0.000000	-8.770000	0.0000
45.00000	0.000000	-3.950000	0.0000
3.200000	0.000000	-13.50000	0.0000
48.50000	0.000000	-0.5000000	0.0000
24.50000	0.000000	-24.72230	0.0000

So, there are three sections of blade i.e. the mean, the tip and the root. For each section the incident angle will vary after fixing the angle of each airfoil. It can be projected on particular surface of hub, mean and tip. Splitting of surface is next surface; multi-section in surfacing workbench module, “CATIA V5” module will be used for this purpose.

3.1.3 Sections of turbine blades by CATIA V5 module

The number of blades calculated is 125 for first design circular pattern. Keeping only consecutive blade geometry other geometries can be hidden. From table 3.7, radii at section plane 2 and 3 have been plotted and after doing multi-section operation in CATIA, the hub, tip and mean surface have been found. Next step is required to project airfoil sections at particular angles as shown in fig. 3.3, airfoil which is already plotted.

Multi-section is the next step to get smooth surface of blade then blade is having complete surrounding surface only need to close it from upper and bottom surface i.e. hub surface and tip surface.

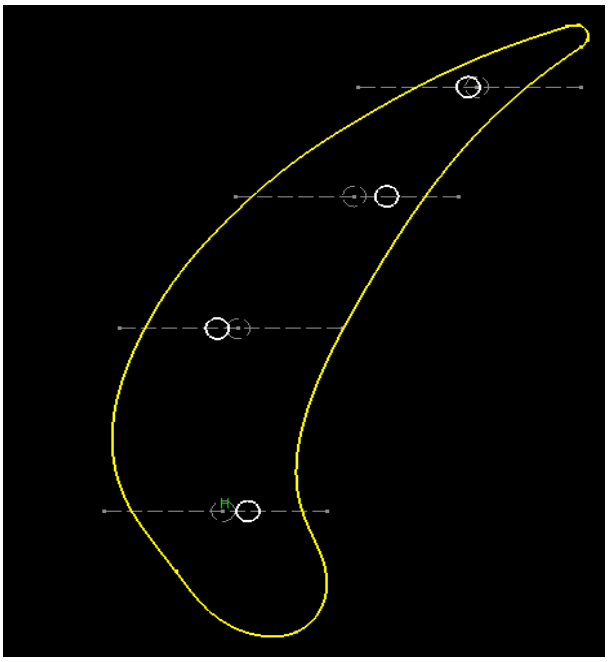

Fig. 3.3 Location of holes for standard design and zigzag design

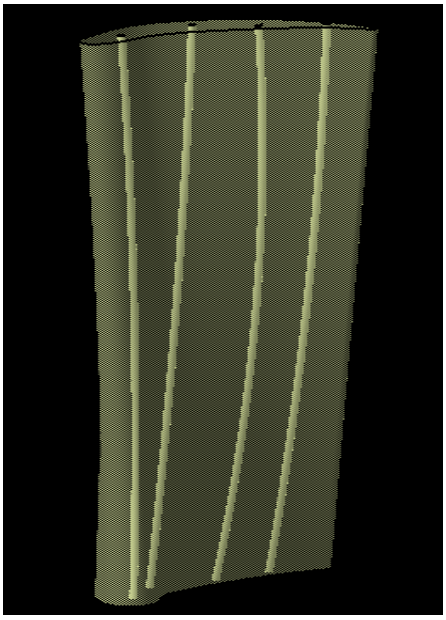

Fig. 3.4 Inner view of multi-sectioned tube

For internal cooling system, design should be calculated and visualized by keeping mechanical strength of blade. The strength of the material, leading edge is subjected to high initial temperature blade cooling holes passage are shown in figure 3.4. Four (4) numbers of holes have been assumed enough to transfer the heat efficiently and it is retaining mechanical strength of the blade [22, 25, 32 and 37].

The thermal design, including durability assessment, of the turbine vanes is based on the combustor exit temperature profile. This profile represents a typical worst case situation at hot spot locations, showing a nearly flat radial profile with a maximum temperature of 1888^0K. The blade internal geometry is cooled through convection, while external surfaces are locally film cooled from the leading edge shower head holes and tip pressure side holes. There are no film cooling holes on either the pressure or suction surfaces of the airfoil.

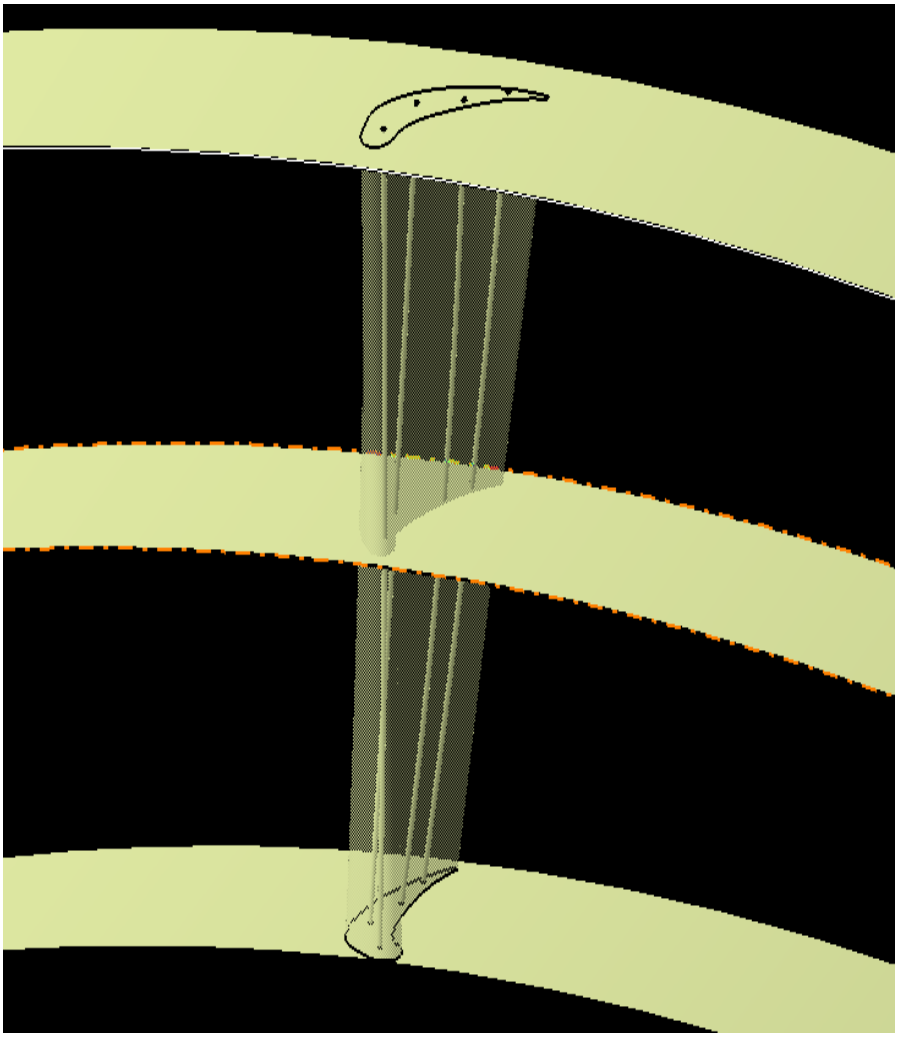

Fig. 3.5 Core engine inlet flow

The total cooling air requirement is 2.75% of the core engine inlet flow. Secondary air stream flow is supplied from bottom holes dimensions found as 0.601 mm and for zigzag the eccentricity given is 10% of total horizontal distance of line on same plane and center of cooling hole with mass flow rate as mentioned above 2.75 % of main stream flow with pressure

16,61,646 Pa and temperature 829^0C. Diameter intentionally kept small otherwise secondary loss will be high and it may cause flow separation. So, the design of diameter as internal surface contact region has been chosen. Figure 3.5 shows the core engine inlet flow developed in CATIA software.

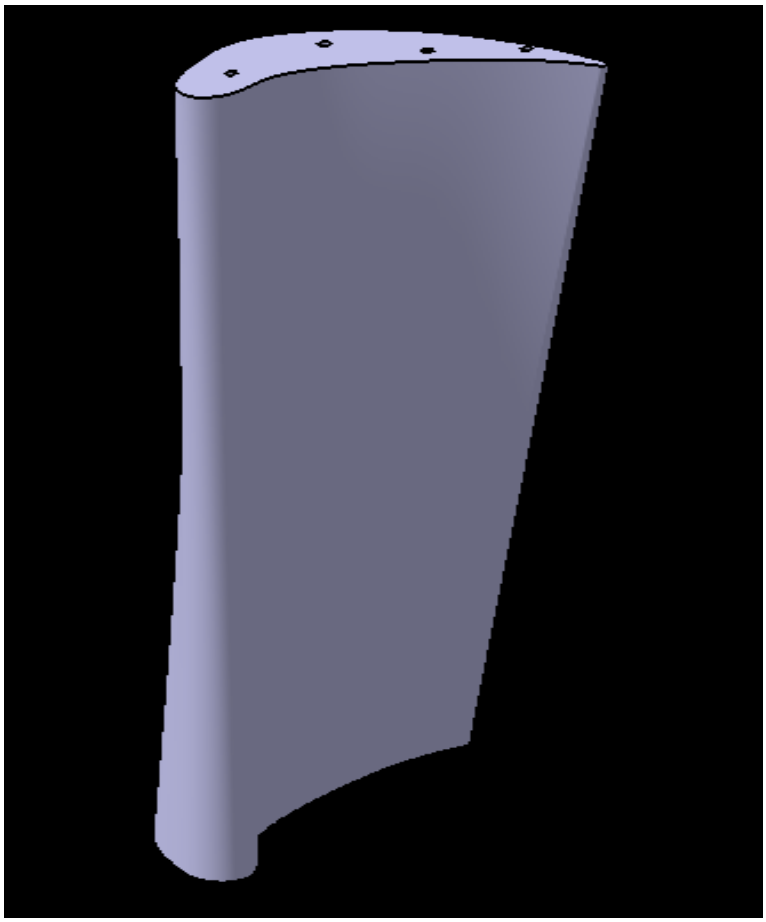

Fig. 3.6 Solid blade with cooling holes

After getting closed surfaces extraction of periodic volume because simulation of entire 125 blades is impossible with that much data. Therefore, alternative is of periodic volume extract the fluid domain and simulate it with per component boundary conditions and extrapolate results for whole stage. The figure 3.7 represents the periodic volume, which is one of the difficult task to do and a brief procedure to extract periodic fluid volume is presented. First an offset surface of consecutive blades has been shown in three blades projection. Those offset surface should be exactly at the middle of consecutive two blades some times because of angle of twist it won't be

possible at that time. One should offset edges of profiles at each plane those are root, mean, tip and then go with multi-section operation likewise from other side also by following same procedure. Now extrude the surface to get inlet and outlet domains close those surfaces by cylindrical surface which is created for airfoil profile projection. Make ‘joint’ operation by selecting all surfaces from fluid domain body and make closed solid body as shown in figure 3.7.

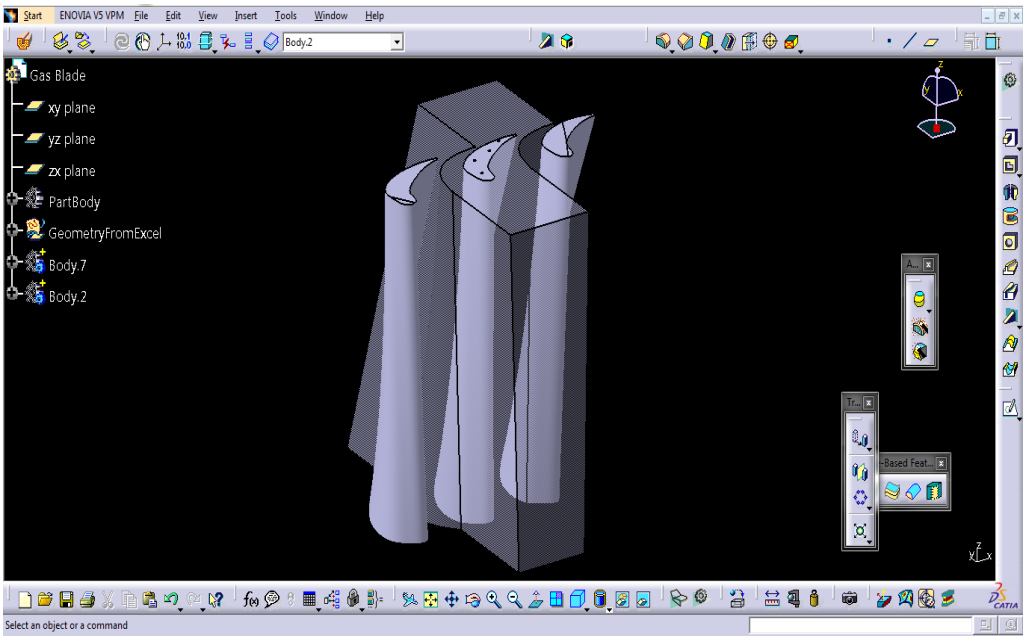

Fig. 3.7 Extracted periodic fluid volume

Tip clearance taken for the simulation is 1.28% of the height of the blade in this reference they tested various blade tip clearances for low compression pressure ratio turbine by experiment and CFD simulations, so the prescribed tip clearance can be taken and shown in figure 3.8.

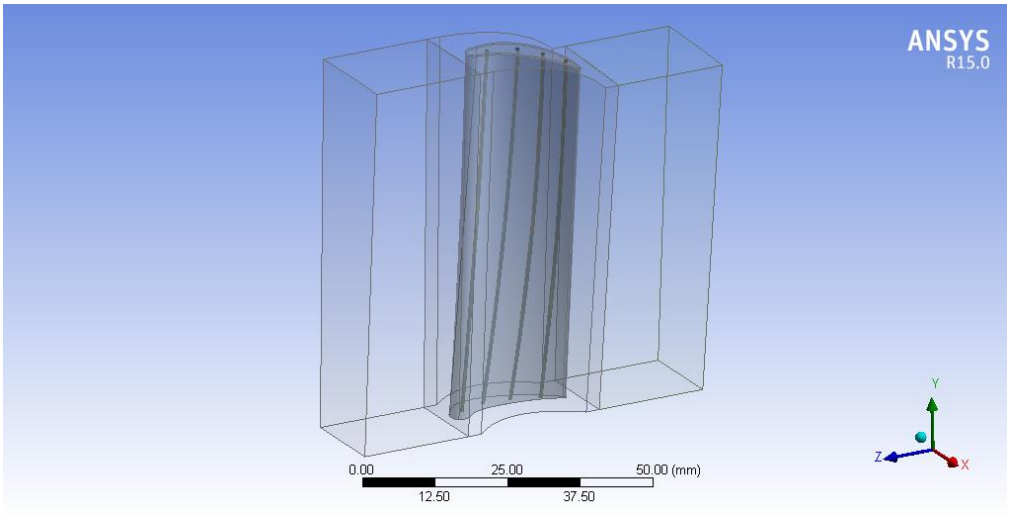

Fig. 3.8 Fluid domain with tip clearence

3.2.1 DESIGN FOR PRESSURE RATIO 30

The same procedure has been followed for the calculations of various parameters for blade design. The pressure ratio has been increased up to 30 by keeping rest of the parameters same.

Table 3.10 Given Input data and Assumed data [72]

Parameters	Values
Pressure Ratio	30
Turbine Inlet Temperature (K)	1200
Compressor Inlet Pressure (bar)	1.01325
Compressor Inlet temperature(K) T01	300
Specific heat for air (Cpa)	1.005
Specific Heat for gas (Cpg)	1.15
Ambient Pressure (bar)	1.01
R	0.296
γ	1.4
λ	0.05
Air Mass Flow Rate(Kg/s)	60
Axial Inlet Velocity (m/s)	175
ϕ	0.2

Calculation for Gas Engine Compressor which is required for some input parameters of Turbine Blade calculation.

$C_1 = C_{\alpha 1} = 175\ m/s$

$T_1 = T_{01} - \left(\frac{V^2}{2C_p}\right) = 300 - \left(\frac{175\times175}{2\times1.005\times1000}\right) = 284.76\ K$

T_1= 284.76 K

$$\frac{P_1}{P_{01}} = \left(\frac{T_1}{T_{01}}\right)^{\frac{\gamma}{\gamma-1}} \quad (41)$$

P_1= 0.841575491 bar

$$\rho_1 = \frac{100\times P_1}{R\times T_1} \quad (42)$$

$\rho_1 = \frac{100\times0.841575491}{R\times284.76}$

$\rho_1 = 1.029737629\ Kg/m^3$

$$r_t{}^2 = \left(\frac{m}{(\pi\times\rho\times C_{\alpha1}\times)[1-(r_r/r_t)^2]}\right) \quad (43)$$

Using interpolation method

$$Y = Y1 + \frac{(X+X1)(Y2-Y1)}{X2-X1} \quad (44)$$

$r_t = 0.41372\ m$

Table 3.11 revolution per second (angular velocity) chosen according to radii ratio

r_r/r_t	r_t (m)	N (rev/s)
0.4	0.2137	260.6
0.45	0.2194	253.9
0.5	0.2262	249.3
0.55	0.2346	237.5
0.6	0.2449	227.5

r_r/r_t has been chosen as 0.5 from table 3.9 for N= 250 rev/s

$$U_t = 2\pi \times r_t \times N \quad (45)$$

$U_t = 649.5423649\ m/s$

Calculation for Gas Turbine Blade is given by

$$T_2 = T_1 \left(\frac{P_2}{P_1}\right)^{\frac{\gamma-1}{\gamma}} \quad (46)$$

$T_2 = 792.78$ K

Pressure after compression = 30.3975 bar, P_3 = 29.7896 bar (compressor efficiency assumed to be 98%)

$$C_{pa}(T_2 - T_1) = C_{pg}(T_3 - T_4) \quad (47)$$

$T_4 = 769.3480039$ K

$$P_4 = \frac{P_3 \times T_4}{T_3} \quad (48)$$

Pressure at exit of turbine = 19.09877569 bar

Temperature coefficient is given by;

$$\psi = \frac{2 \times C_{pg} \times \Delta T}{U^2} \quad (49)$$

Change in temperature ΔT will be 354.8646 K

$\psi = 2.347682357$

If the rotational speed, which is assumed to be fixed by the compressor, had led to an ill-proportioned annulus, it would be necessary to rework this preliminary design. E.g. r_t/r_r could be increased by decreasing the axial velocity, i.e. by using a lower value of the flow coefficient ϕ. This would also decrease the nozzle efflux velocity, but it has been found that it was comfortably subsonic and so can be decreased if necessary.

Swirl increases the losses in the jet pipe; swirl is governed by angle $\alpha_3 = 0$.

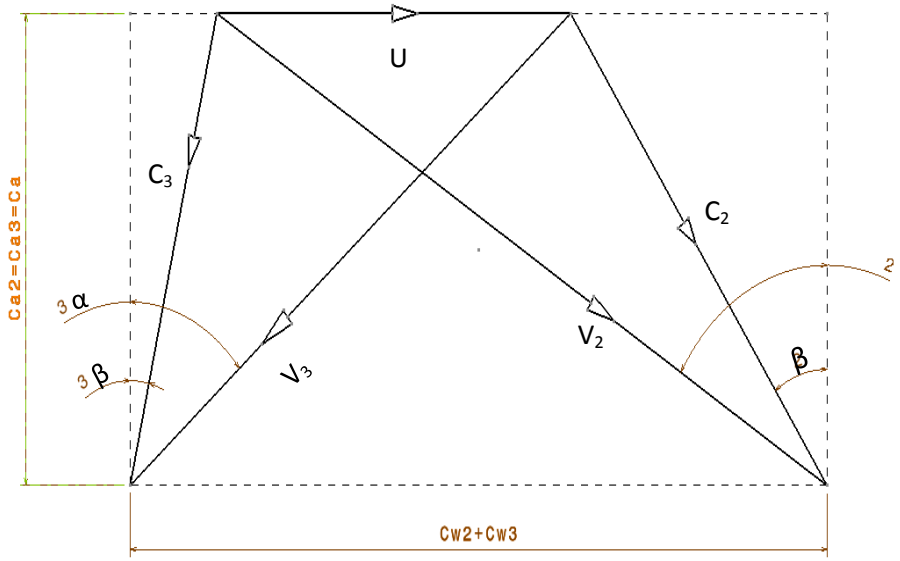

Fig. 3.9 Velocity Triangle for pressure ratio 30

$$\tan\alpha_3 = 0 = \tan\beta_3 - \frac{1}{\emptyset} \quad (50)$$

$$\tan\beta 3 = \frac{1}{2\emptyset}\left(\frac{1}{2}\psi + 2\Lambda\right) \quad (51)$$

$\Lambda = 0.413079411$

Including three-dimensional effects, the reaction increases from root to tip of the blades, and a degree of reaction of only 0·413 at the mean diameter might mean too small value at the root. Negative values must certainly be avoided because this would imply expansion in the nozzles followed by recompression in the rotor and the losses would be large. Perhaps, a modest amount of swirl will bring the reaction to a more reasonable value with $\alpha_3 = 10$. With this assumption, the value of other angles can be calculated at mean section as follows;

$$\tan\alpha_3 = 0.1763 = \tan\beta_3 - \frac{1}{\emptyset} \quad (57)$$

$\tan\alpha_3 = 0.1763$, $\alpha_3 = 10$, $\tan\beta_3 = 5.176326981$, $\beta_3 = 79.06559$, $\Lambda = 0.4483448$

$$\tan\beta_2 = \frac{1}{2\emptyset}\left(\frac{1}{2}\psi + 2\Lambda\right) \quad (58)$$

$\tan\beta_2 = 0.692878911$, $\beta_2 = 34.71727202$

$\tan\alpha_2 = 5.69287$, $\alpha_2 = 80.03717$

$$C_{a2} = U \times \emptyset \quad (59)$$

$C_{a2} = 649.5423 \times 0.2 = 129.908473$ m/s

$$C_2 = \frac{C_{a2}}{\cos\alpha_2} \quad (60)$$

$$C_2 = \frac{129.9084}{\cos 80.03717} = 750.8762 \text{ m/s}$$

Change in the temperature at inlet of turbine rotor,

$$T_{02} - T_2 = \frac{{C_2}^2}{2C_p} \quad (61)$$

$T_2 = 954.86$ K

$$T_2 - T_2' = \lambda n \frac{{C2}^2}{2Cp} \quad (62)$$

$$T_2' = 954.86 - 0.05\frac{750.8762^2}{2Cp} \quad (63)$$

$T_2' = 942.6061244$

$$\frac{P_{01}}{P_2} = \left(\frac{T_{01}}{T_2'}\right)^{\gamma/(\gamma-1)} \quad (64)$$

$$\frac{29.7896}{P_2} = \left(\frac{1200}{942.6061244}\right)^{1.4/(1.4-1)}$$

$P_2 = 12.796$ bar

$$\rho_2 = \frac{P_2}{R \times T_2} \quad (65)$$

$$\rho_2 = \frac{12.79 \times 10^2}{0.296 \times 954.86} = 4.527 \text{ kg/m}^3$$

$$A_2 = \frac{m}{\rho_2 \times C_{a2}} = \frac{75}{4.527 \times 129.90} = 0.127517876 \text{ m}^2 \quad (66)$$

$$A_{2n} = \frac{m}{\rho_2 \times C_2} = \frac{75}{4.527 \times 750.8762} = 0.022061761 \text{ m}^2 \quad (67)$$

$$C_{a1} = C_1 = C_3 = \frac{C_{a3}}{\cos \alpha_3} \quad (68)$$

$C_{a1} = C_1 = C_3 = 684.8821$ m/s

Temperature equivalent of the inlet (and outlet) kinetic energy is given by,

$$\frac{{C_1}^2}{2 \times C_p} = 203.940 \text{ J} \quad (69)$$

$$T_1 = T_{01} - \frac{C1^2}{2 \times C_p} \quad (70)$$

$T_1 = 996.0593$ K

$$\frac{P_1}{P_{01}} = \left(\frac{T_1}{T_{01}}\right)^{\gamma/(\gamma-1)} \quad (71)$$

$P_1 = 15.8380$ bar

$\rho_1 = 5.37186$ Kg/m^3

$A_1 = 0.0203854$ m^2

$T_{03} = T_4 =$ Exit temperature

$$T_3 = T_{03} - \left(\frac{{C_3}^2}{2c_p}\right) \quad (72)$$

$T_3 = 565.407$ K

$P_3 = 6.4989124$ bar

$\rho_3 = 3.8831800$ Kg/m^3

$A_3 = 0.148674422$ m^2

Centrifugal velocity of turbine is given by;

$$U_t = 2\pi N r_m \quad (73)$$

$$r_m = \frac{U_t}{2\pi N} = \frac{649.5423}{2 \times \pi \times 250} = 0.4137212 \text{ m}$$

$$A = 2\pi N r_m h = \left(\frac{U_m h}{N}\right) \quad (74)$$

$$h = \left(\frac{NA}{U_t}\right) \quad (75)$$

Table 3.12 Calculated areas and height at particular sections

Stations	**1**	**2**	**3**
A	0.020385464	0.127518	0.148674
h	0.007846087	0.04908	0.057223
rt/rr	1.019146222	1.126111	1.148588

Aspect ratio has been taken as 3 to reduce the secondary losses [39]. According to this number, cord length is

$$c = \frac{0.04908+0.057223}{2\times3} = 0.017717\text{m}$$

Pitch distance s from calculated value of cord length, $s = 0.01470$

$$\text{Number of blades} = \frac{2\times\pi\times r_m}{s} = 176.683$$

Angles calculation,

$$r_t = r_m + \frac{h}{2} \quad \text{and} \quad r_r = r_m - \frac{h}{2}$$

Table 3.13 root, tip radii list at respective planes

Section	**2**	**3**
r_t	0.438261197	0.442333
r_r	0.389181306	0.38511

Gas angles calculation at plane 2 for tip section is given by,

$$\tan\alpha_2 = \left(\frac{r_m}{r}\right) \times \tan\alpha_{2m} \quad (76)$$

$$\tan\alpha_{2t} = 0.917691369 \times \tan 80.33055007 = 5.386$$

$$\alpha_{2t} = \tan^{-1}(5.386) = 79.481^{\circ}$$

Table 3.14 Radii ratios at respective planes

Section	2	3
r_m / r_r	1.063055305	1.074294
r_m / r_t	0.944006118	0.935317
r_r / r_m	0.940684831	0.930844
r_t / r_m	1.059315169	1.069156

$$\tan\beta_{2t} = \tan\alpha_2 - \left(\left(\frac{r_t}{r_m}\right) \times \frac{U_m}{C_{a2}}\right) \quad (77)$$

$$\tan\beta_{2t} = \tan 79.48187 - \left(\left(\frac{0.403233}{0.37004}\right) \times \frac{580.9683}{116.19}\right)$$

$$\tan\beta_{2t} = -0.0624491$$

$$\beta_{2t} = -3.57343^\circ$$

Gas angles calculation at plane 3 for tip section:

$$\tan\alpha_3 = \left(\frac{r_m}{r}\right) \times \tan\alpha_{3m} \quad (78)$$

$$\tan\alpha_{3t} = 0.915916 \times \tan 10 = 0.161500702$$

$$\alpha_{3t} = 9.17409^\circ$$

Similarly, the values of all the angles for root section also calculated and found as follows.

α_2 = 80.61729236

β_2 = 53.43907

α_3 = 10.72628

β_3 = 78.33484

Table 3.13 shows all the angles of the different section of blade calculated in the above article.

Table 3.15 angles for three sections of blade (tip, mean and root)

Blade Angles	α_2	β_2	α_3	β_3
Mean	80.03717554	34.71727	10	79.06589
Tip	79.45911484	4.433654	9.365014	79.71474
Root	80.61729236	53.43907	10.72628	78.33484

3.2.1BLADE PROFILE (For pressure ratio 30)

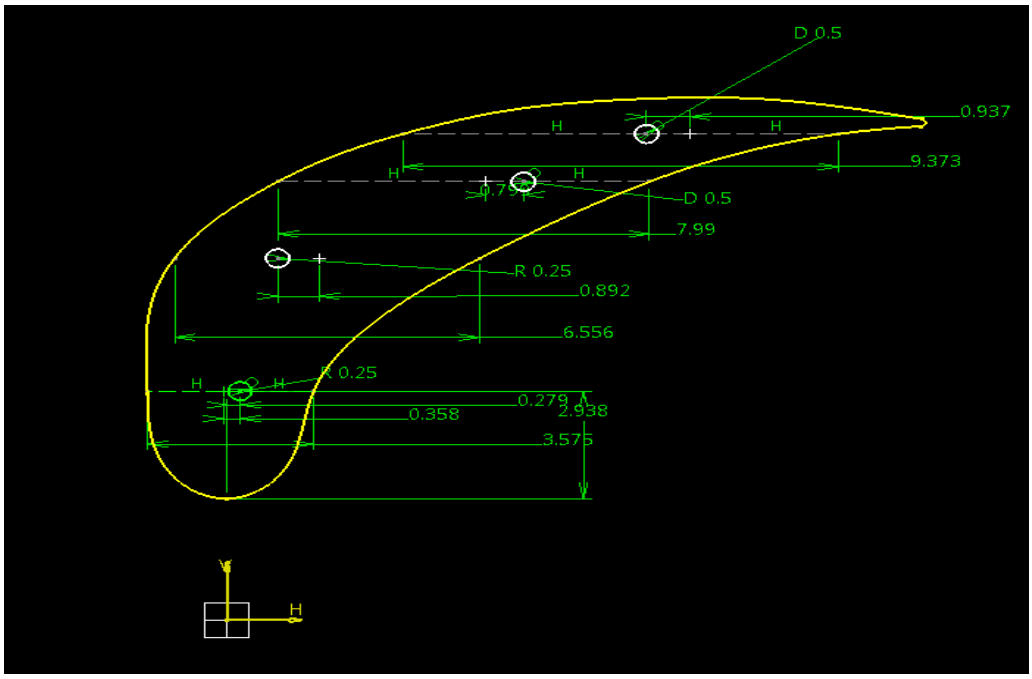

Fig. 3.10 Airfoil section with angle of orientation for mean surface

The same procedures have been followed for the development of airfoil section of the blade with angle orientation as discussed in previous article. The developed blade profile for the current work is shown in the figure 3.12.

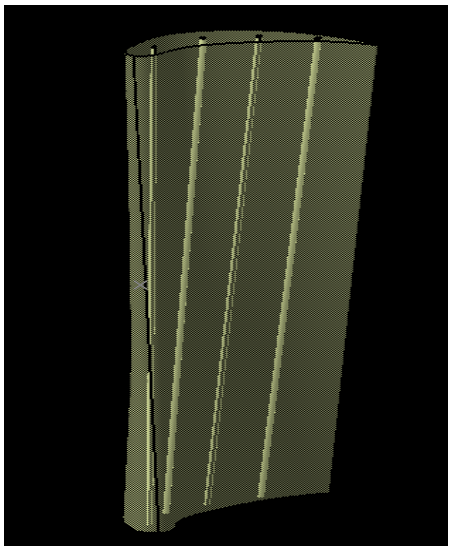

Figure 3.11 Inner view of multi-sectioned tube developed in CATIA

For internal cooling system design should be calculated and visualized by keeping mechanical strength of blade in view. Strength of the material should not be changed. The leading edge is subjected to high initial temperature so in volume of blade cooling holes are distributed as shown in fig. 3.14. Four (4) numbers of holes assumed for transfer of heat efficiently from previous work and it is retaining mechanical strength of the blade as well [23, 38].

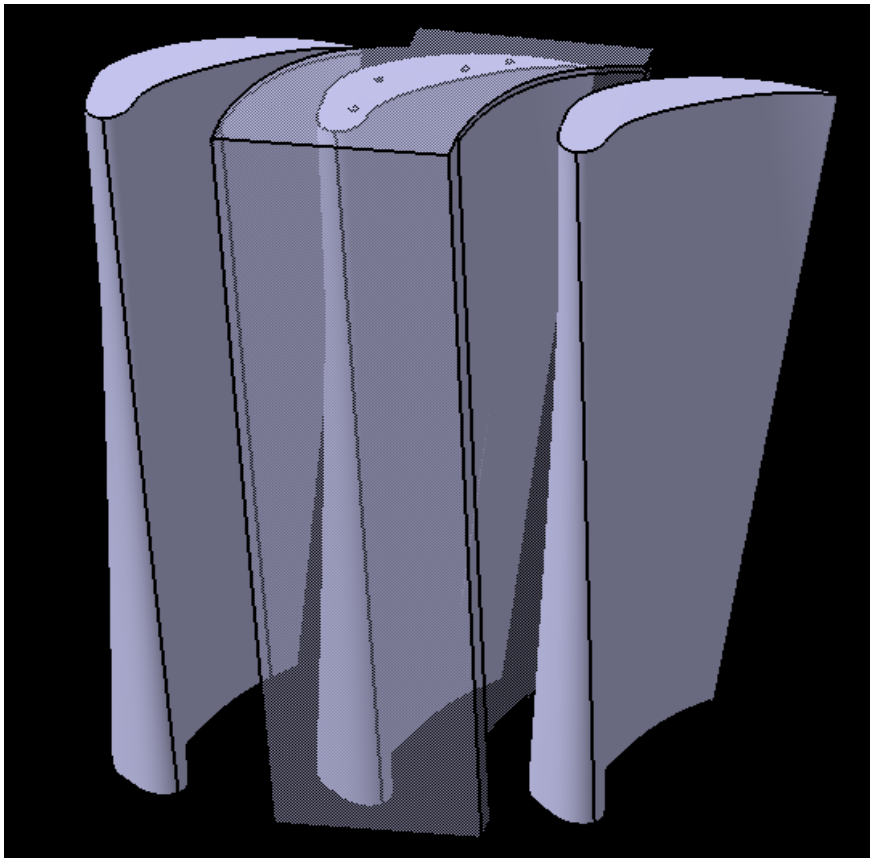

Fig. 3.12 Extracted periodic fluid volume

Tip clearance taken for the simulation is 1.28% of the height of the blade. In this reference, various blade tip clearances for low compression pressure ratio turbine by experiment and CFD simulations is tested, so the prescribed tip clearance can be considered. Similarly, the design of blade cooling is analyzed for temperature at the inlet of turbine 1200 K and 1400 K.

3.3 CFD Simulation and ANSYS Analysis

CFD is one of the branches of fluid mechanics that uses numerical methods and mathematical algorithms to solve and analyze problems that involve fluid flows. Computers are used to perform the millions of calculations required to stimulate the interactions of fluids with complex surfaces used in the engineering [18].

3.3.1 Need for CFD analysis

CFD is used in a vast number of fields automotive, aerospace, chemical, electrical, pharmaceutical, and biomedical. Biomedical most of the research is based on the process of working of the diseases, other things are easily it can be visualize, but still it can't replace experimental methods of determination.

CFD is now being used in:

- ✓ **Lift and drag of aircraft:** CFD is used in conjunction with wind tunnel tests to determine the performance of various configurations.
- ✓ **Flows over missiles**: This, again, is an area where there is a need for lift, drag and side force data, so that simulations of performance can be made. As with aircraft, CFD and wind tunnel tests are used.
- ✓ **Flames in burners**: There is a need to understand the complex interactions between fluid flow and chemical reaction in flames. This can assist in the production of more efficient designs for burners in boilers, furnaces and other heating devices.
- ✓ **Air flow inside lungs:** lungs are tested as the porous region which draw the air from outside and transferred to branches of this elastic sac, this is important in case of diseases of lungs.
- ✓ Dispersion of pollutants into rivers and oceans.

From this list, it is clear that the applications can be extremely varied in nature. Despite this, the computer predictions of the different problems can be made with computer software and hardware that is not specific to a given problem. Now that these computer tools are widely available, CFD has been brought out of the research laboratory and is used by many more people. It can even be used in the engineering design process.

3.3.2 Analysis procedure

Following points describe the general approach for solving a flow problem by using any CFD software. [19] [26]

- ➢ Describing a flow problem in engineering

- Defining the geometry of the problem.
- Dividing the volume occupied by the fluid into discrete cells. The mesh may be uniform or non-uniform.
- Defining the boundary conditions. This involves specifying the fluid behavior and properties at the boundaries of the problem for the transient problems the initial conditions.
- Defining the physical modeling, for example the equations of motions + enthalpy + radiation + spices conservation.
- The simulation is started and the equations are solved iteratively as a study state or transient.
- Finally a post processor is used for the analysis and visualization of the resulting solution.

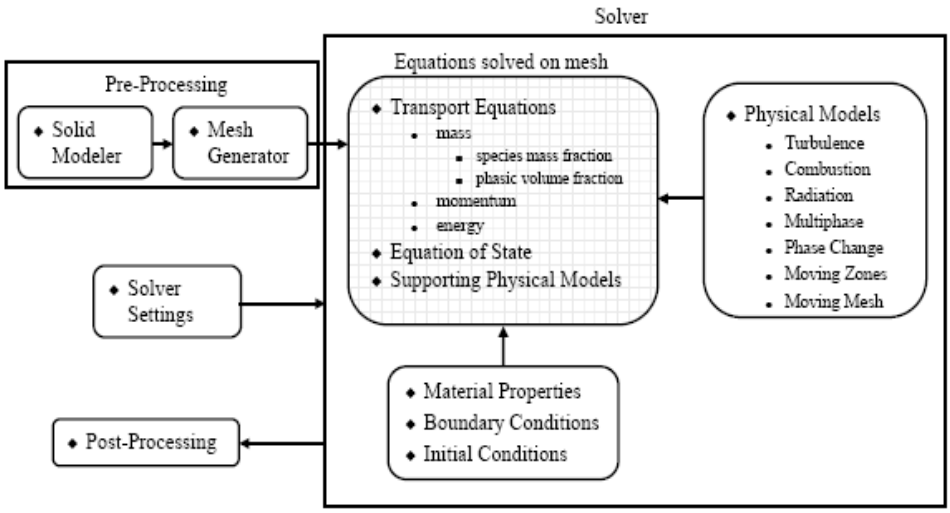

Fig. 3.13 Analysis procedure in CFD [11]

3.4 Describing the problem

Producing a computer simulation of a flow problem requires the analyst to provide a large amount of data to the solver program. It is the quality of this data, in terms of both suitability and accuracy that may well determine the quality of the results of the simulation. The key to a sound analysis is the production of a specification of the flow problem. This is a clear exposition of the reasons why the simulation is being carried out and of what the physical flow situation is. Once it has been produced it can be translated into the set of data that is required by the simulation package.

3.5 Producing a specification

A specification for a flow problem must be sufficiently detailed so that the analyst can obtain from it all the information necessary to define the flow problem to a CFD solver program. This

information comes from a good understanding of the flow problem which the analyst must obtain be talking with the people who require the results of the simulation. In particular the analyst must know three things:

- Why it is that the simulation is required.
- What the geometry of the problem is, in broad terms.
- What the possible flow behavior might be.

3.6 Defining the geometry

Once the problem specifications are determined, the actual specification can be made [19]. When looking at any flow problem it is important to be able to describe the physical boundaries that contain the fluid. This is particularly important for engineering flow problems where it is usual for at least some part of the boundary to be a man-made object and it is a prediction of the effect of this object on a flow that is required from a CFD analysis show the fig 3.16 imported periodic models.

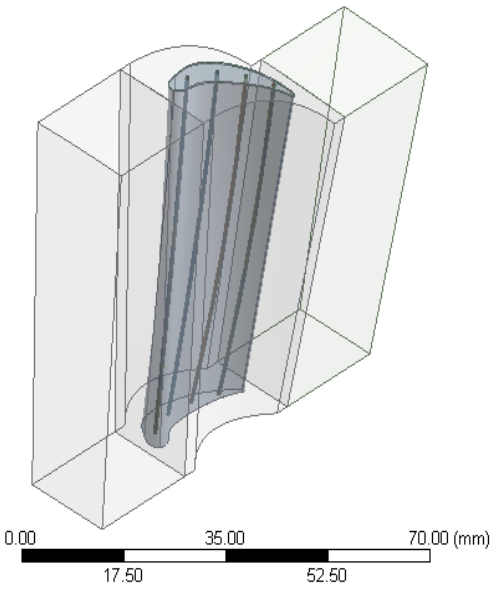

Fig. 3.14 Imported periodic model

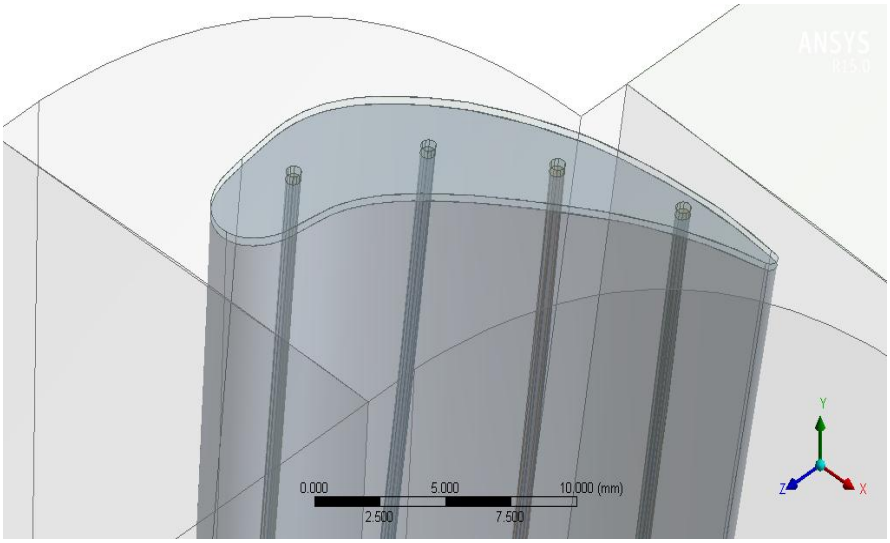

Fig. 3.15 Zoomed view showing tip clearance

From such sources most of the bounding surfaces of the flow domain may be determined precisely. During the specification stage it is sufficient to know roughly where these surfaces are in relation to each other and how they fit together. It is also worth remembering that when a computational model has been built, a complete description of the bounding surfaces is required, and that some of these surfaces might not be physical surfaces as shown in the figure 3.17.

3.7 Meshing

Meshing is the process of discretization of space in which flow takes place. Meshing is the basic step in building a computer model for a flow problem. Depending on the discretization technique used, meshing procedure varies. For finite difference method the values of the variables at the points are used to produce equations for the variables that enable a solution to be determined. This involves a grid of points. However, if we use the finite volume method then the points are arranged so that they can be grouped into a set of volumes and the partial differential equations can be solved by equating various flux terms through the faces of the volumes. Also, if we use the finite element method then the points are grouped to define elements within which the numerical analogue to the partial differential equations can be set up.

These are the basic parts from which meshes are built:

- Nodes, junction of edges of two elements.
- Elements, Control volumes, also known as cells in some documentation.

Which of these parts are needed for a mesh depends on the discretization method being used [21]. In all the discussion that follows terms like volume, cell and element will be used to mean a

sub-domain without implying that a particular discretization technique is being used. With CFD programs a much more restricted set of volumes or elements is available at present. By far the most common volume or element, for use in three-dimensional meshes, is a hexahedron with eight nodes, one at each corner and this is known as a brick element or volume. For two-dimensional applications the equivalent element is a four-nodded quadrilateral. Some finite volume programs have now been released which have the ability to use tetrahedral in three dimensions or triangles in two dimensions. Most finite element CFD codes will allow these elements to be used together with a small range of other element types.

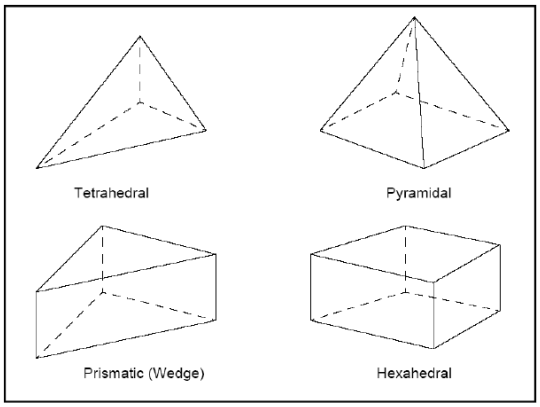

Fig. 3.16 Common sub-domains

The next consideration is regarding the structure of the mesh. This arrangement is known as the topology of the mesh. When using the finite difference method the nodes are the positions in space where the variables are calculated and they are arranged in what looks like a grid of cells. In contrast to this, when using the finite element method, the points are the nodes of the set of elements used to split up the fluid volume and the elements can be arranged in any way, providing that the faces of the elements are aligned correctly. The interaction between the elements takes place when the element equations are added together to form the global equations. With the finite volume method the actual implementation of the numerical solution will determine which scheme of volume placement can be used. Some programs demand that the volumes are placed in the same way as they would be for a grid of finite difference cells and others allow a finite element-like placement. There are two ways in which the mesh structure can be arranged. They are: a regular structure or topology, where the points of the mesh can be imagined as a grid of points placed in a regular way throughout cuboids. These points can then be stretched to fit a given geometry. Note that when the mesh is stretched the connections between the points do not change. Consequently, if any point is considered in the mesh it will be

connected to the same neighboring points both before and after the stretching process. Sometimes these meshes are called structured meshes as they have a well-defined structure or mapped meshes as they can be seen as a cuboids mesh that has been mapped onto some other geometry. When considering these meshes it is useful to think of a local coordinate system within the mesh. This is enables the orientation of the cells relative to each other to be determined, and so before the mesh is transformed the axes of this system are the edges of the cuboid. Once the transformation into the actual coordinate system is being used, the global coordinate system is carried out. The local coordinate system axes become dependent on the position within the mesh.

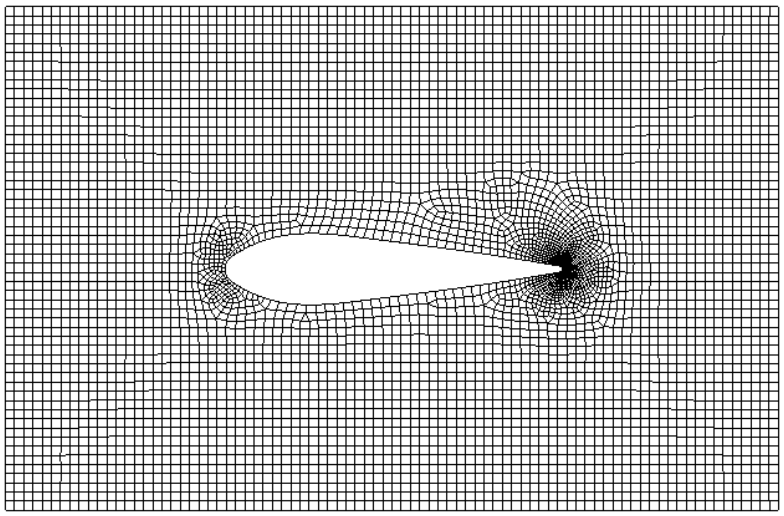

Fig. 3.17 Regular Mesh

An irregular structure or topology, where the points fill the space to be considered but are not connected with a regular topology. Figure 3.19 shows a two-dimensional example of this type of mesh formed with triangular elements. Note that the cell faces do not overlap. The fact that any particular node is attached to an element cannot be known from the form of the mesh, and so a numerical table must exist that describes the arrangement of the mesh by listing which nodes are attached to each element. This contrasts with the regularly structured mesh where knowledge of the location of a cell within the mesh enables the labels of the points at its corners to be found implicitly. A mesh with an irregular structure is often referred to as an unstructured mesh or a free mesh.

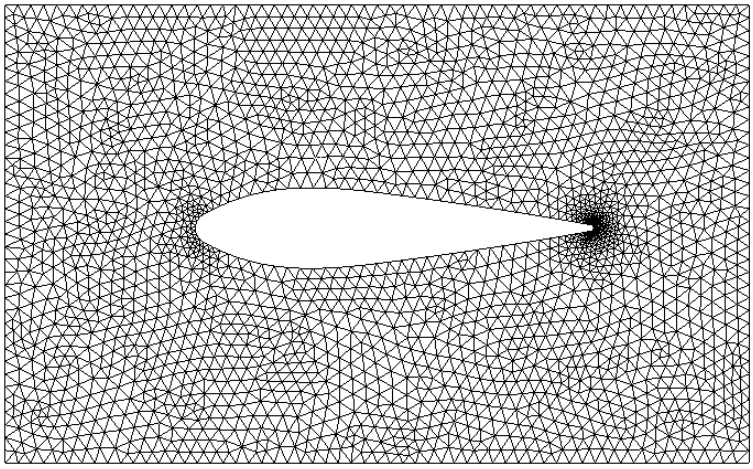

Fig. 3.18 An irregular Mesh

3.7.1 Defining boundary conditions

To calculate the required variables, the governing partial differential equations must be solved and so the boundary conditions for each equation must be specified. When the flow specification was produced the boundaries were defined in terms of the geometry of the flow domain, and now these boundaries have to be found in terms of the mesh that is being used. This involves defining the boundaries as a collection of cell or element faces.

Now the boundaries of the mesh in terms of cell faces are used. Few such entities can be grouped before their boundary conditions are determined.

3.7.2 Grouping Faces Together

If the boundary faces are grouped together into sets of faces, each set of faces can then be given an index that will allow the set to be related to a boundary condition. Sometimes, the boundary condition on a set of faces will be unique to that set, however, in some cases; the same boundary condition may well be applied to several sets of faces. In this latter case, each of the sets can be given the same index and then the index can be linked to the given boundary condition. Finally, it is useful to know that some CFD solvers will find all the cell faces on the boundary of the mesh. This list of faces can then be compared to the boundary faces that have been specified by the user. It is common for any unspecified boundary faces to be assumed to be solid walls. This can save a great deal of effort for the user if the mesh is for a flow problem such as a complex internal flow. These meshes can have multiply connected passages, the boundary faces of which

can be very difficult to view. By considering all unspecified faces to be solid walls, the user does not have to specify these faces and the saving in effort is large if this is done.

3.7.3 Boundary conditions

After the boundaries of the problem are defined and appropriate faces are grouped then the boundary conditions for all these groups must be defined. For each partial differential equation that has to be solved, the numerical method that is used determines which boundary conditions can be specified. Often, the software will predict a flow which has the derivatives of the velocity normal to a boundary calculated as zero if no other specification is made. Of course, if the analyst wishes, such conditions at the boundary can be changed by specifying the appropriate values.

Following are the boundary conditions used in CFD.

- **A solid wall with a turbulent flow over it:** To model this accurately requires many points through the boundary layer as the shear at a solid wall in a turbulent flow is much greater than that for a laminar flow. The computational effort required to do this can be reduced by assuming that the flow velocity varies in a logarithmic fashion through the boundary layer, as found in experiments. Then empirical approximations to the values for the velocity at points just away from the wall can be used. Similarly, the boundary conditions for the additional turbulence parameters, such as the turbulent kinetic energy and its rate of dissipation, can be set in an automatic way to some empirically-derived values.
- **A free surface:** Here, the fluid pressure is fixed but the fluid velocity and the shape of the boundary are not known. These surfaces occur, typically, when we model the surface of a liquid in contact with air, for example when calculating the flow around a ship. Special CFD programs can handle these boundaries, but if the surface shape does not have need to have the effects of waves modeled then we can use a symmetry plane as an approximate model of these boundaries.
- Moving walls, such as a piston in an internal combustion engine, where a solid surface moves in the flow.
- An inlet with a turbulent flow coming through it. Here the turbulence parameters are convicted into the fluid flow domain and the levels of the variables that are brought in must be specified.

3.7.4 Physical modeling

This part includes modeling of

- Governing equations

- Flow conditions
- Initial conditions

As already discussed, there are three governing equations for any flow problem, the continuity equation, the momentum equation and the energy equation. The first two equations are a must for any flow problem. The energy equation will be used only if there is any energy transfer involved in the problem.

Defining the flow conditions involves in determining those properties that will depend on the problem but not on the fluid that is flowing. Some examples of these additional properties are the thermal conductivity of a fluid which is needed if we are simulating heat transfer problems, or an effective turbulent viscosity which is needed for the simplest turbulence models, defining whether a flow is laminar, incompressible one or a turbulent incompressible one in case of solving problems involving turbulent flow of the fluid, the turbulence effects have to be modeled.

Many solution algorithms require that some form of initial flow field is specified for the solver. This could be due to the flow actually being time dependent, where the initial state of the variables is required to start the calculation, or it could be due to the CFD solution algorithm using a quasi-time-varying solution algorithm to calculate a steady state solution. Equally, the non-linearity of the problem will demand some initial guess for the variables which will have to be supplied either as a series of default values or by the user. Usually, the specification of the initial conditions is fairly straightforward. Sometimes the initial conditions are specified for groups of cells with a constant value of a variable being set within each group.

3.8 Solution

3.8.1 Iteration of solution

When using a CFD package the details of the numerical solution process will usually be hidden from the user. However, some features of the process are common to all packages and the controls that have to be used are often similar, even though the values of the control parameters may be algorithm- or problem specific or both. In particular, if we consider the non-linearity of the equations, this forces the solution process to be iterative, regardless iteration convergence of

whether the problem is time dependent or not. This means that an initial solution, normally a guessed solution, is required at the start of the solution process, and then the numerical equations are used to produce a more accurate approximation to the numerically correct solution, which is one in which all the variables satisfy the governing equations. This new approximation, the updated solution, is then used as the new starting solution and the process is repeated until the error in the solution is sufficiently small. Each repetition of the solution process is known as iteration. Sometimes during an iterative process the updated solution at the end of one iteration and be very different from the solution at the start of the iteration.

3.8.2 Residuals

Fortunately, the numerical equations that we wish to solve can also be used to find such a measure of error. These measures of error can be used to see if a solution process is converging, and they are known as residual errors or residuals. At the end of each iteration, the latest solution can be used to generate all the terms in the various partial differential equations. For example, if all the terms in the momentum equation, equation are placed on the left hand side of the equation and the individual components of the equation formed from the solution for the velocities and pressure, then these terms can be summed and the sum should be zero. As the solution is only an approximation to the required values of the variables, the sum will not be zero. It is this sum that is the residual error.

3.8.3 Running Solver and Troubleshooting

At the start of any analysis, the user should instruct the solver program to perform only a few iterations. This enables the user to perform convergence checks on the solution process by looking at the values of the residuals either on the screen or in a data file and seeing if they are reducing or increasing. After running something like ten iterations the initial trends in the residuals should be clear. If they are reducing the solution process is clearly converging and this is the desired situation, whereas if they are increasing further thought is required before the convergence properties of the solution can be determined. Some typical graph of the residual value for one of the flow equations plotted against iteration number are shown in following figure 3.21. However, if the residuals are still increasing after ten iterations then the differences in the residuals from iteration to iteration need to be examined. If the difference is increasing from iteration to iteration, the process is diverging, but if the differences are reducing then the process is probably converging.

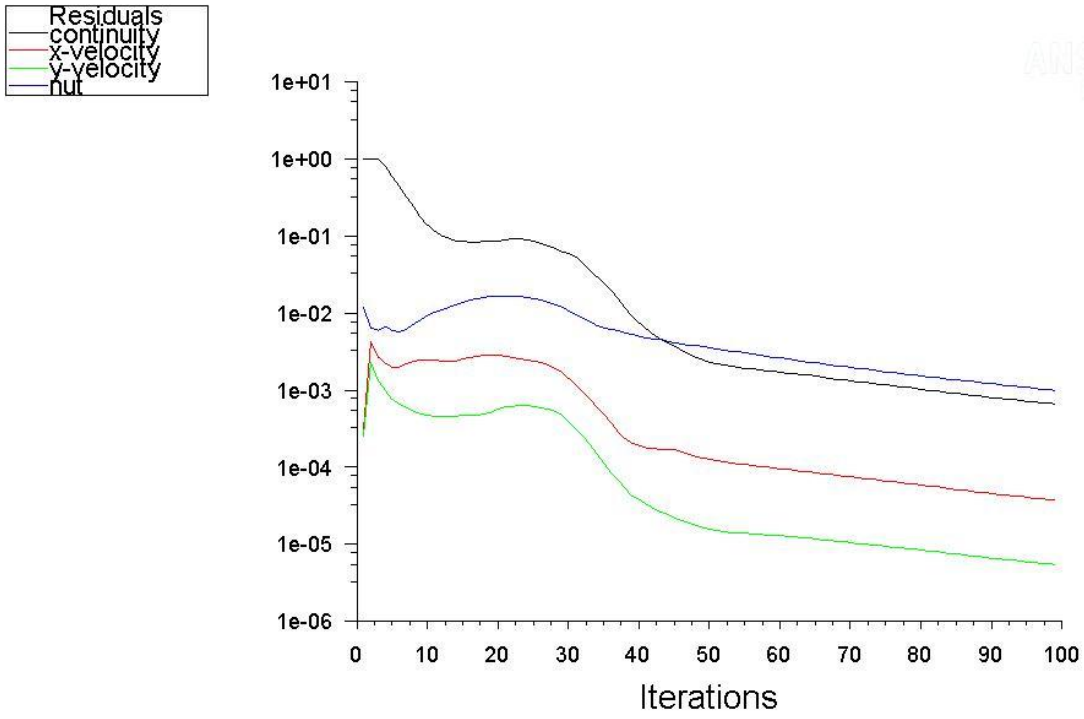

Fig. 3.19 Iterations solution [27]

If divergence occurs, then the first remedy is to check the meshing quality though mesh metric showing good quality of meshing it is possible one much skewed element will prevent solution from conversion next is computer model for obvious errors. This can be done by reading any of the input data that has been written by the solver program and by meticulously checking the data stored by the pre-processor. The computer model should reflect the original specification that was produced at the beginning of the analysis. If nothing obvious is found then the next step is to change the relaxation factors or the time step. If a converging solution is still not achieved, then it is probable that there is some sort of error in the problem statement, never blame standard codes.

3.9 Analyzing the results

When the numerical solution is obtained it is necessary to determine whether or not it bears some relationship to the physical reality. If it is likely that it does, then the required technical information can be extracted from the results. When the solver runs it produces a large amount of data that has to be analyzed. This analysis might be undertaken so that some cause of divergence in the solution process can be identified, so that the quality of the solution can be examined or so

that useful technical information can be extracted if it is a converged solution. First we must consider what information will actually be available to us when we want to analyze the results.

The type of information produced by the solver program can usually be controlled by the user but it often consists of:

- Values of the residual error for the various partial differential equations that have been solved. These are listed as a function of the iteration number or time step. These values give some idea as to whether the solution is progressing to a converged solution. This is usually stored as ASCII data so that it can easily be read later.
- Values of some of the variables at a limited number of locations, known as monitor locations, for every iteration or time step. This data also gives an indication of the progress of the solution towards a converged solution. For time-varying solutions it also gives a limited history of the development of the flow with time. Again this is usually ASCII data.
- A complete list of the flow variables at all the nodes of the domain or all the cells of the domain as appropriate for the way in which the solver works. These lists, also known as dumps of the data, are produced at the end of the solution process, but the solver can also be instructed to produce such a list at intermediate stages in the process. This might be necessary if the results at several discrete times are needed to describe a time-varying flow. This is normally binary data to reduce the storage space that is required, but ASCII forms can also be requested to make reading of the data easier, if the amount of data is small, or to allow a transfer between computers.
- Mesh data. This is sometimes produced by the pre-processor but might be produced by the solver program. It includes the coordinates of the points in the mesh and, if necessary, the connectivity list. Depending on the CFD package, such things as cell volumes and face areas might also be stored. This data is usually held in binary form to reduce the required storage, but again ASCII data

3.9.1 Using Graphics software for observing results

The graphics software itself is usually supplied as part of the CFD software package and is known as a post-processor. Sometimes, however, this software is combined together with the pre-processor to form a single interactive program that is used for both creating the computer model and post-processing. These programs enable a user to see the geometry of the flow problem, the mesh and the results of the simulation by producing pictures of the available data,

usually in color. Displaying the data in a visual way condenses the vast amount of information that a CFD solver can generate into a usable format.

By entering commands the analyst can use the CFD post-processing software. These commands direct the software to build up the required picture of the data on the graphics screen. This file can be created by the user with a text editor or it could be written by the software itself in some cases. When generating the pictures, the stages that are followed are similar regardless of the type of data being displayed. The display process involves, first of all, displaying some part of the geometry or mesh on the screen. Then, the picture is manipulated so that the required view is displayed before the solution itself is shown. This final display might be some of the velocity data, shown as a set of vectors, or the contours of scalar variables such as the fluid pressure or the turbulence modeling variables. These three stages; show the geometry, modify the view and display the results; can be performed in any order but it is usual to display the actual results last of all. As this post-processing part of the analysis process is highly interactive, the user can often move between these three stages in a seemingly random fashion. However, for most simple cases, it will be most useful if the order given above is followed. The following sections deal with each of these three stages in turn.

3.10 Meshing and Simulation

3.10.1 Meshing

Meshing is done in Ansys Meshing, meshing should be fine enough to capture the physics at the same time that should be of possible highest quality. We have adjusted some of the parameter to get high quality mesh, switching proximity and curvature based refinement it will mesh small entities like edges and surface with greater details and we took care of unnecessary smaller entities so we can mesh the geometry so. Values given to take any surface as proximity is 0.15mm and for curvature the value is 0.1 mm, maximum element size for surface mesh 3.5mm and for everything else 4.0mm, to get the conformable mesh for middle volume (R1) we already have done form a new part, and other two will give non-conformable meshing as in fig. after getting particular quality we should give the appropriate name to the respective surfaces.

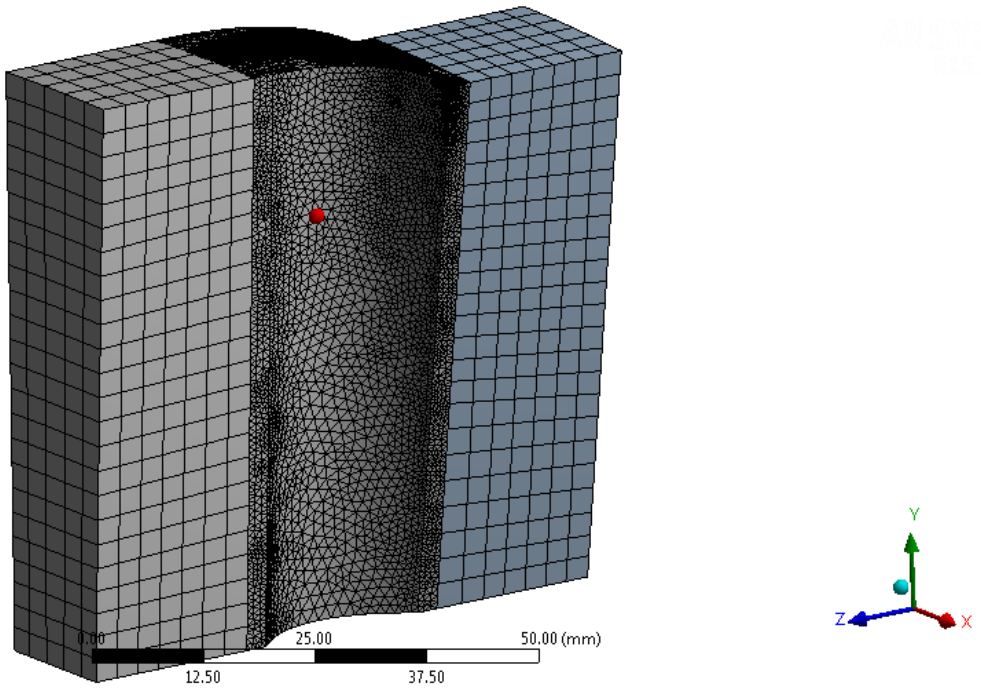

Fig. 3.20 Hybrid mesh used for geometry

Now, the boundary conditions for the turbine blade section can be created. This is done by once again name selection. The boundary type of wall is default select the unmentioned boundary conditions. The next boundary to define is the outer vertical faces that will be defined as velocity inlet, and hot pressure outlet. The next boundary to define is the bottom face of turbine blade cooling holes that will be defined as secondary inlet, and top face of turbine blade cooling holes is interface to clearance volume as show in fig 3.22 and 3.23.

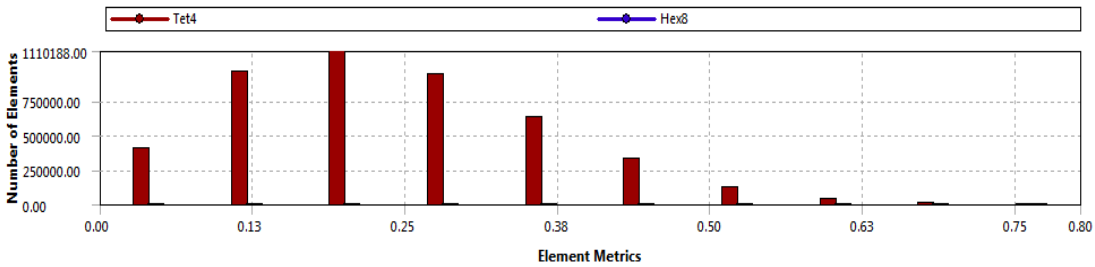

Fig. 3.21 Mesh metric graph

3.10.2 CFD Simulation in ANSYS Fluent

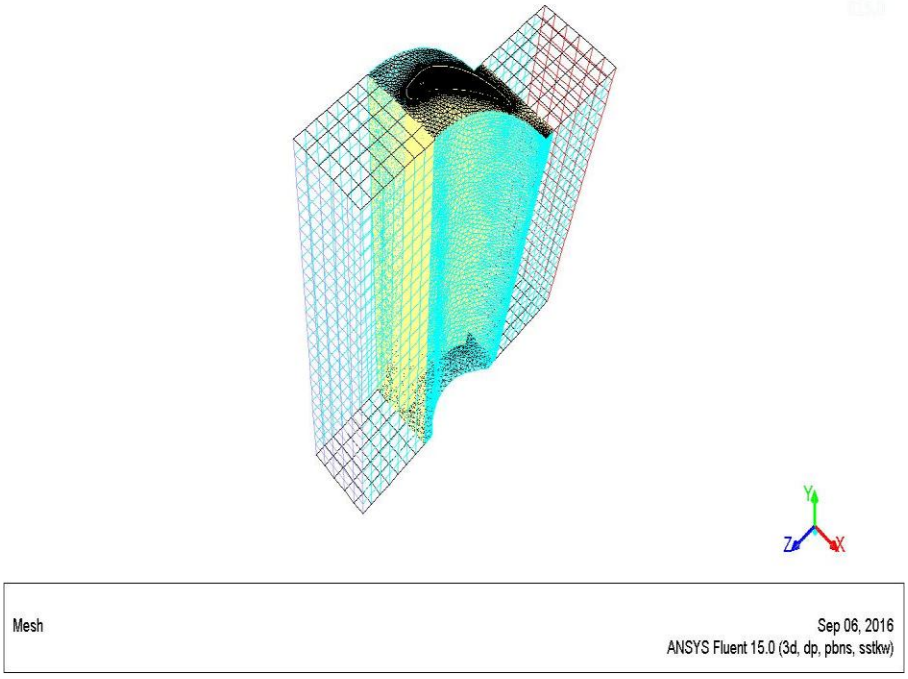

Fig. 3.22 Mesh in Ansys fluent showing detailed boundary conditions by different colors

Ansys "Fluent" is one of the oldest fluid flow simulation commercial software, it is most robust compare to other if number of elements needs to simulate is more. Standard procedure followed to simulate. Import the mesh in this case we will double click on setup of the tree given for fluent analysis system. As shown in fig 3.24 check the meshing quality, check the scaling, and report the quality in general tab. Keep pressure based solver because it can be used for incompressible fluid to compressible fluid of some extend, it was found that fluid velocity is not very high to consider as density based solver. Velocity found was near to 105 m/s maximum so Mach number is near to 0.3 so pressure based solver will work correctly. Simulation is steady state because it will give the visualization of developed flow. Next is turbulence model and energy equation, Reynolds number was calculated for each and every case it found near to 65,000 so limit for laminar flow is 20,000 around an obstacle so obviously it is a turbulence flow, flow through tubes is absolutely laminar so it has been initiated laminar and thermal heat transfer we want to see as output so surely we should on energy equation.

Energy equation is types of transport equation in which conduction diffusion, species, viscous dissipation will get calculated addition to that enthalpy of source also calculate. Generalized equation looks like follows,

$$\frac{\partial(pE)}{\partial t} + \nabla.[V(\rho E + p)] = \nabla.[k_{eff}\nabla T - \sum_j h_j J_j + \tau_{eff}.V] + S_h \quad (78)$$

Energy per unit mass is defined as

$$E = h - \frac{p}{\rho} + \frac{V^2}{2} \quad (79)$$

3.11 SST-K-ω model-shear stress transport (two equation models):

This two equation models are calculating not only kinetic energy but also turbulence scale or equivalent. The starting point of all two equation models is the Boussinesq approximation, and kinetic energy is calculated by the following equation,

$$\rho\frac{Dk}{Dt} = \tau_{ij}\frac{\partial \bar{u}_i}{\partial x_j} - \rho\beta f_\beta k\omega + \frac{\partial}{\partial x_j}\left[\left(\mu + \frac{\mu_t}{\sigma_\varepsilon}\right)\frac{\partial k}{\partial x_j}\right] \quad (80)$$

$$\mu_t = \alpha \times \rho\frac{k}{\omega} \quad (81)$$

$$\rho\frac{D\omega}{Dt} = \alpha\frac{\omega}{k}\tau_{ij}\frac{\partial \bar{u}_i}{\partial x_j} - \rho\beta f_\beta \omega^2 + \frac{\partial}{\partial x_j}\left[\left(\mu + \frac{\mu_t}{\sigma_\omega}\right)\frac{\partial \omega}{\partial x_j}\right] \quad (82)$$

$$\omega = \text{specific dissipation rate} \approx \frac{\varepsilon}{k} \propto \frac{1}{\tau}$$

These are the equation of two equation model by menter SST-k-ω. This model gained high popularity in various engineering fields because of following regions,

- ✓ Can be used to integrate to wall without use of any damping function
- ✓ Accurate and robust for wide range of boundary layer flows with pressure gradient
- ✓ Most widely used in the aerospace and turbo-machinery communities.

Several sub-models are available like compressibility effect which we have used here. And viscous heating has not been used to transfer the heat from contacted and remain contacted fluid because fluid after expanding will not be having high density. Blended function is applied to limit the turbulence viscosity, to do so modification had done in near wall function where log law of fluid will be applicable, so this modification is applicable only for fluid flow near to the wall where fluid boundary layer follow log law, this blending equation is as follows.

$$\rho\frac{D\omega}{Dt} = \frac{\gamma}{v_t}\tau_{ij}\frac{\partial \bar{u}_i}{\partial x_j} - \rho\beta\omega^2 + \frac{\partial}{\partial x_j}\left[\left(\mu + \frac{\mu_t}{\sigma_\omega}\right)\frac{\partial \omega}{\partial x_j}\right] + 2\rho(1 - F_1)\sigma_{\omega 2}\frac{1}{\omega}\frac{\partial k}{\partial x_j}\frac{\partial \omega}{\partial x_j} \quad (83)$$

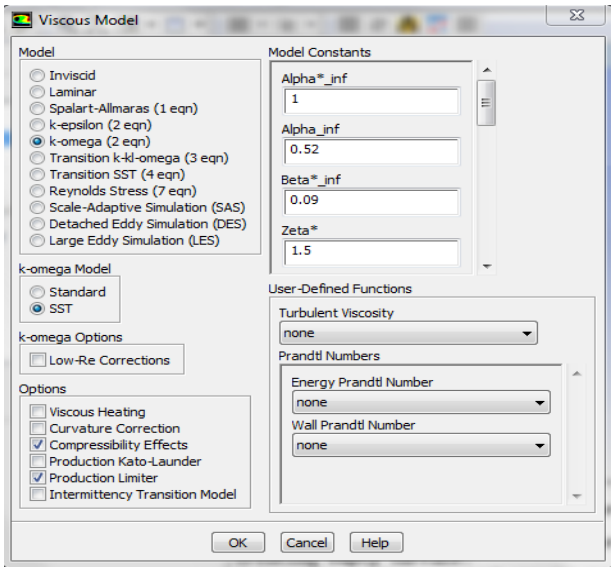

Fig. 3.23 Turbulent model tab

As per calculation done in design section air/exhaust gas is coming in turbine with pressure 19.85 bar with temperature of 1200 K and mass flow rate per component is 0.48 This is the values for primary inlet and for secondary inlet it has been calculate 2.75% of mass flow rate of total engine inlet is coming 0.0033 kg/s.

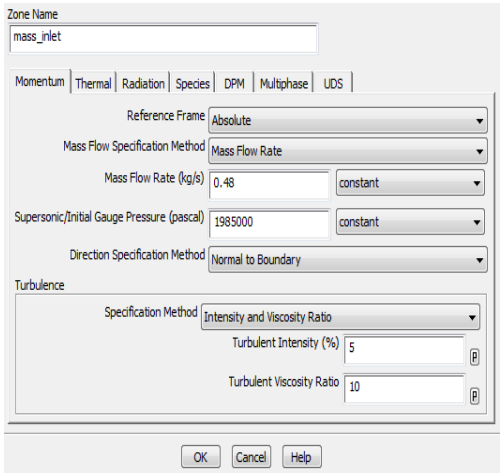

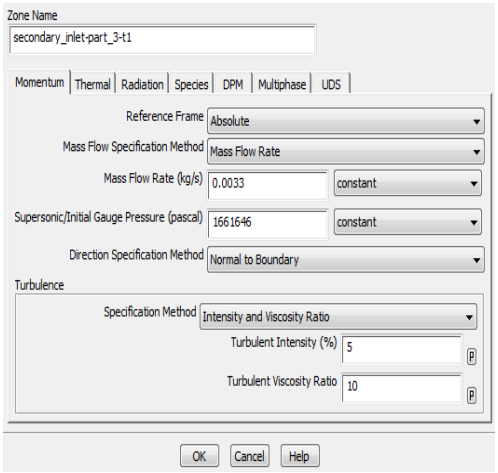

Fig. 3.24 (a) Primary mass flow **(b) Secondary mass flow**

Pressure outlet is calculated already so it can feed those values, after this periodic boundary condition need to mention by TUI method return > mesh > Modify zone > make periodic, give particular surface ID's and it will show us one of the surface has deleted. Next tedious task we

should do is providing interfaces by defining the proper name combination it will show us zone surface can't create surface from sliding interfaces, creating empty surface. After this check the each shadow coupled surfaces and material assigned to those surfaces compute the reference values from mass inlet and give reference zone as stationary-1 domain.

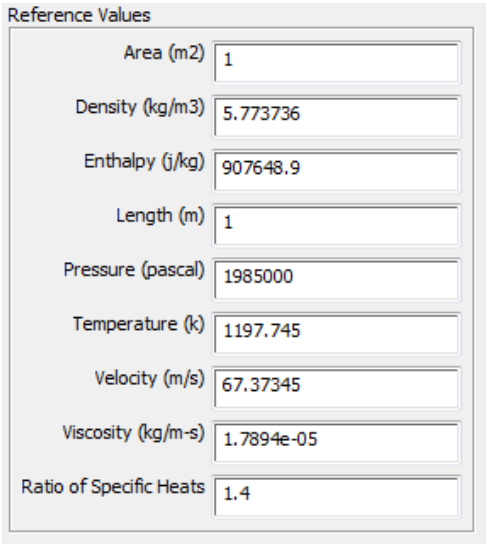

Fig. 3.25 Reference values calculated from inlet

3.12 Solution Methods

The pressure-based coupled solver (PBCS) is applicable for most single phase flows, and yields superior performance to the standard pressure-based solver. In this momentum and pressure equations are calculated simultaneously it can converge very rapidly but required more memory 1.5 to 2 times as segregated solver. Solver variables are stored in center of the cell, to interpolate this central value to faces of the element this govern by discretization. Most of the convective terms are calculated by second order discretization because it is essential with tri/tetra mesh or when flow is not aligned to mesh, it takes more time to converge but it is 2^{nd} order accurate. Gradient discretization used is Least square cell based because it is same accurate as Green Gauss node based but take less time.

Pressure gradient for other simulation used as PRESTO! Used for highly swirling flows, flows involving steep pressure gradients (porous media, fan model, etc.), or in strongly curved domains. For higher temperature (1400K) analysis we used this PRESTO!

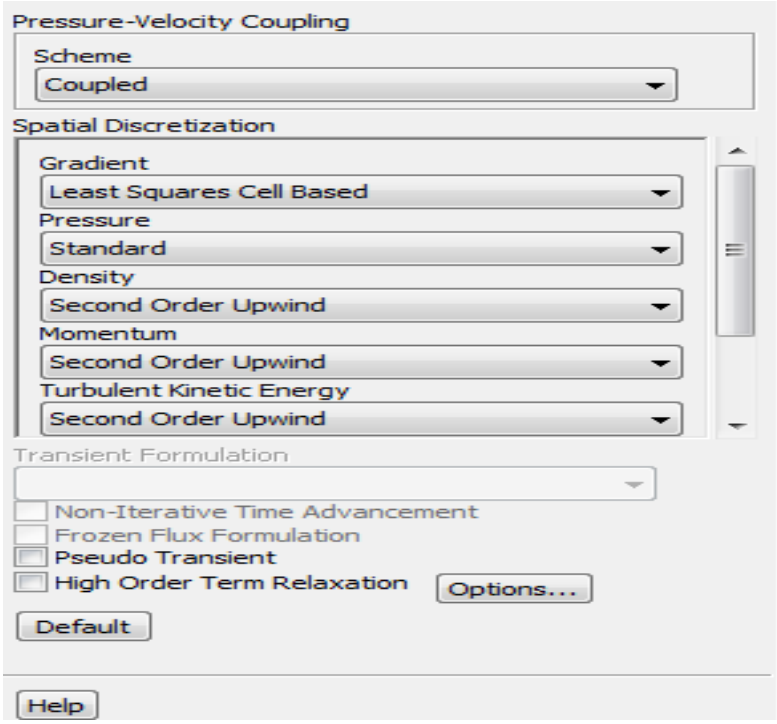

Fig. 3.26 Pressure-velocity coupling in ANSYS

Hybrid initialization is used to get the better initialization; this provides a quick approximation of the flow field, by a collection of methods.

• It solves Laplace's equation to determine the velocity and pressure fields.

• All other variables, such as temperature, turbulence, species fractions, volume fractions, etc., will be automatically patched based on domain averaged values or a particular interpolation.

3.12.1 Modification done under relaxation factors

Under relaxation factor is factor of transient term for particular equation assigned for that much of the time, according to that fluctuating component will get multiplied, so for most of the values are changed in this tab. If value is too high, the model will be unstable, and may fail to converge. Value is much too low, it will take longer (more iterations) to converge. Default settings are suitable for a wide range of problems; you can reduce the values when necessary. The Courant number is the main control for stability when using the coupled solvers. A transient

term is included in the density-based solver even for steady state problems. The Courant number defines the time step size, it given as seven which is seen in figure 3.29.

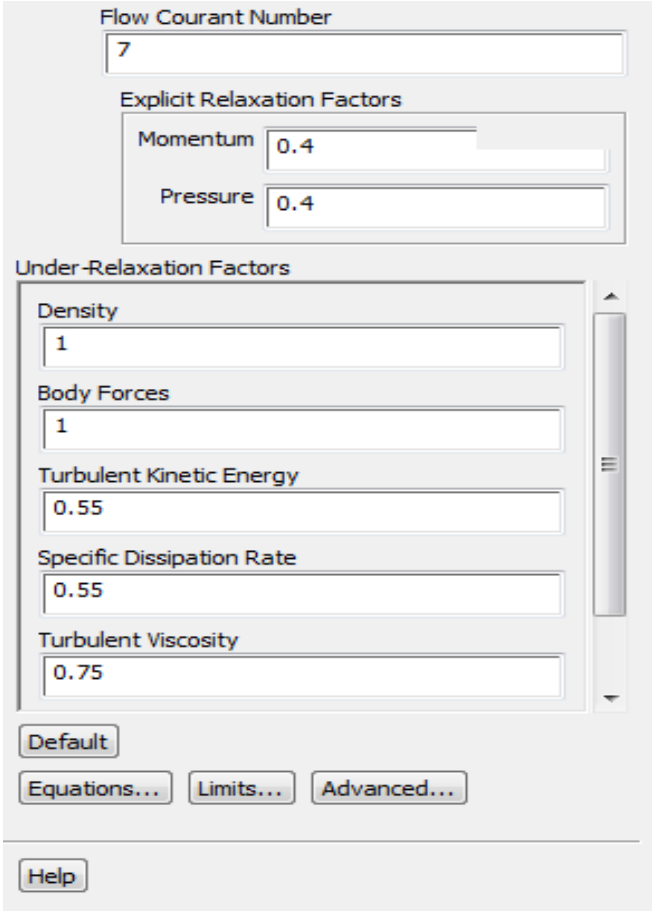

Fig. 3.27 Solution Control flow in ANSYS

For turbulent kinetic energy and specific Dissipation rate value kept 0.55, turbulent Viscosity 0.75, for momentum and pressure 0.4, for energy value is 0.5.Here one more topic has used called FMG initialization; Full Multi-Grid (FMG) Initialization solves the flow problem on a sequence of coarser meshes, before transferring the solution onto the actual mesh.FMG Initialization is useful for complex flow problems involving large pressure and velocity gradients on large meshes. Euler equations are solved with first-order accuracy on the coarse-level meshes. It can be used with both pressure and density based solvers, but only in steady mode.

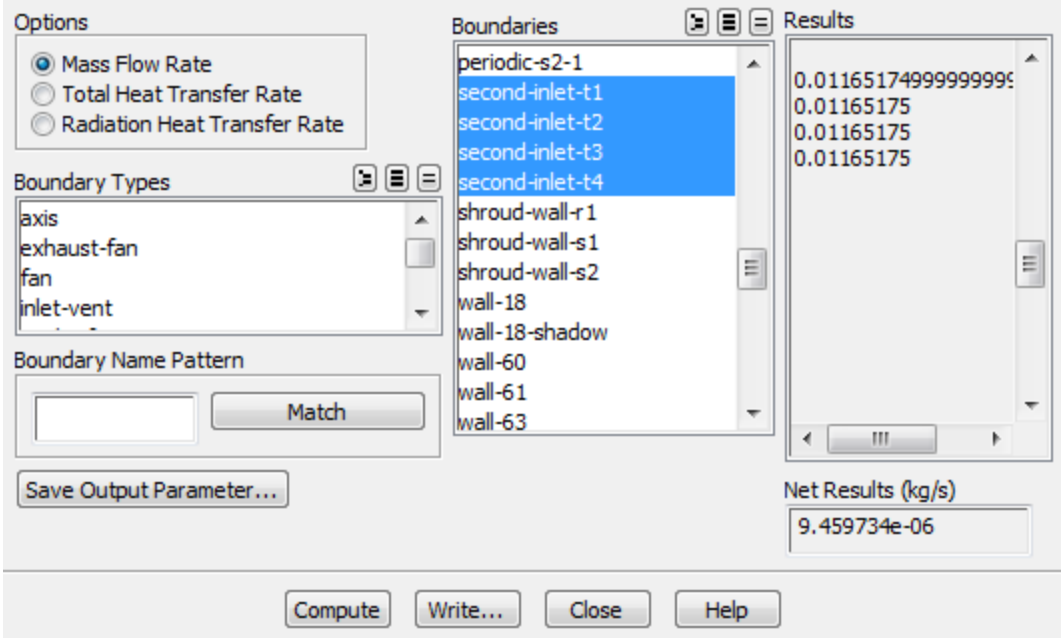

Fig. 3.28 Report flux for pressure ratio 30 and inlet temperature 1200 K

Check the case in run calculation tab generally; a decrease in residuals by three orders of magnitude indicates at least qualitative convergence. At this point, the major flow features should be established which can be determined in figure 3.30.

RESULTS AND DISCUSSION

In the present analyses, two type of cooling hole patterns have been chosen namely; straight lined pattern and zigzag lined pattern for cooling of turbine blades material.

Two different materials have been taken for the analysis of gas turbine blade. The materials, titanium alloy and alloy steel are considered for the analysis [31, 32 and 34]. Also there are four combinations between temperature and pressure which have been selected for the present analysis as shown in table 4.1.

Table 4.1 combination of pressure and temperature for analysis

S. No.	Material	Temperature	Cooling pattern type	pressure
1	Alloy Steel	1200	Straight lined	20 bar
2	Alloy Steel	1400	Straight lined	20 bar
4	Titanium Alloy	1200	zigzag lined	30 bar
5	Titanium Alloy	1400	zigzag lined	30 bar

4.1 Results for 20 Pressure Ratio for inlet temperature 1200K

Primarily, 20 bar pressure and 1200 K temperature have been selected and the results are shown in the following paragraphs.

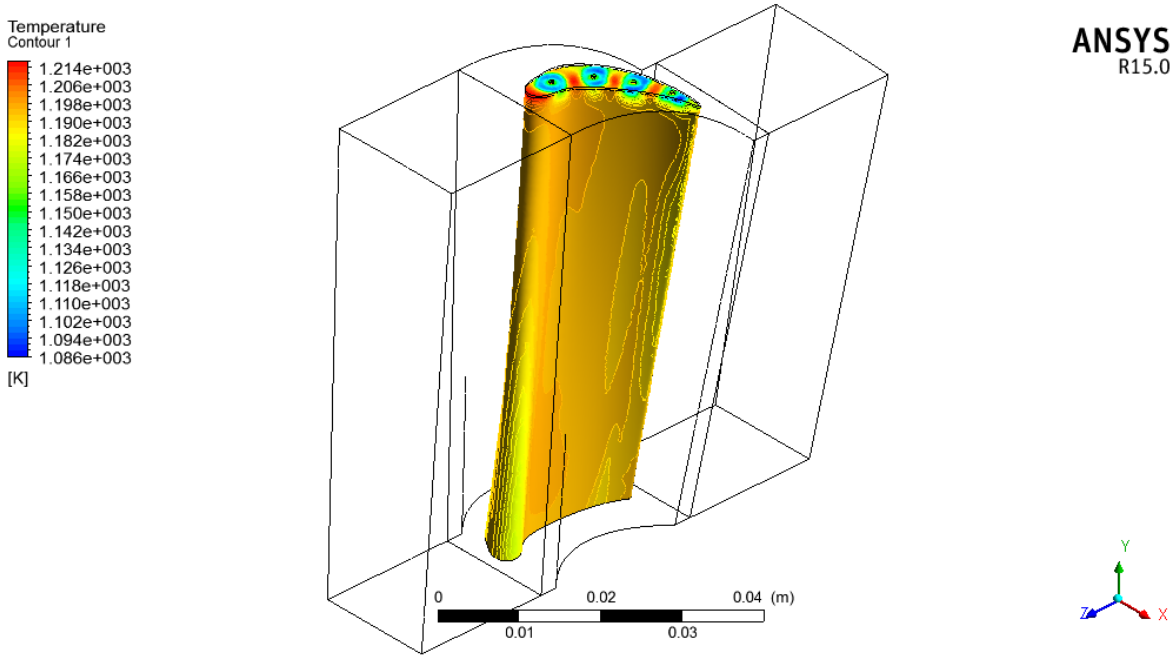

Fig. 4.1 Temperature plot for Straight lined pattern for Titanium blade

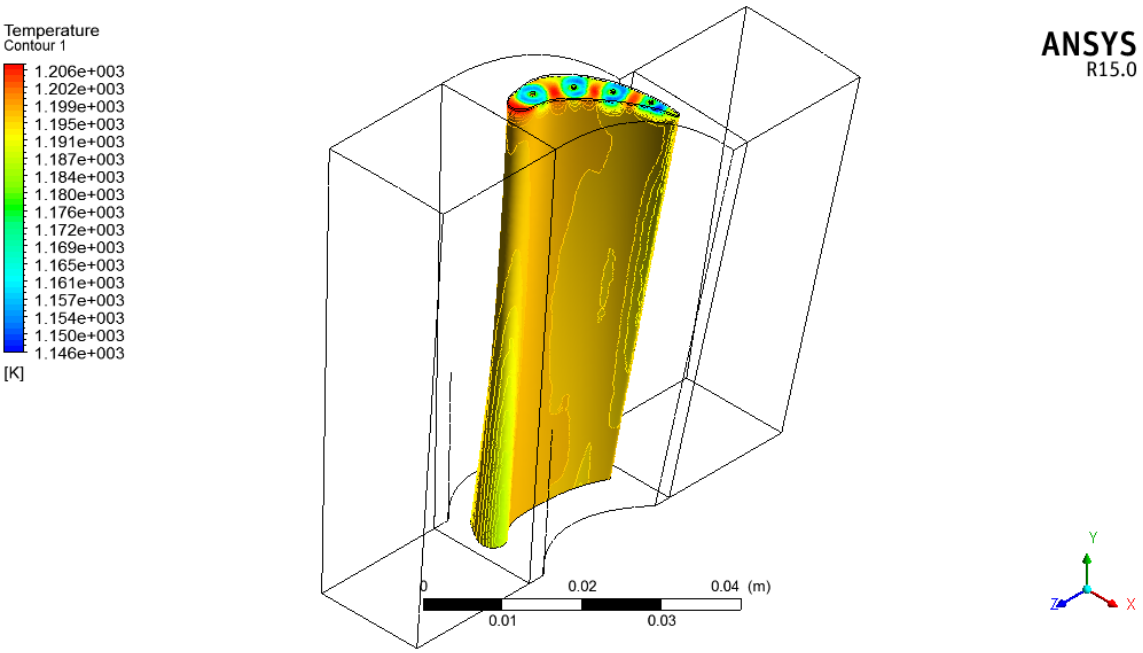

Fig. 4.2 Temperature plot for Straight lined pattern for steel blade

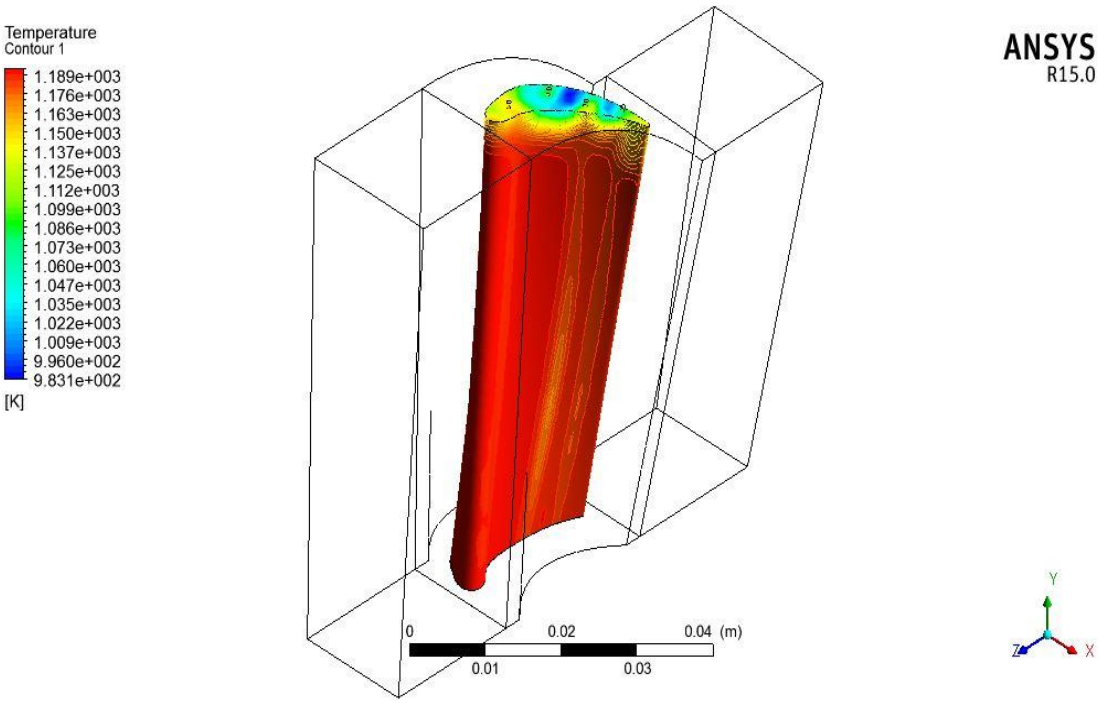

Fig. 4.3 Temperature plot for zigzag lined pattern for Titanium blade

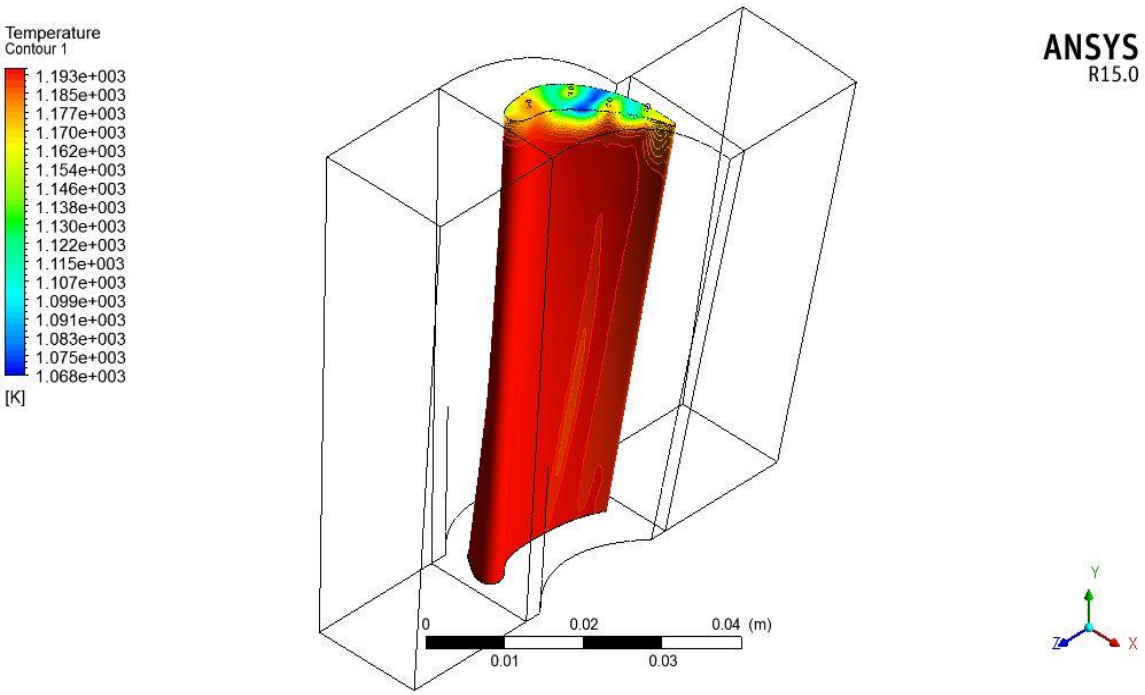

Fig. 4.4 Temperature plot for zigzag lined pattern for steel blade

Fig. 4.1 and fig. 4.2 represent the temperature plot for straight lined pattern for Titanium blade and steel blade respectively. It has been found that the change in temperature for titanium alloy straight lined holes blade design is 128^0C and for alloy steel blade is 60^0C. Therefore, titanium alloy blade transferring more heat as compared to alloy steel. This is due to fact that, the heat transfer capacity of titanium is better than steel. Fig. 4.3 and fig. 4.4 show the temperature plot for zigzag lined pattern for titanium alloy and alloy steel blade material respectively. Change in temperature for zigzag lines pattern for titanium alloy blade material is 205.9^0C and for alloy steel blade is coming only 128^0C. This is again; the reason for better heat transfer is heat transfer capacity of titanium alloy.

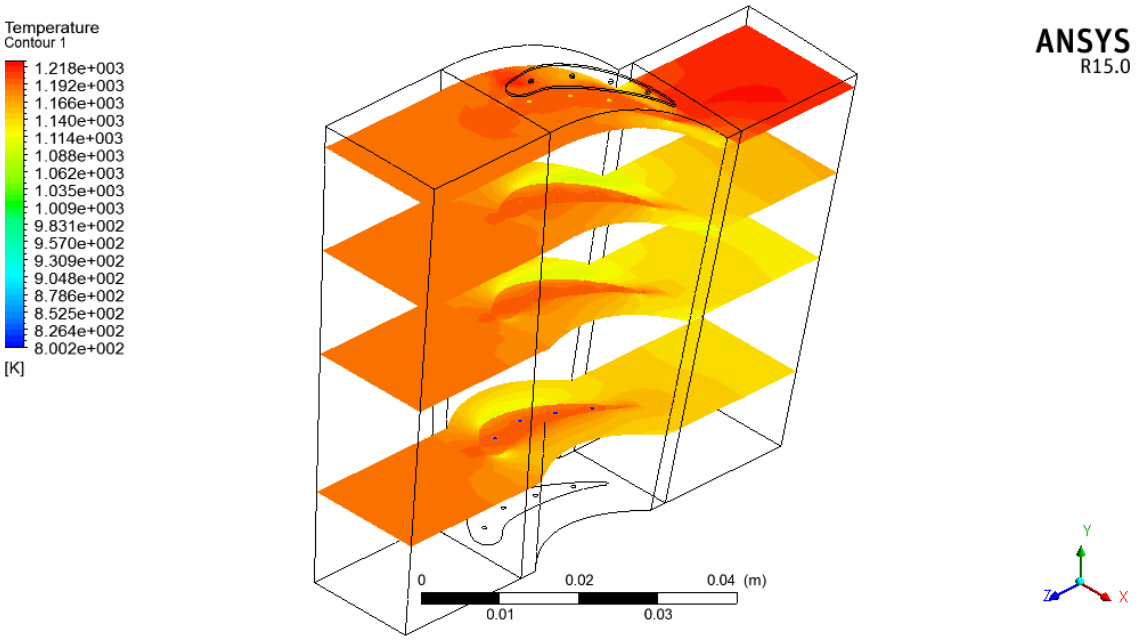

Fig. 4.5 Temperature Plot on Planes for straight lined pattern Titanium Blade

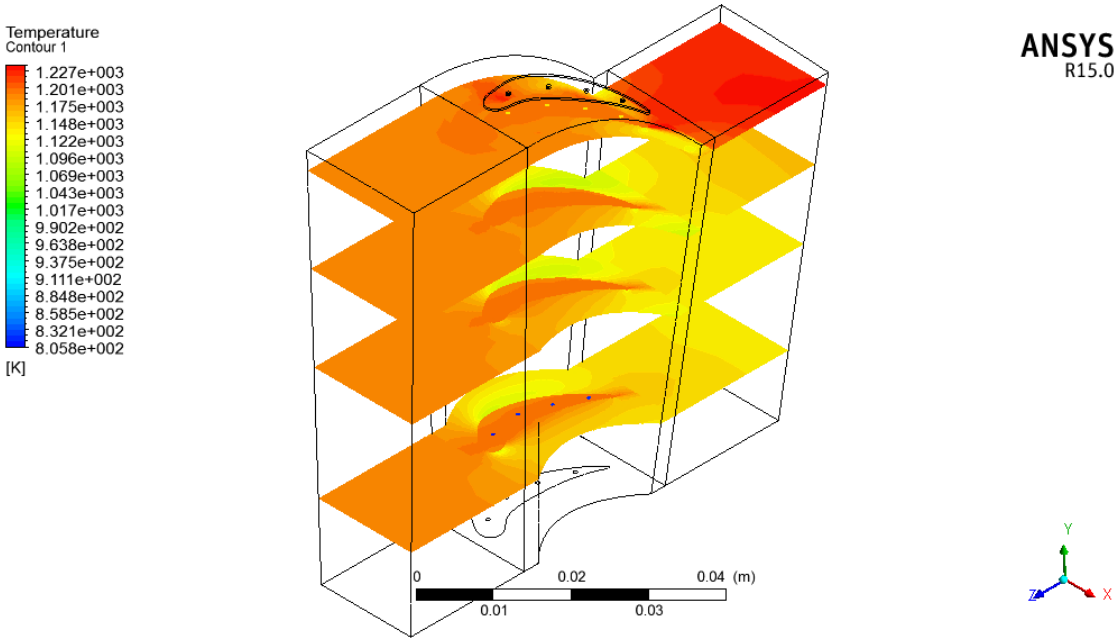

Fig. 4.6 Temperature Plot on Planes for straight lined pattern Steel Blade

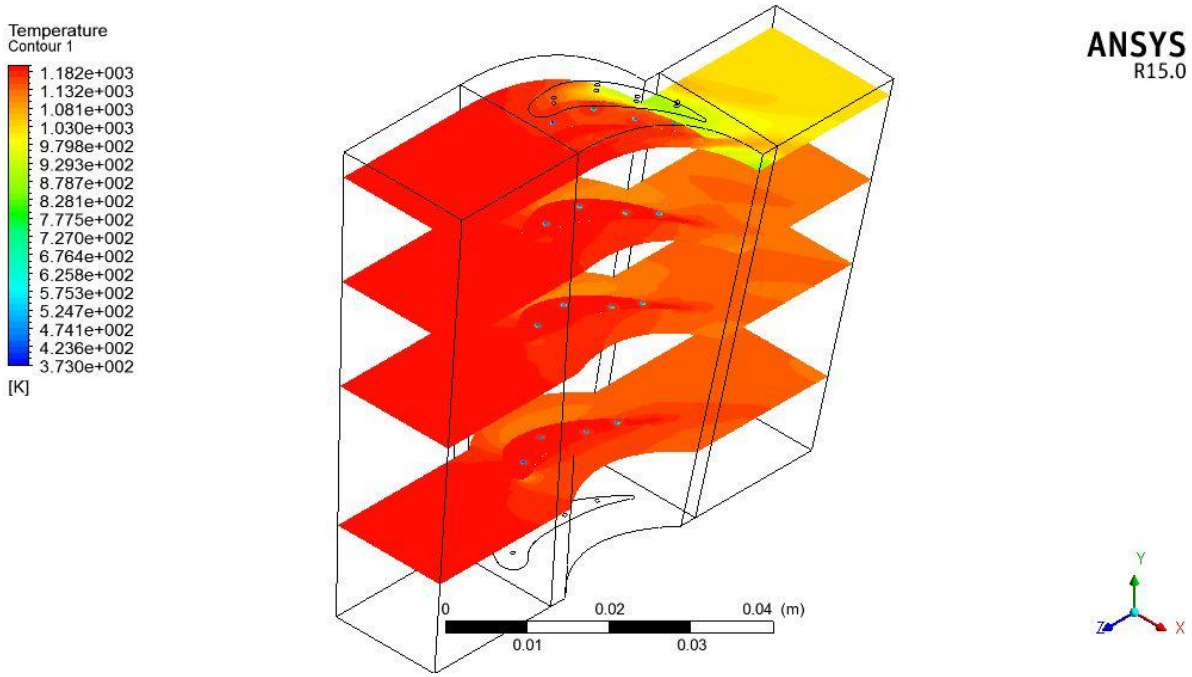

Fig. 4.7 Temperature Plot on Planes for zigzag lined pattern Titanium Blade

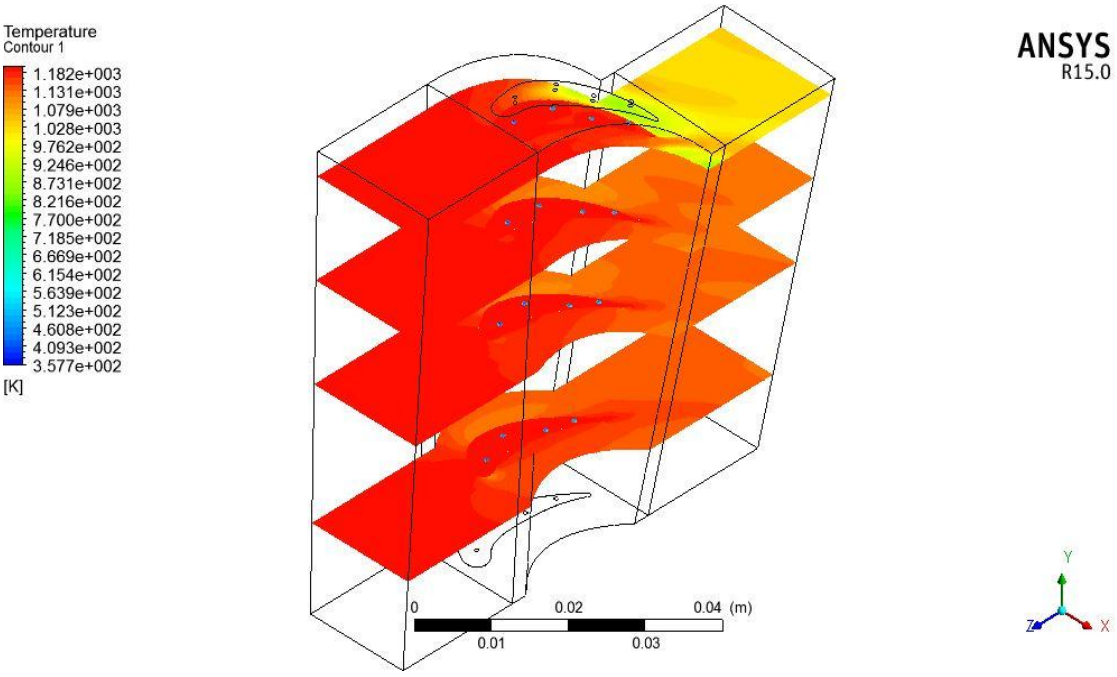

Fig. 4.8 Temperature Plot on Planes for zigzag lined pattern Steel Blade

Fig. 4.5 and fig. 4.6 represents temperature plot showing control volume temperature for both the materials having straight lines pattern cooling holes. For the entire domain, temperature

decreases towards the bottom side. Exit temperature for all designs is same while the blade temperature is 20^0C less for zigzag design as compared to straight lined design. Temperature of secondary fluid while exiting from steel blade is very high it means it is reached to is highest capacity to bear the heat, titanium is having much higher temperature rise, this plot is actually intended to resolve core temperature of blade and temperature at interface of blade and fluid domain. Fig. 4.7 and fig. 4.8 represent the same variation for zigzag pattern of both the fluids.

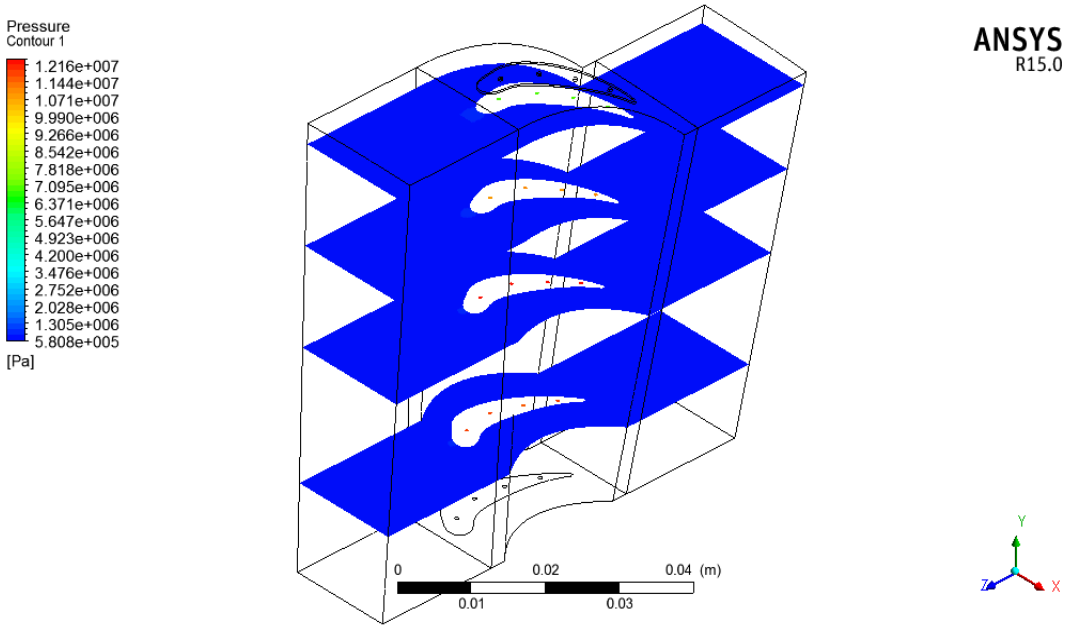

Fig. 4.9 Pressure Plot on Planes for straight lined pattern Titanium Blade

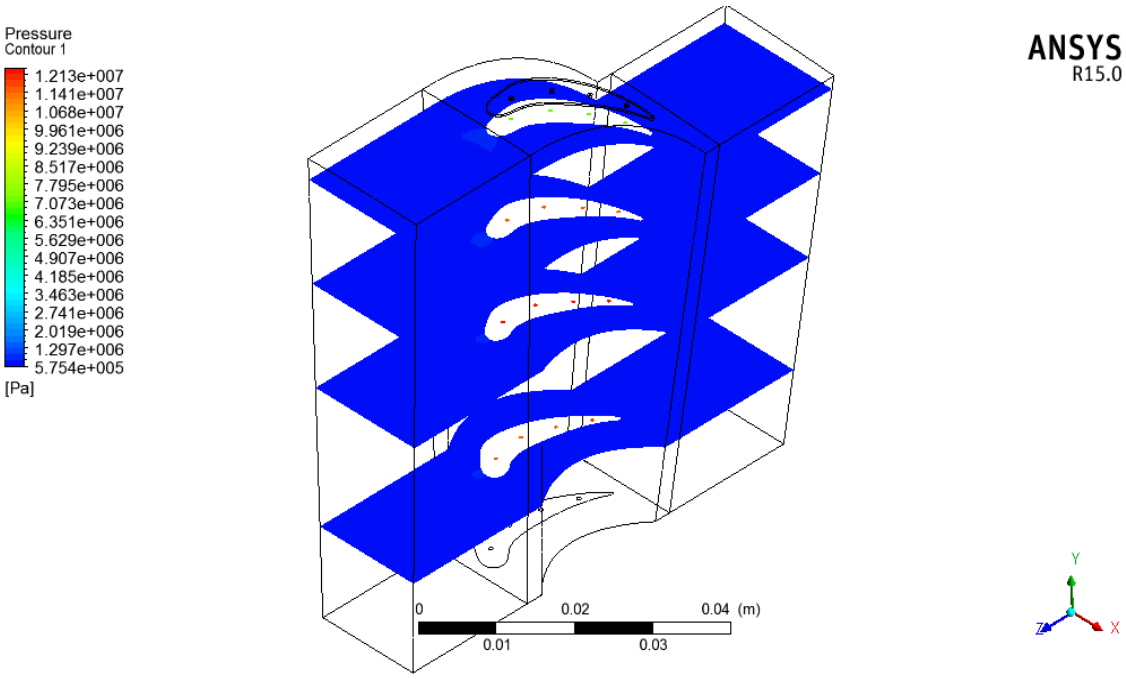

Fig. 4.10 Pressure Plot on Planes for straight lined pattern Steel Blade

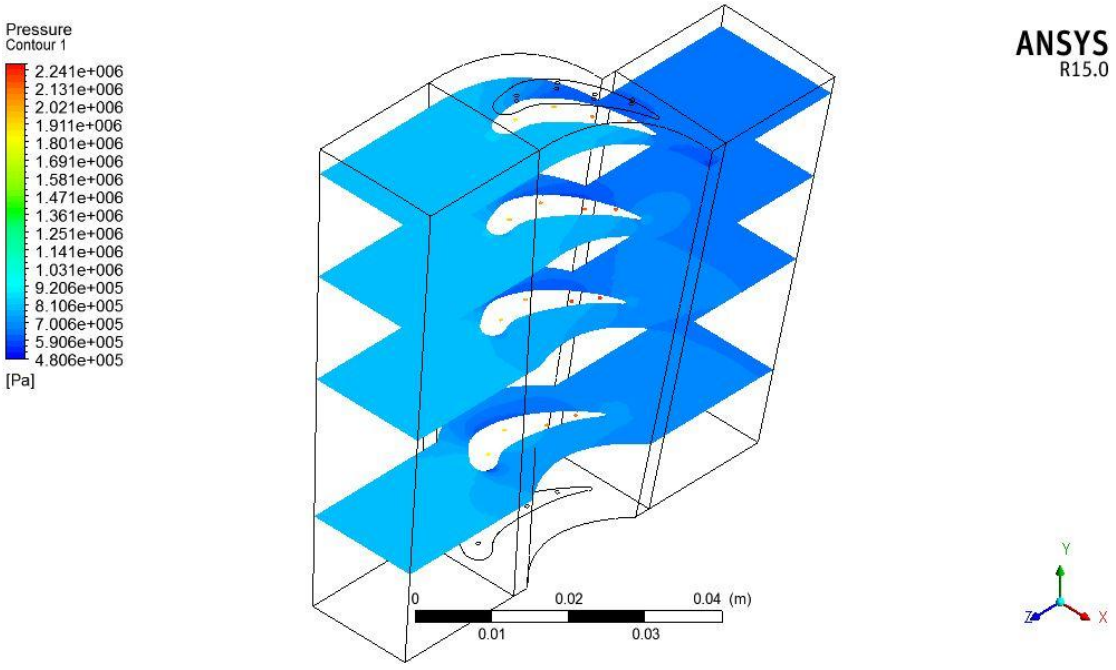

Fig. 4.11 Pressure Plot on Planes for zigzag lined pattern Titanium Blade

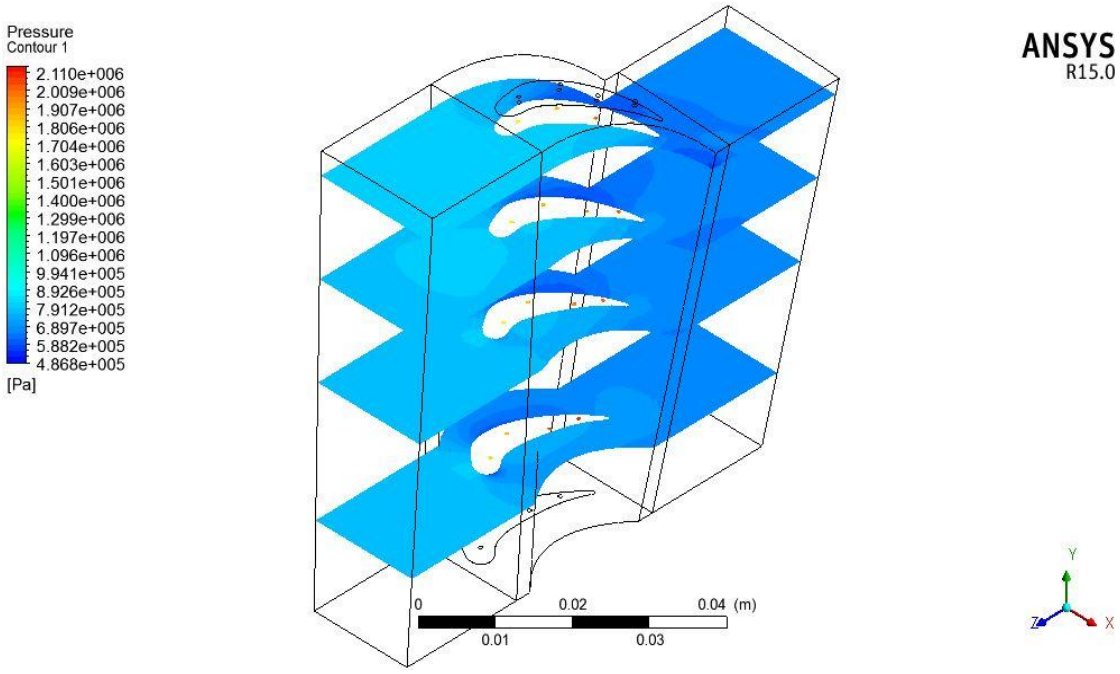

Fig. 4.12 Pressure Plot on Planes for zigzag lined pattern Steel Blade

Fig. 4.9 and 4.10 represents pressure plot on planes for straight lined pattern titanium blade steel blade. Pressure is uniformly distributed on planes shows the pressure inside the tube is highly varying and therefore, temperature could be high causing less stability of the blade strength easy to subject for creep. Pressure in first tube is lower than the last tube indicating more heat is absorbed at trailing edge in second design of zigzag pattern. More pressure variation can be seen across the blade in second design that is effectiveness of turbine have increased slightly. Outside, fluid pressure is lower than inside fluid so there will not be any chocking of fluid. All the designs are seems to do satisfactorily in that case. Fig. 4.11 and fig. 4.12 show the pressure plot on planes for zigzag lined pattern titanium blade steel blade. As it can be observed that the pressure is almost same on blade surface for each of the material but for zigzag pattern, maximum value of pressure is lower with alloy steel blade by 30000 Pa (gauge pressure). Pressure in zigzag pattern is lower in titanium alloy blade material than other designs, showing more efficient to increase the pressure drop across the blade. This is due to fact that in the zigzag pattern, the flow of fluid is initially streamlined but after getting heated with the transfer of heat it gets turbulent.

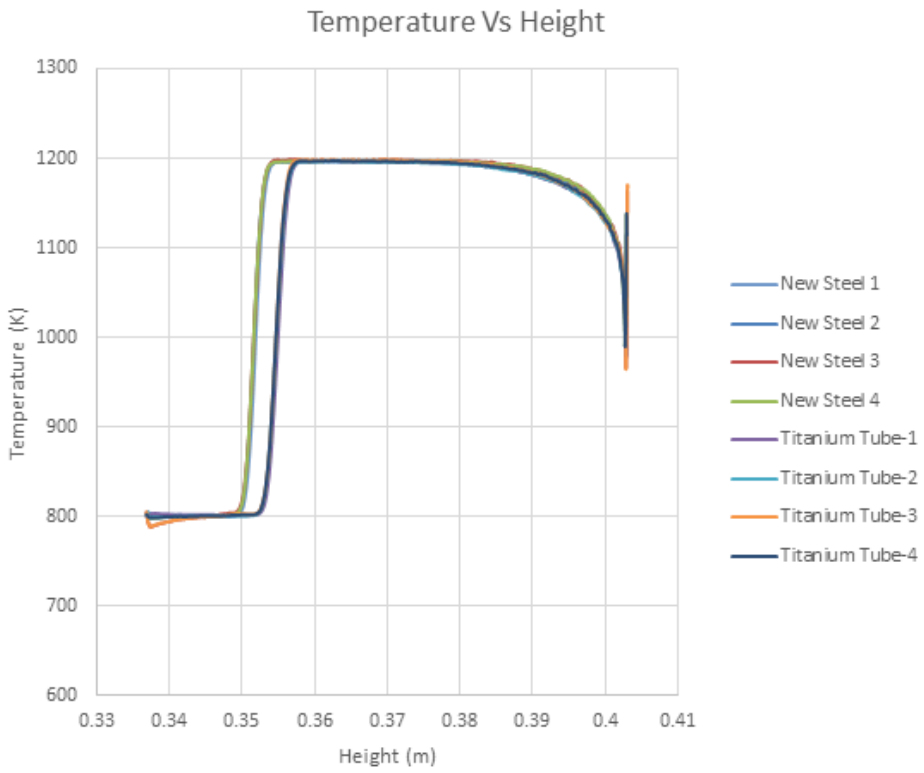

Fig. 4.13 Temperature variation with blade height of Straight lined pattern

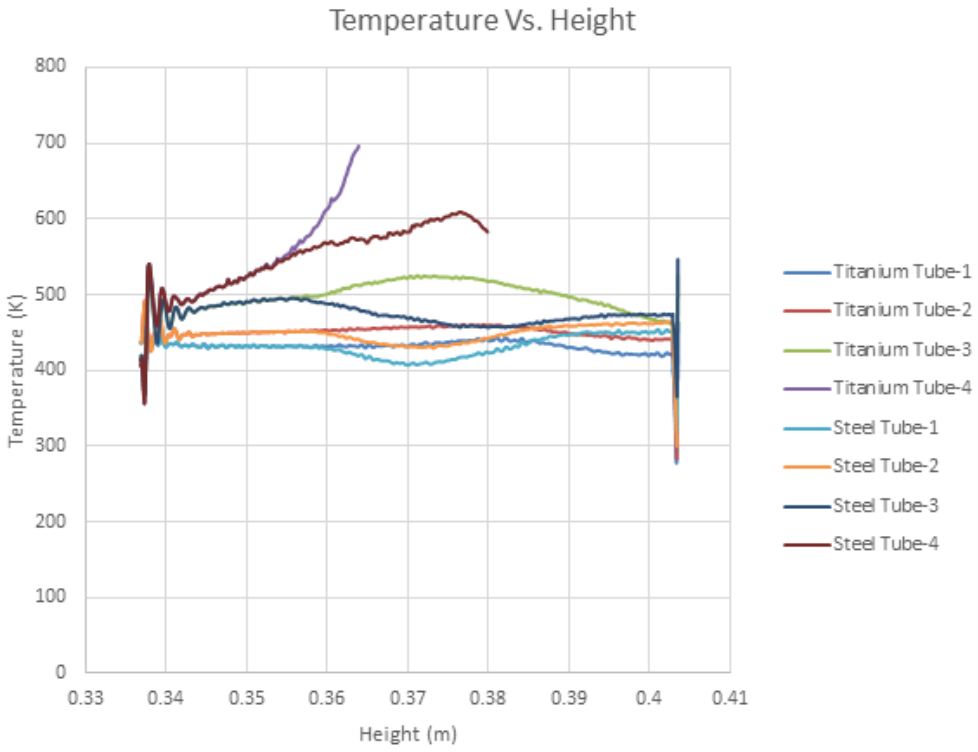

Fig. 4.14 Temperature variation with blade height of zigzag lined pattern

Fig. 4.13 and 4.14 are showing for straight lined cooling pattern and zigzag cooling pattern of both the blade materials respectively. All cooling tubes are having same temperature variation among them for straight lines pattern. For alloy steel blade cooling, fluid is getting heated very rapidly from 800^0K to 1200^0K then it seems almost constant for small height of blade. When it reaches to upper blade opening, again it gets cool down. After coming out from upper opening, it is mixed with primary flowing fluid. This sudden change in temperature may cause development of thermal stresses in the blade material. Other characteristics are almost same except heating rate of the cooling fluid.

For zigzag pattern, change in temperature is uniform in all tubes, except last one as shown in fig. 4.14. Due to location of the hole as it exist very near to the outer most surface. Hence, it will get heated exceptionally, that may cause to serious issue. Due to this, it will change the eccentricity of offset. Other characteristics of second design are showing almost same changes in terms of temperature. Because of diffusion, as soon as the fluid entering from the bottom side it is getting cooled rapidly.

4.2 Results for 20 Pressure Ratio for inlet temperature 1400K

In this article, the turbine inlet temperature has been increased by 200^0K to 1400K for the same pressure ratio i.e. 30.

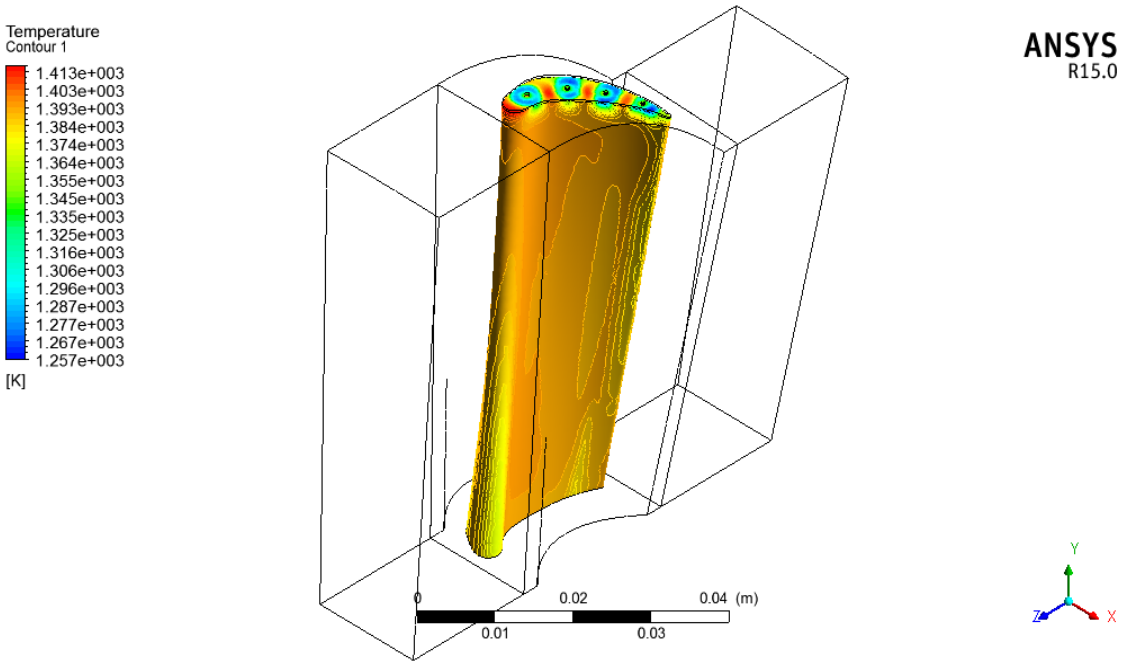

Fig. 4.15 Temperature plot for Straight lined pattern for Titanium blade

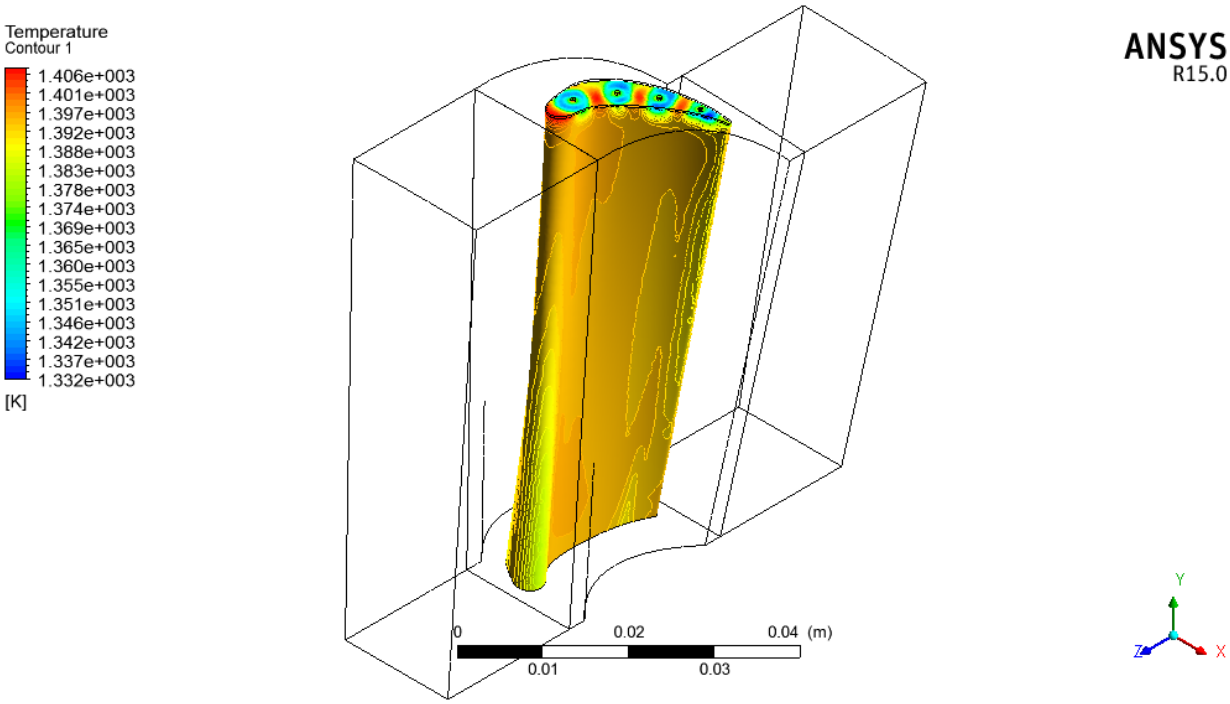

Fig. 4.16 Temperature plot for Straight lined pattern for steel blade

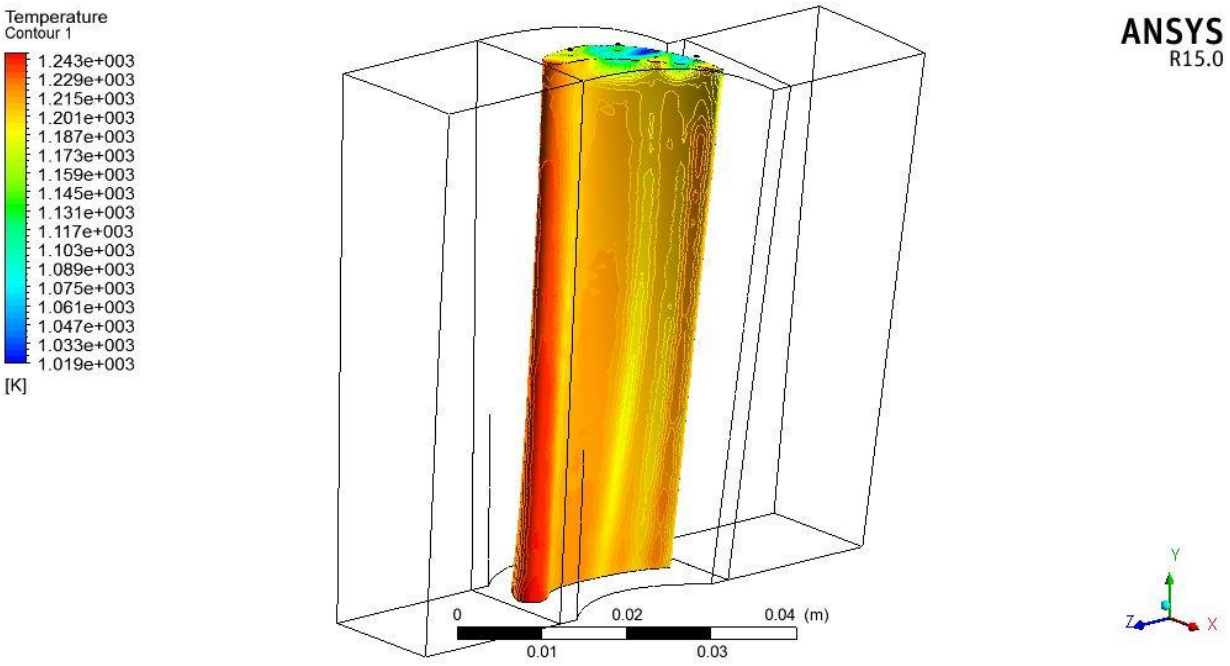

Fig. 4.17 Temperature plot for Zigzag lined pattern for Titanium blade

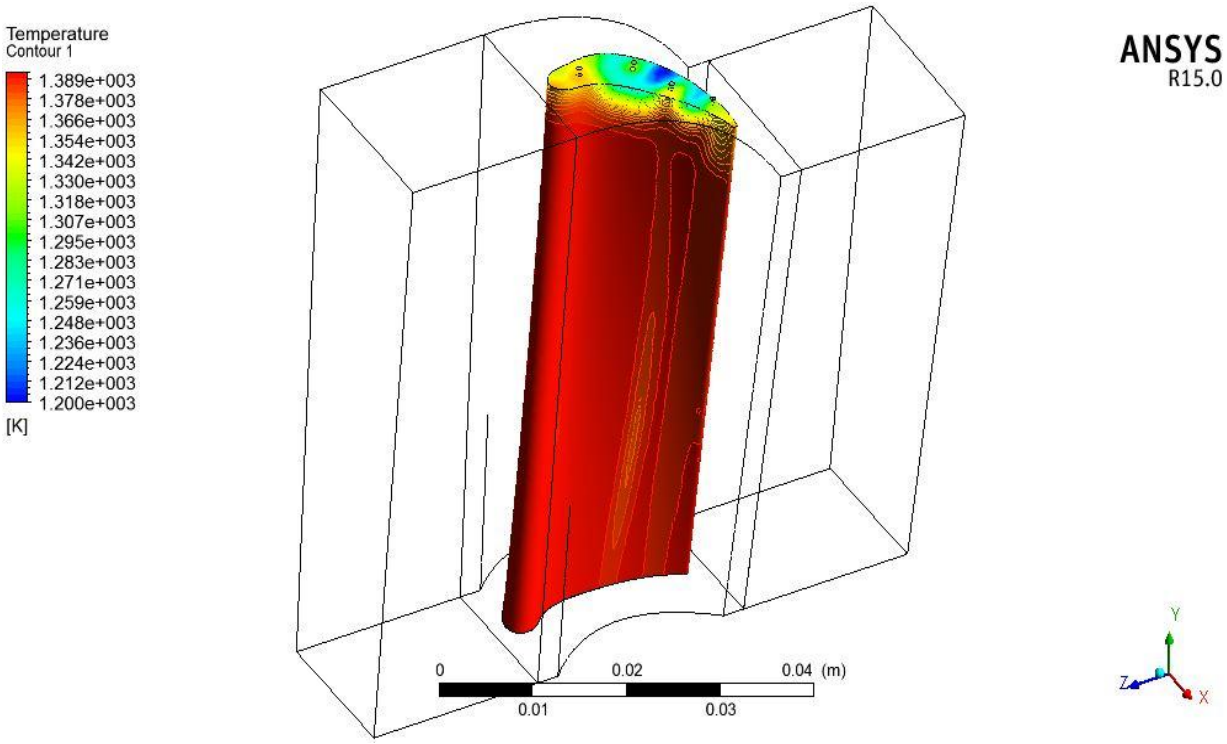

Fig. 4.18 Temperature plot for Zigzag lined pattern for steel blade

Fig. 4.15 through fig. 1.18 showing change in temperature due to straight lined holes and zigzag holes patterns. It has been observed that, change in temperature in titanium and steel straight lined holes blade design is 156^0C and same for steel blade is 74^0C, so titanium transferring more heat than steel. On comparing zigzag design pattern, change in temperature for zigzag titanium blade is 224^0 and for steel blade is only 189^0C.

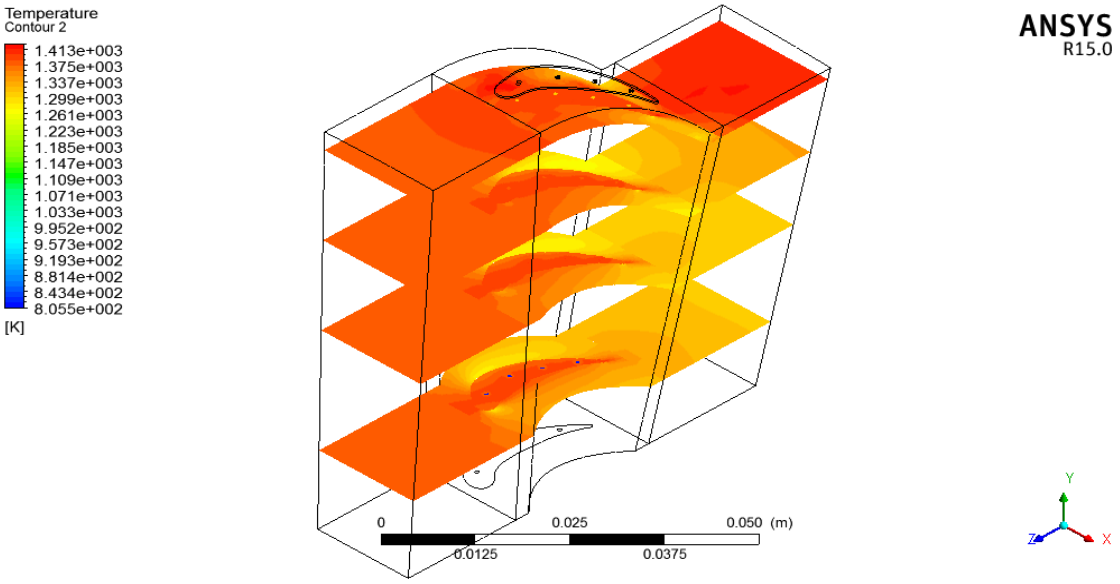

Fig. 4.19 Temperature Plot on Planes for straight lined pattern Titanium Blade

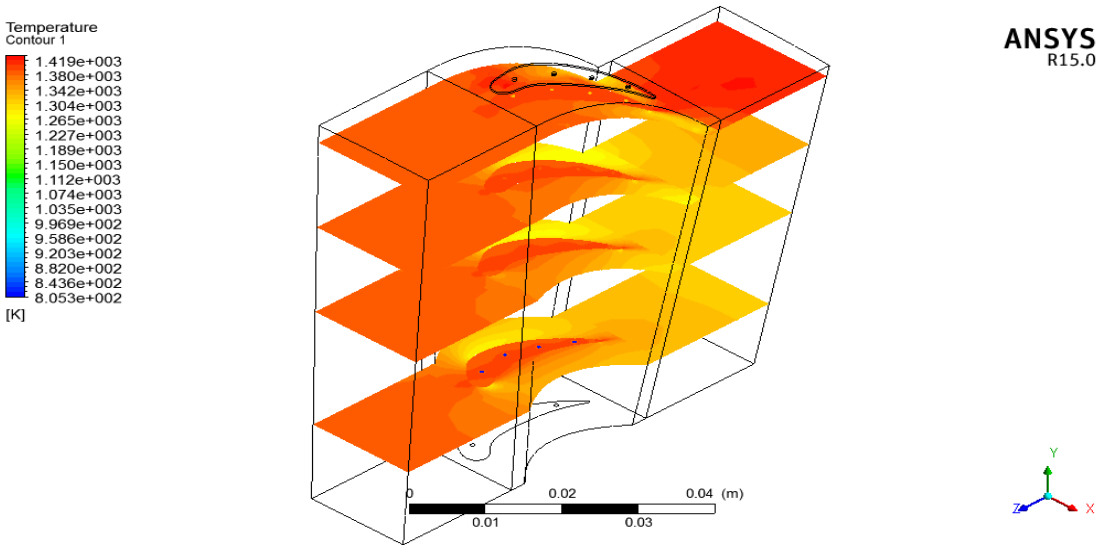

Fig. 4.20 Temperature Plot on Planes for straight lined pattern Steel Blade

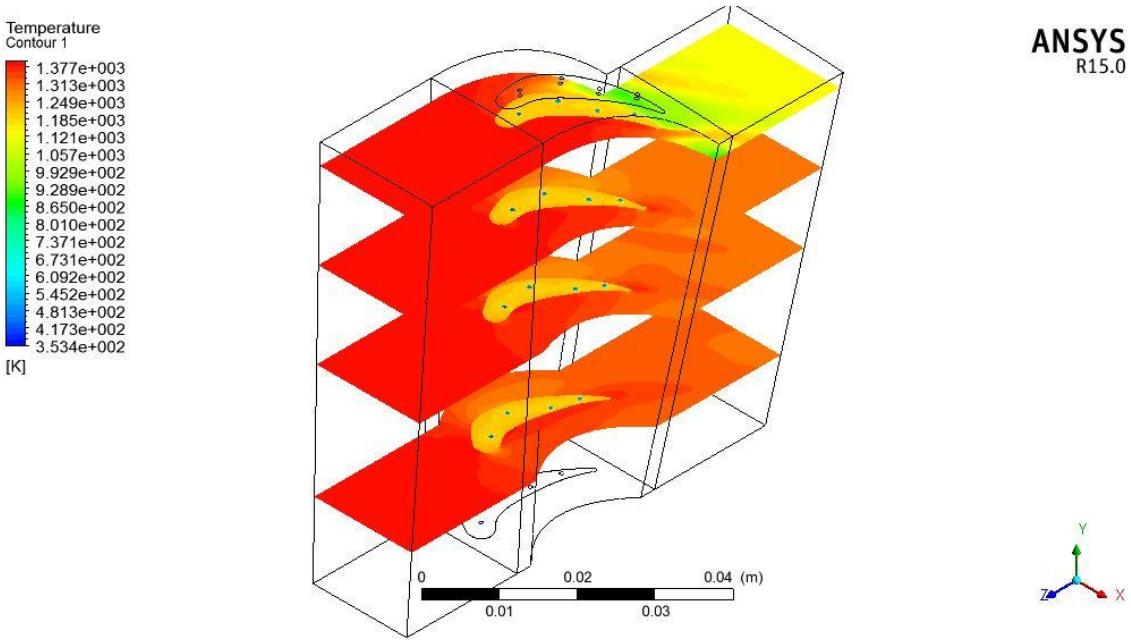

Fig. 4.21 Temperature Plot on Planes for Zig-zag lined pattern Titanium Blade

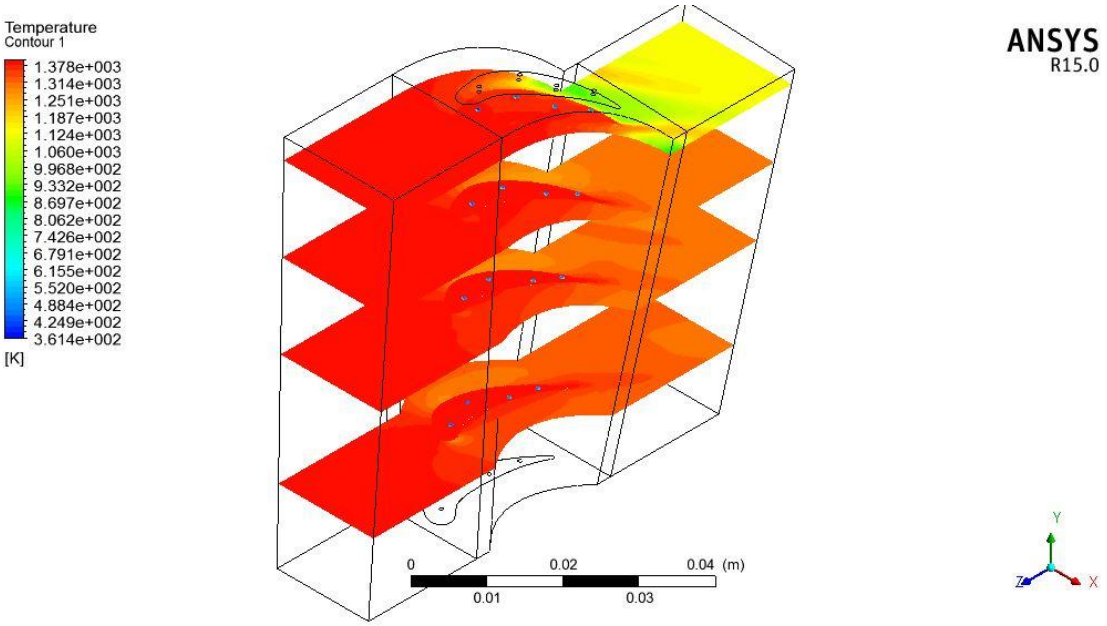

Fig. 4.22 Temperature Plot on Planes for Zigzag lined pattern Steel Blade

Fig. 4.19 through 4.21 represents the plot for the variation of temperature in the hole patterns for both the materials and both the patterns. Above temperature plot showing control volume temperature for all domain temperature decreases towards the bottom side. Exit temperature for all designs is same while the blade temperature is 38^0C less for zigzag design as compared to

straight lined design. Temperature of secondary fluid while exiting from steel blade is very high that's mean it is reached to is highest capacity to accept the heat, titanium is having much higher temperature rise, this plot is actually intended to resolve core temperature of blade and temperature at interface of blade and fluid domain.

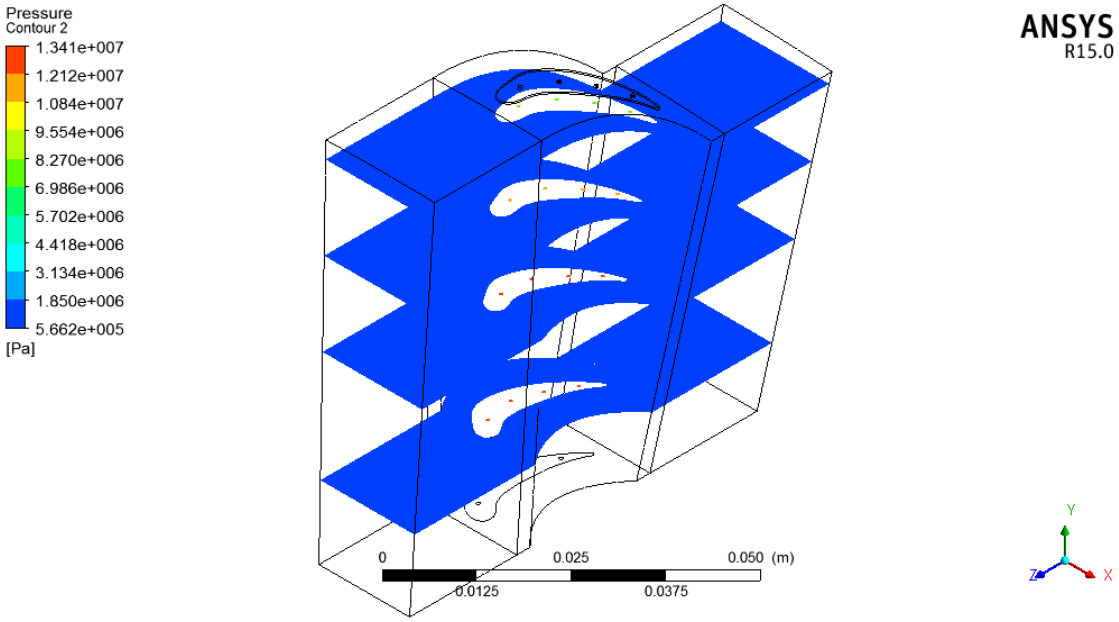

Fig. 4.23 Pressure Plot on Planes for straight lined pattern Titanium Blade

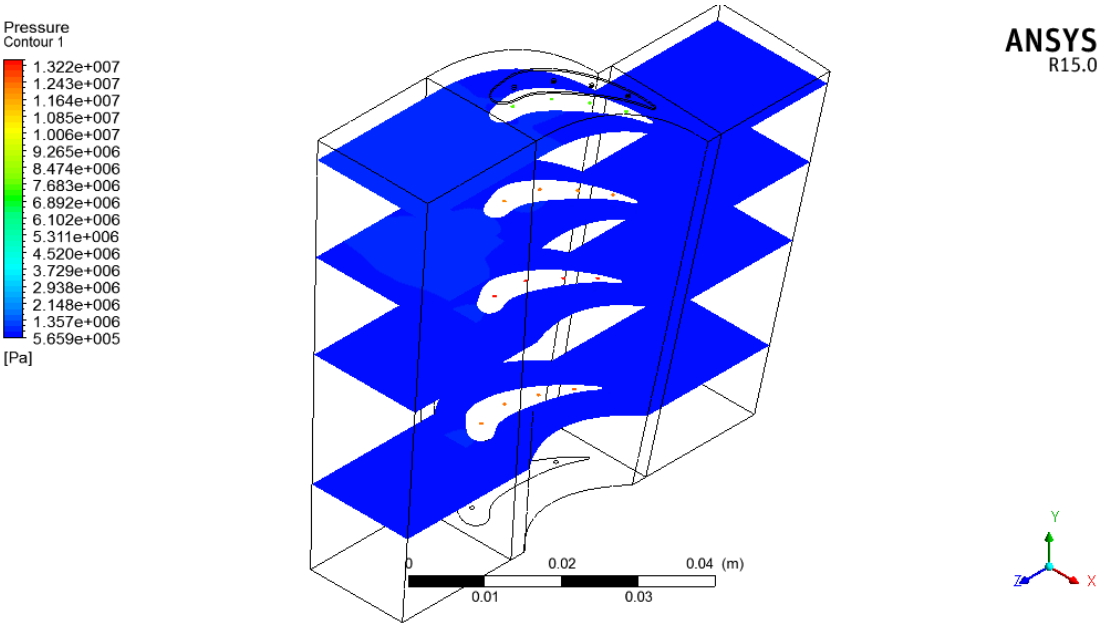

Fig. 4.24 Pressure Plot on Planes for straight lined pattern Steel Blade

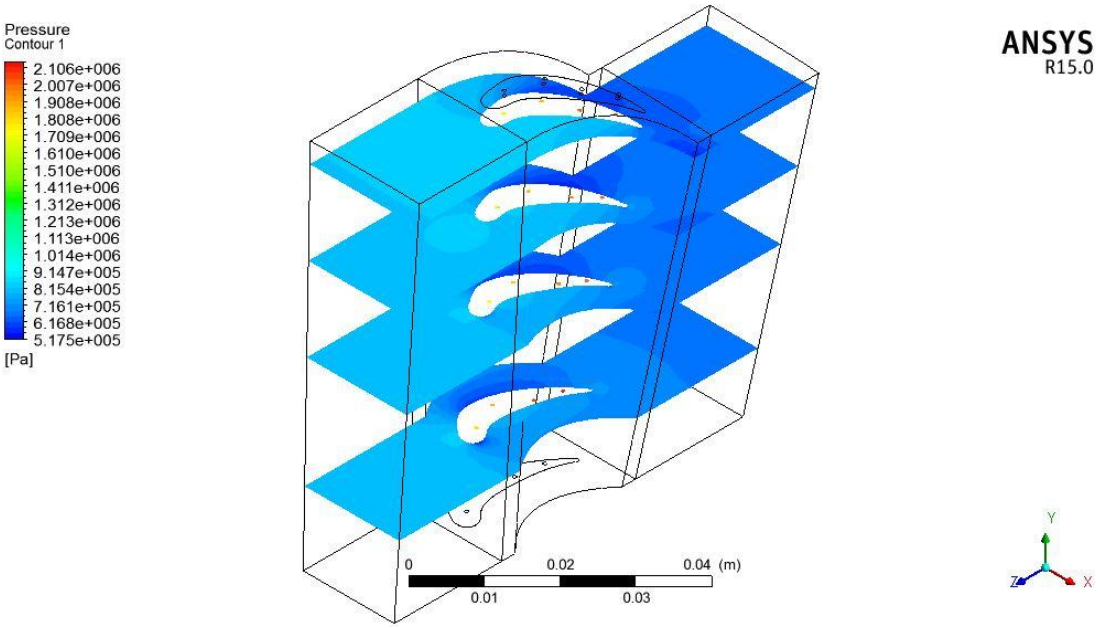

Fig. 4.25 Pressure Plot on Planes for Zigzag lined pattern Titanium Blade

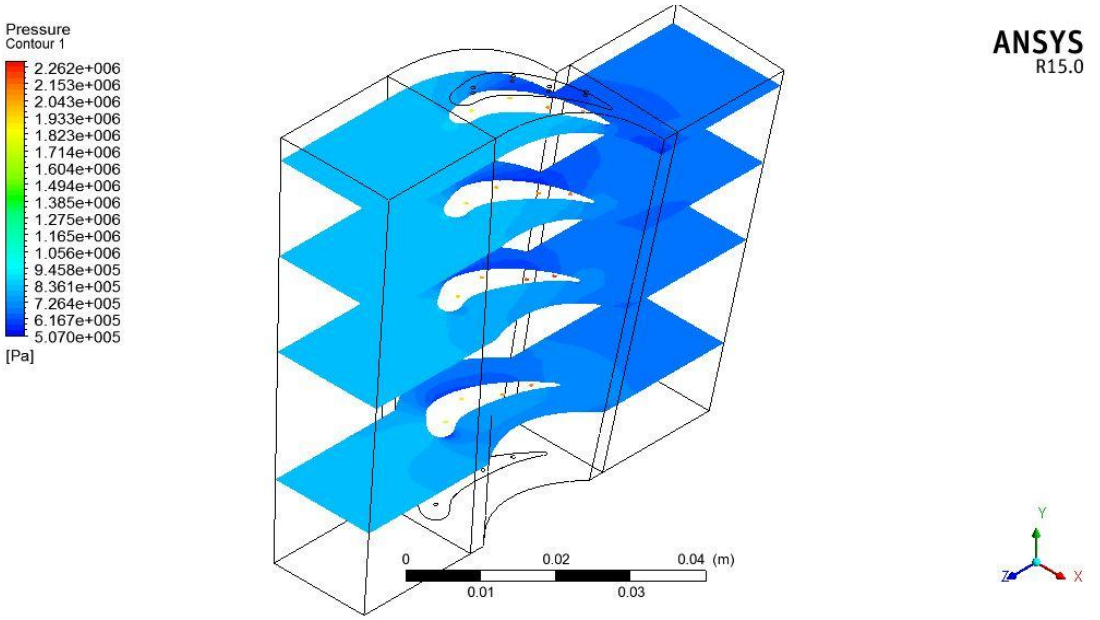

Fig. 4.26 Pressure Plot on Planes for Zigzag lined pattern Steel Blade

Fig. 4.23 and fig. 4.24 pressure plot on planes for straight lined pattern Titanium Blade and steel blade respectively. Pressure is uniformly distributed on planes shows the pressure inside the tube is highly varying if it is so temperature also could be high, causing less stability of the blade strength easy to subjected for creeping, pressure in first tube is lower than the last tube indicating more heat is absorbed at trailing edge in second design of zigzag pattern. More pressure variation

can be seen across the blade in second design that is effectiveness of turbine have increased slightly. Outside fluid pressure is lower than inside fluid so there will not be any chocking of fluid so all designs are seems to do well in that case. Fig. 4.25 and fig. 4.26 represent pressure plot on planes for zigzag lined pattern titanium blade and steel blade respectively. It has been observed pressure is almost same on blade surface for each of the material but for maximum value of pressure is higher in zigzag pattern with steel blade by 27000 Pa (gauge pressure). Lower pressure in zigzag pattern for titanium blade material compared to other designs, showing more efficient to increase the pressure drop across the blade.

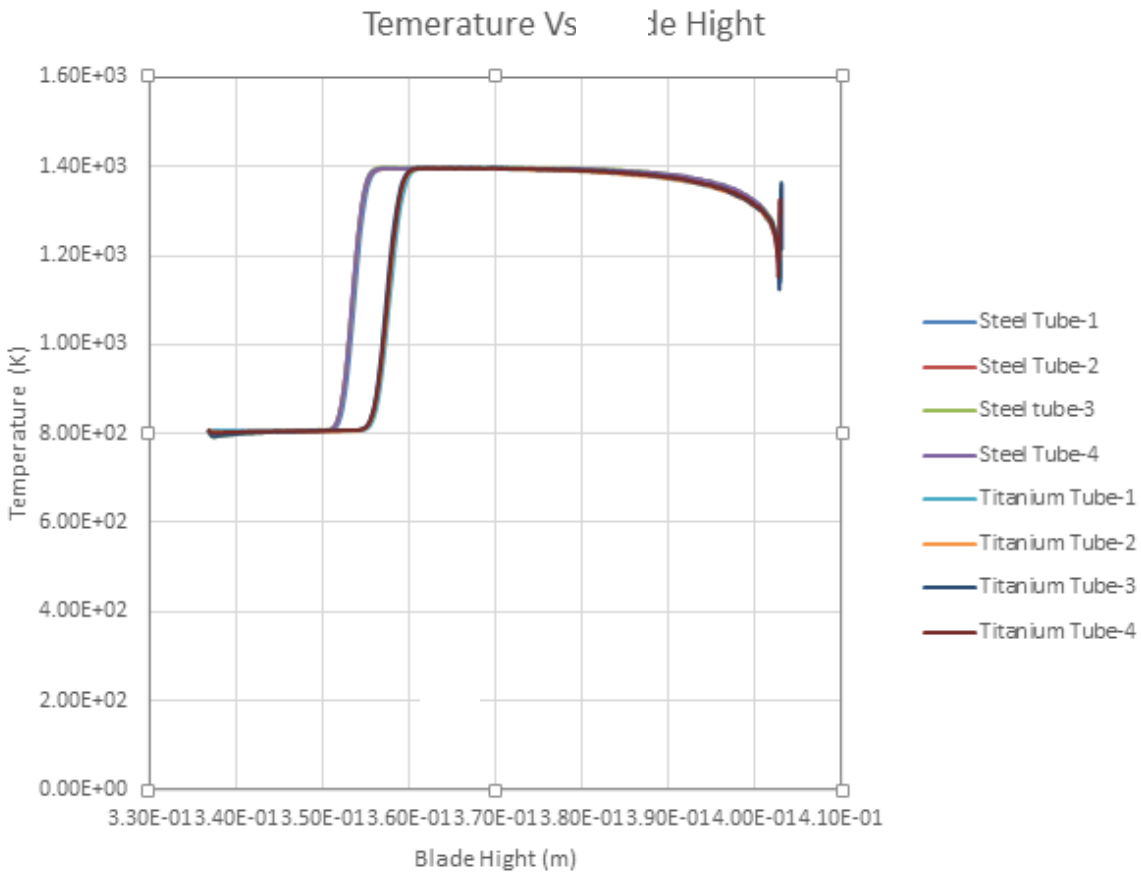

Fig. 4.27 Comparison for Straight lined pattern steel Blade

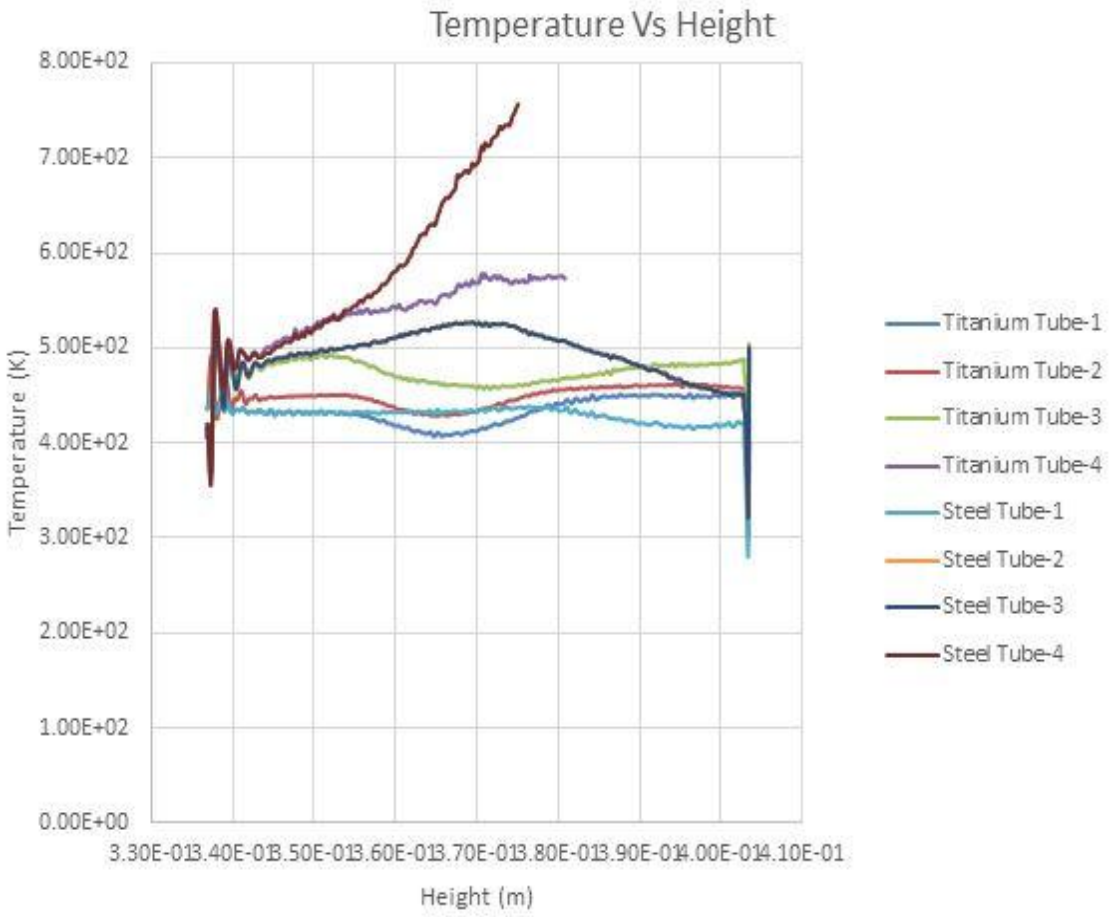

Fig. 4.28 Comparison Graph for zigzag lined pattern Titanium Blade

Fig. 4.27 and 4.28 represents graphical plot showing in all designs for particular one blade all cooling tubes are having same temperature variation among them. First design steel blade cooling fluid is getting heated very rapidly from 800K to 1200K then it is staying constant for some distance and when it is very near to blade upper opening once again it is cooled, after coming out from upper opening it is mixed with primary flowing fluid. This sudden very change in temperature may cause development of thermal stress; other characteristics are almost same excepting heating rate of the cooling fluid.

For second design, change in temperature is uniform in all tubes, except last one, because it is very near to the outer most surface. So, it will get heated exceptionally, that may cause to serious issue. For that reason, one may change the eccentricity of offset. Other characteristics of second design are showing almost same changes in terms of temperature. Because of diffusion, as soon as the fluid entering from the bottom side it is getting cooled rapidly, that temperature is nothing but the starting point temperature.

4.3 Results for 30 Pressure Ratio Design for inlet temperature 1200 K

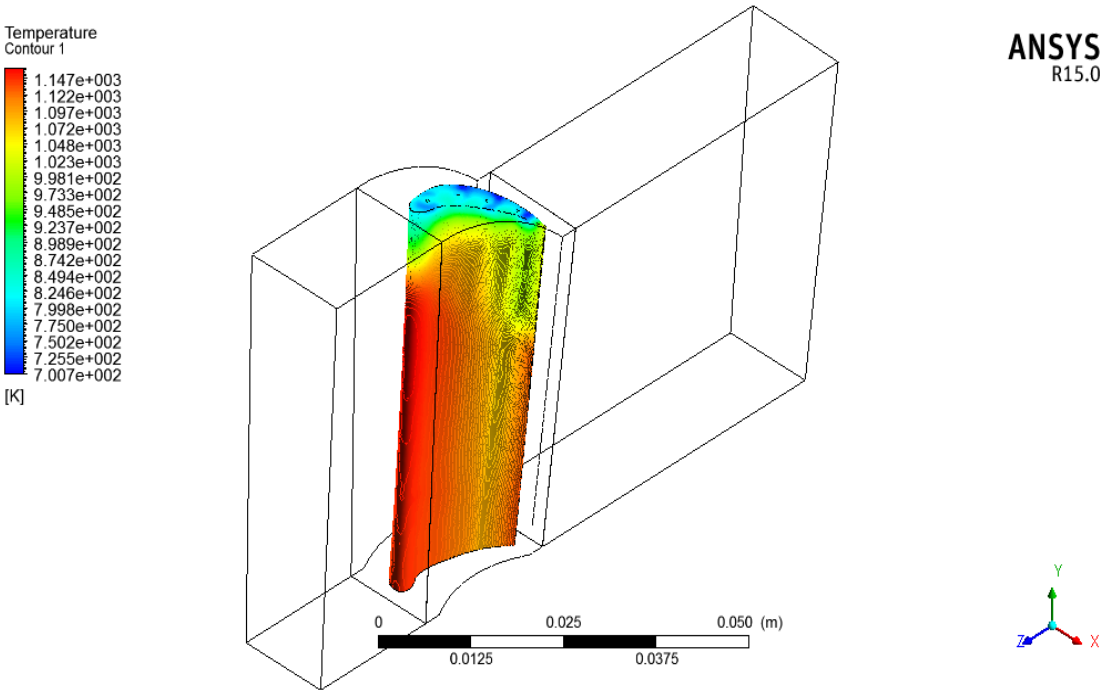

Fig. 4.29 Temperature of blade for Titanium blade (straight lined pattern)

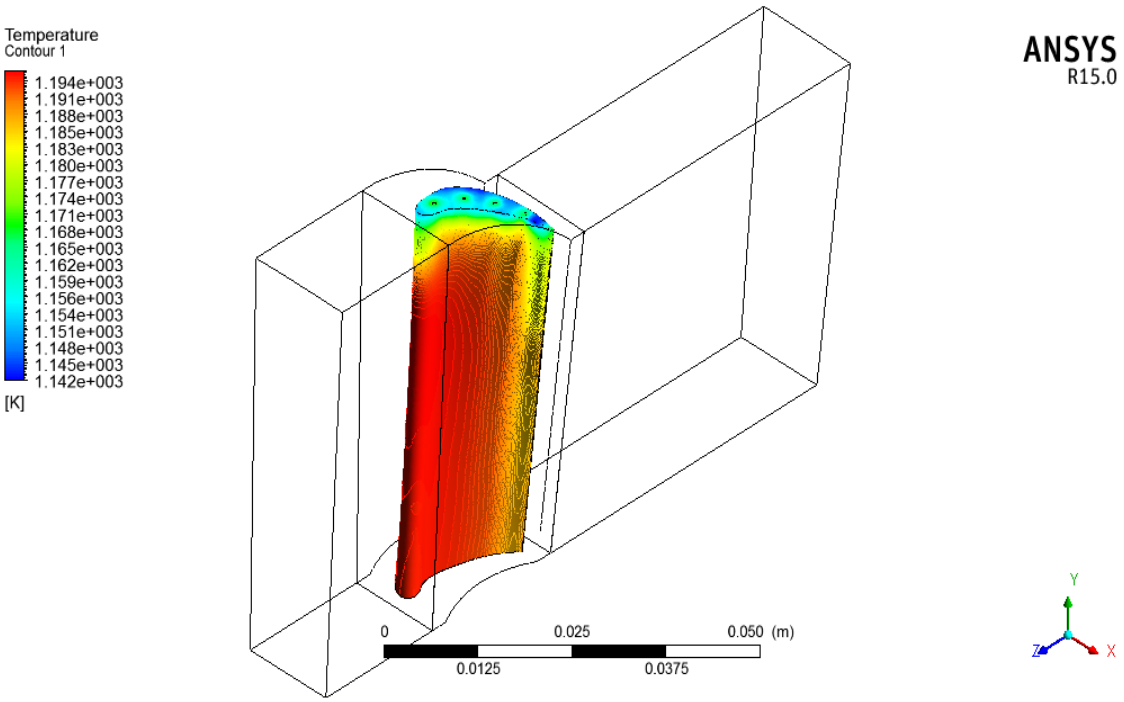

Fig. 4.30 Temperature of blade for Steel blade (straight lined pattern)

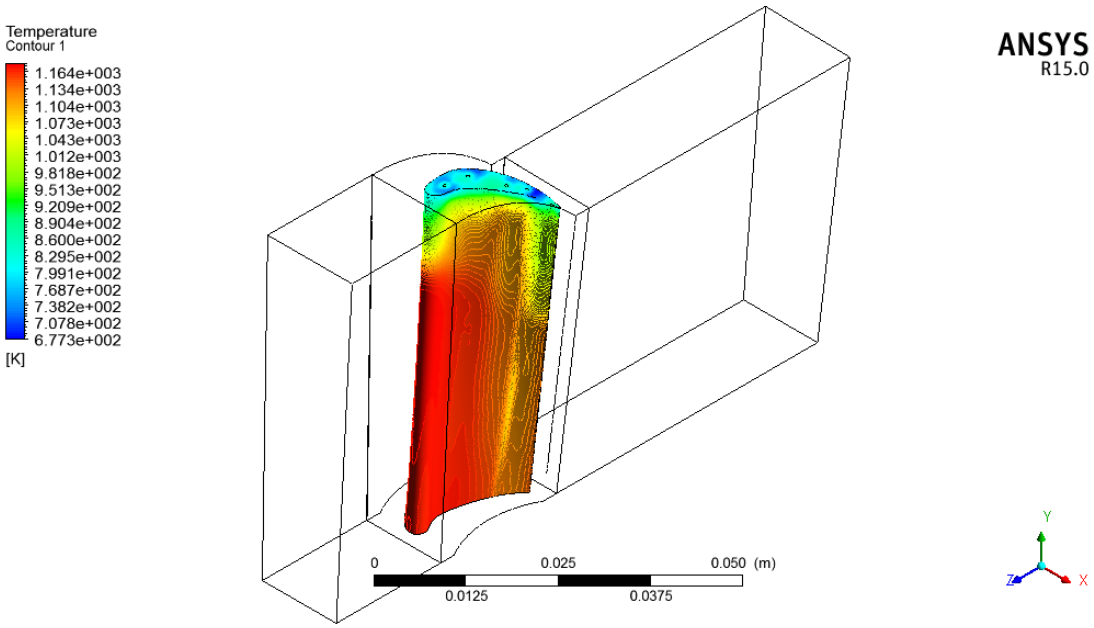

Fig. 4.31 Temperature of blade for Titanium blade (Zigzag lined pattern)

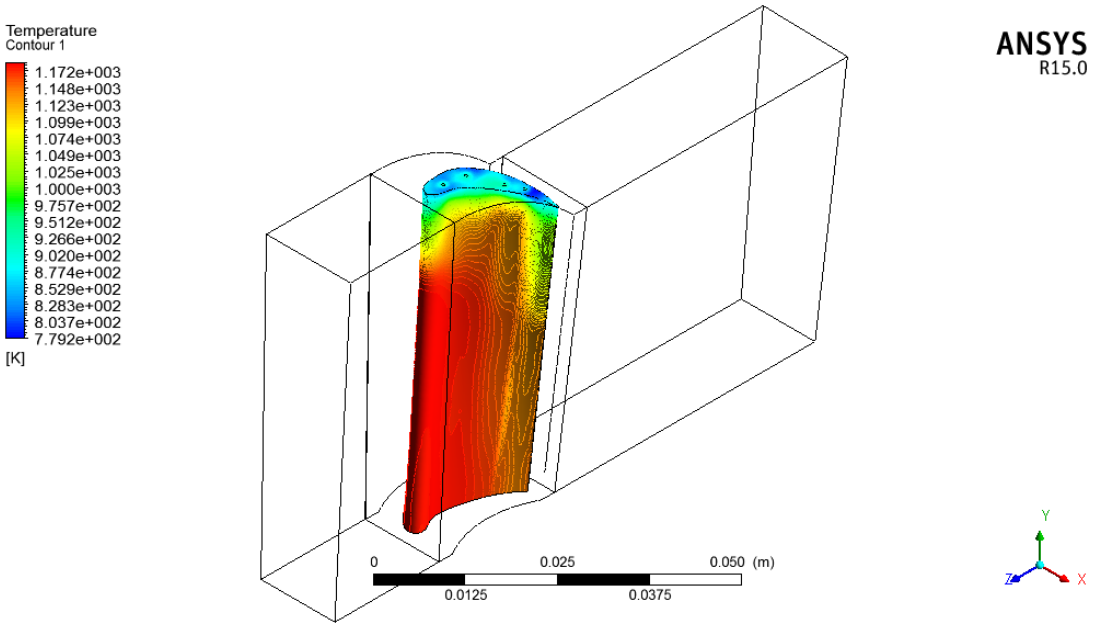

Fig. 4.32 Temperature of blade for Steel blade (Zigzag lined pattern)

By keeping the pressure and temperature of secondary inlet constant it has been observed that this is causing increase in velocity of secondary fluid causing lower heat transfer coefficient. There are two reasons for that one is blade height is less than blade height present in design for pressure ratio 20. Ultimately blade surface got decrease which was in contact previously. Here,

contour plots are almost same for each design and maximum temperature present in both designs is also almost same approximately by 17-22^{0}C. Volume averaged temperature in zigzag pattern for titanium blade is 1115K for steel blade is 1140K for titanium with straight lined pattern 1081.37K and for steel with straight lined pattern 1191.21K. Leading edge is exposed to higher temperature always there is no chance of making any kind of perforation because aerodynamics of blade will be poor. Though the contour plots are same, temperature difference is very high and therefore, carefully need for examine the legends of plots.

Pressure distribution causes the turbine to rotate. The pressure contour plots show the comparison. Pressure in first design is concentrated on leading edge and lower in second design. Higher and lower pressure locations are same in both the designs but pressure values are different and if it is exceeding certain value then the blade may deform permanently according to applied position.

This contour plot is showing external cooling, wall heat transfer coefficient for blade its value is positive means it absorbs the heat and not rejecting it from outer surface. Leading edge is highly affected and subjected to high temperature, one can suggest the decrement of cord length from hub to tip of the blade i.e. lowest cord length for tip airfoil that will cause the uniform heating of blade and there may not be induction of thermal stress.

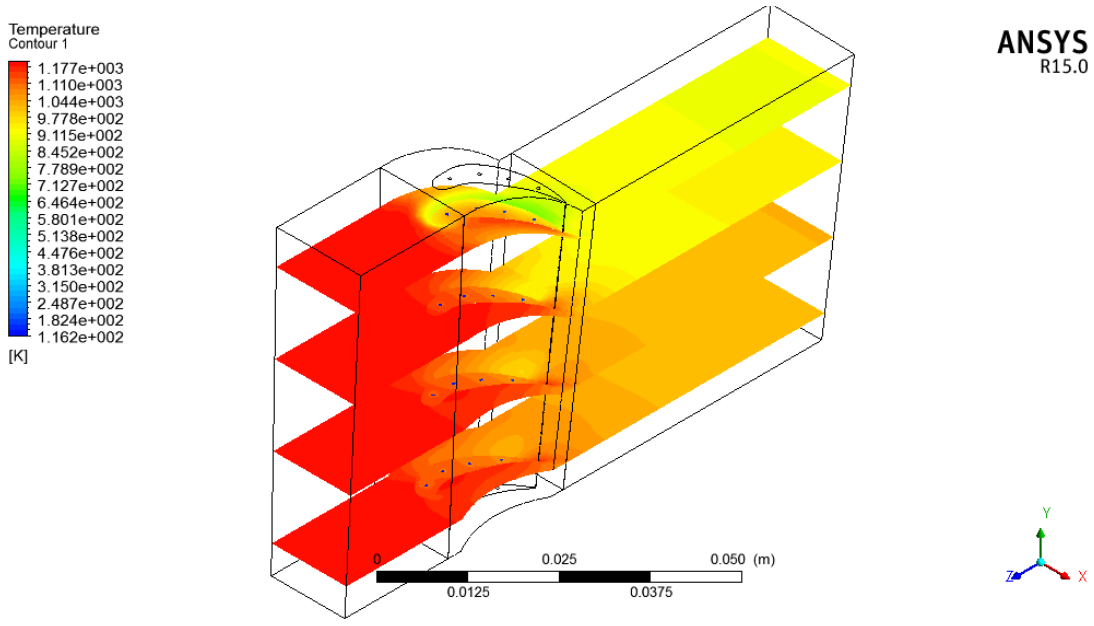

Fig. 4.33 Temperature plot on planes for Titanium blade (Straight lined pattern)

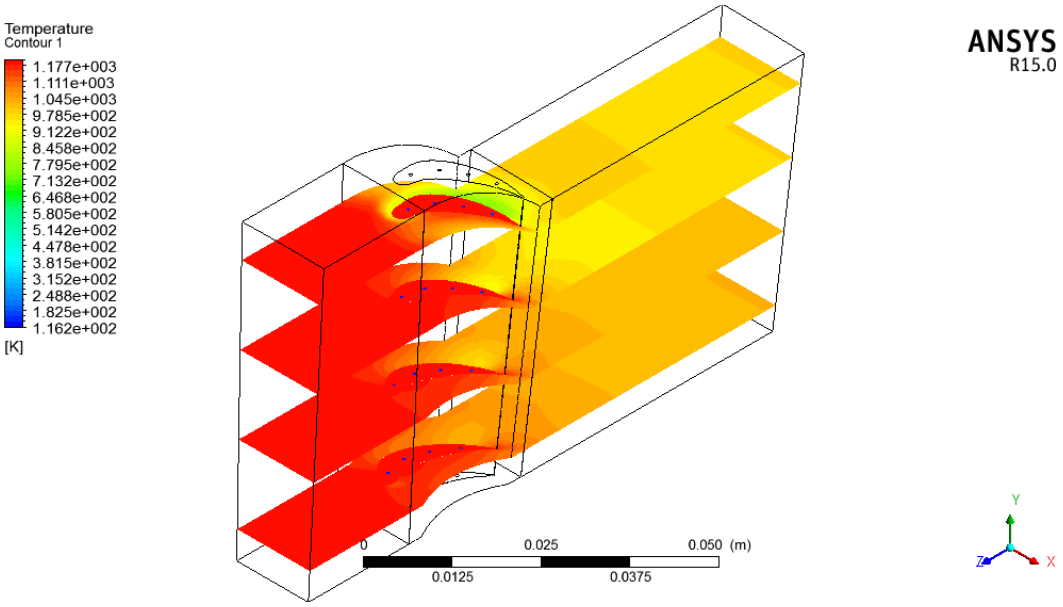

Fig. 4.34 Temperature plot on planes for steel blade (Straight lined pattern)

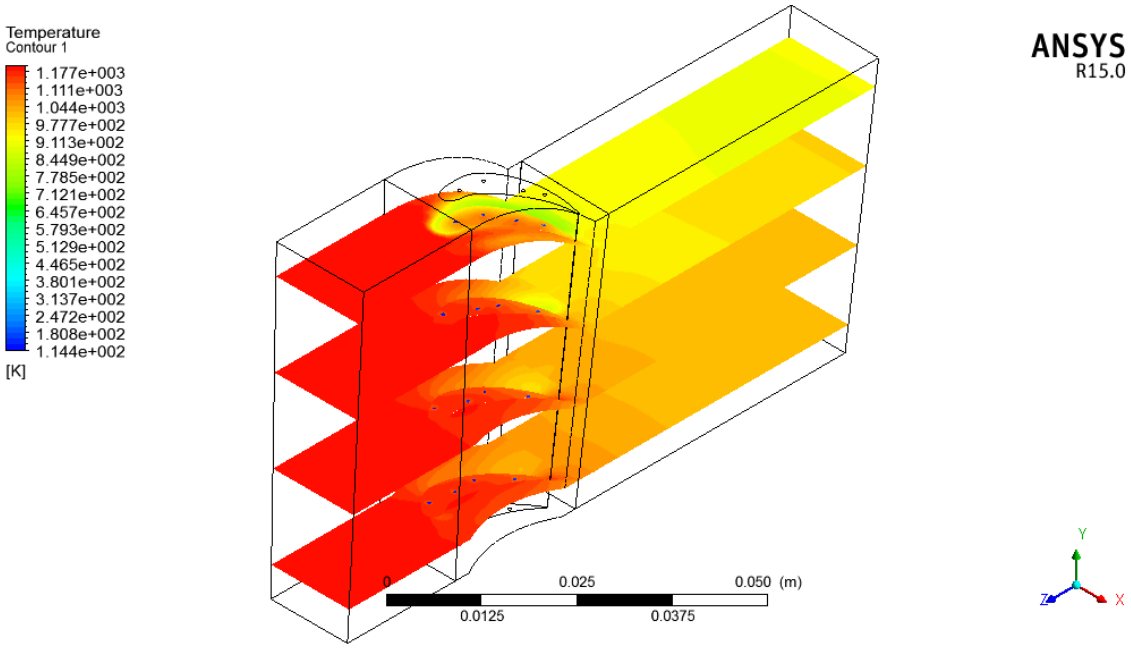

Fig. 4.35 Temperature plot on planes for Titanium blade (Zigzag lined pattern)

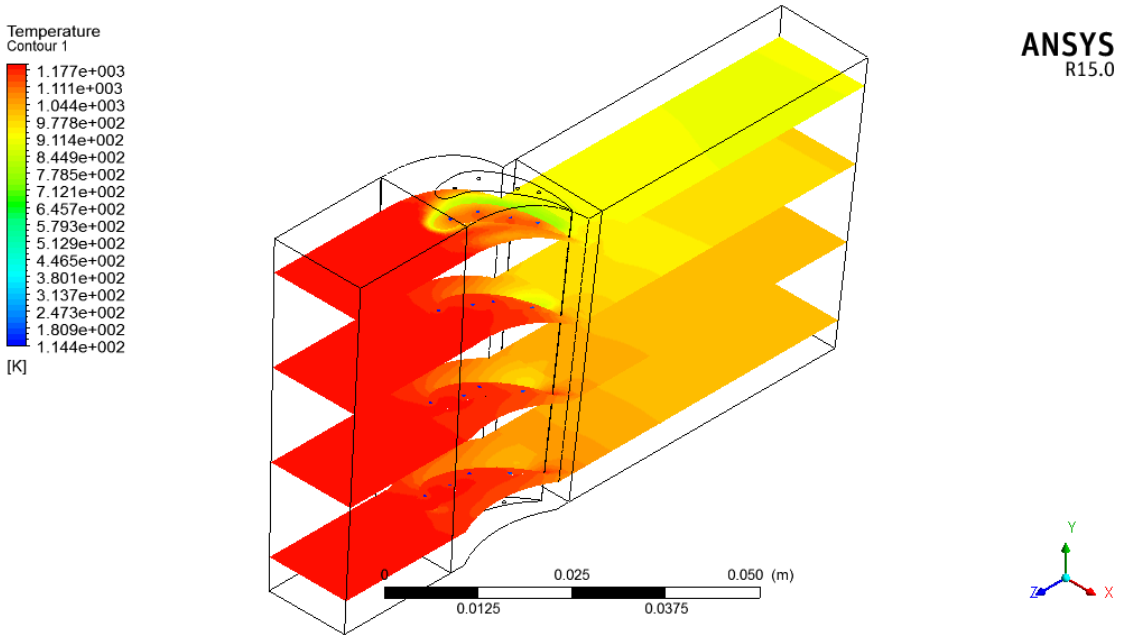

Fig. 4.36 Temperature plot on planes for steel blade (Zigzag lined pattern)

Fig. 4.32 and fig. 4.33 show the temperature plot on planes for Titanium blade and steel blade for straight lined pattern respectively. Here on temperature plot it seems to have almost same distribution. Above temperature plot showing control volume temperature for all domain temperature goes on decreasing towards the bottom side.

Fig. 4.34 and fig. 4.35 represents temperature plot on planes for Titanium blade steel blade for straight lined pattern. Exit temperature for all designs is same while the blade temperature is 20^0C less for zigzag design as compared to straight lined design. Temperature of secondary fluid, while exiting from steel blade is very high. That means it is reached to highest capacity to bear the heat. Titanium is having much higher temperature rise due to its thermal properties. This plot is actually intended to resolve core temperature of blade and temperature at interface of blade and fluid domain.

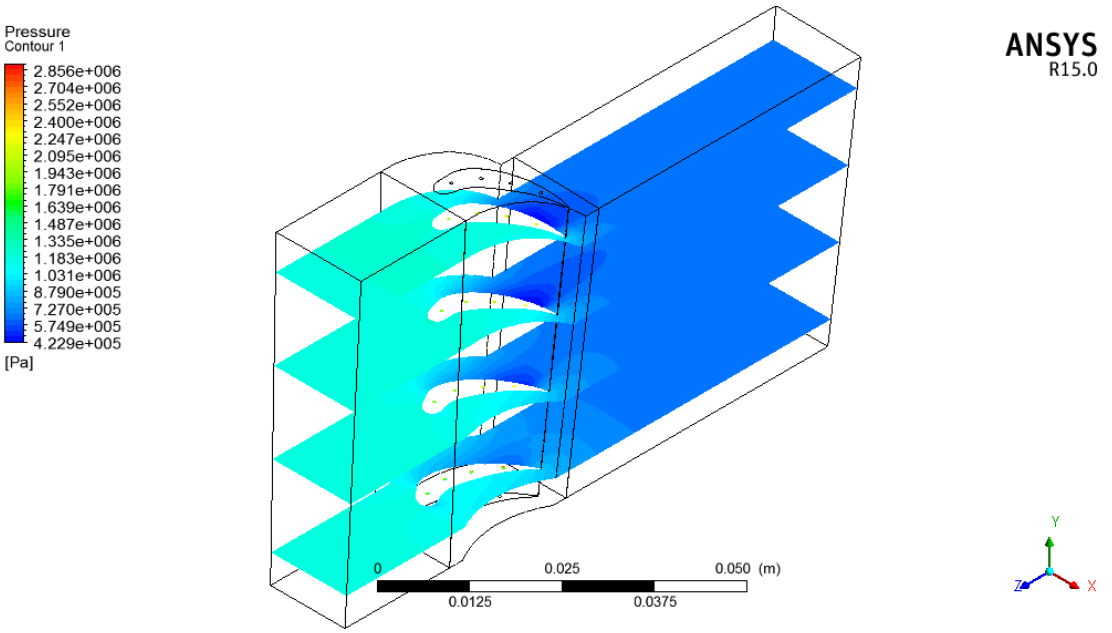

Fig. 4.37 Pressure plot on planes for titanium blade (Straight lined pattern)

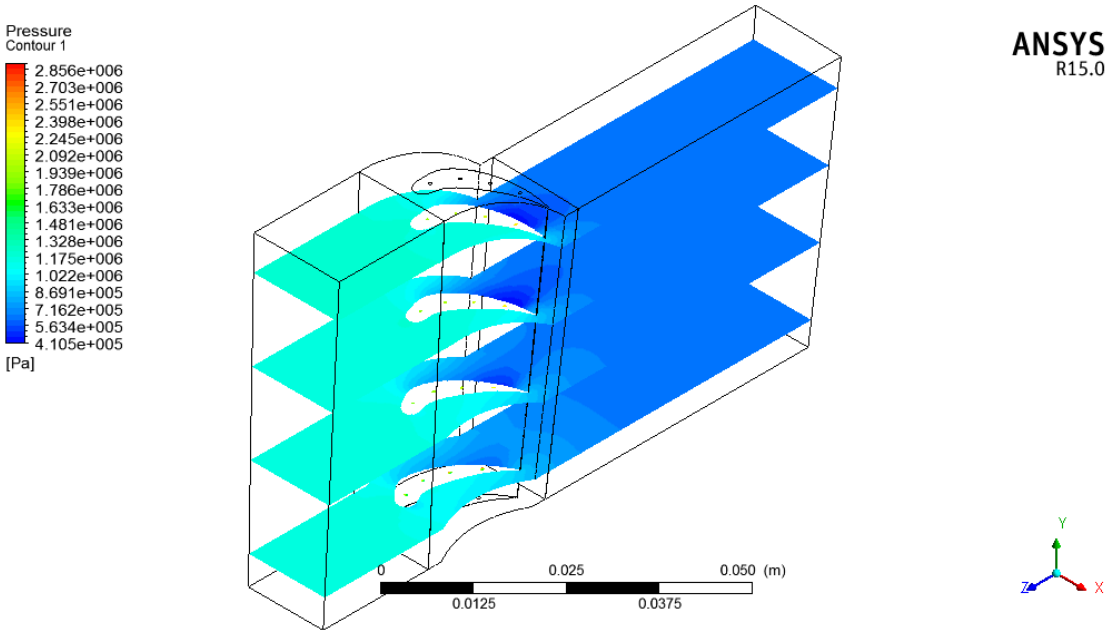

Fig. 4.38 Pressure plot on planes for steel blade (Straight lined pattern)

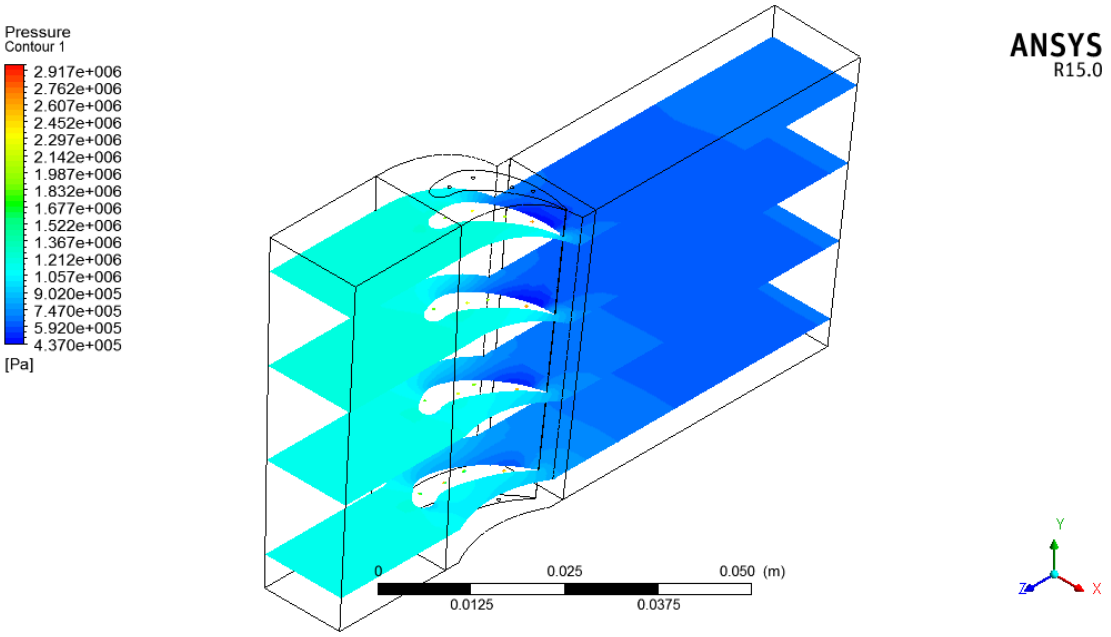

Fig. 4.39 Pressure plot on planes for Titanium blade (Zigzag lined pattern)

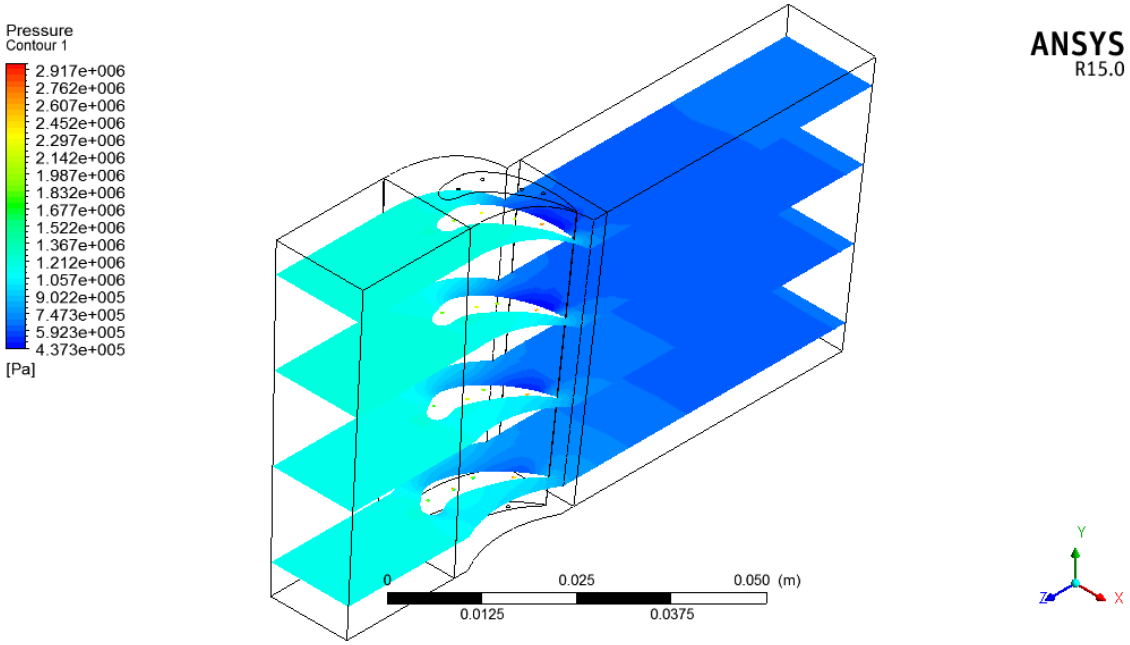

Fig. 4.40 Pressure plot on planes for steel blade (Zigzag lined pattern)

Fig. 4.36 and fig. 4.37 represents pressure plot on planes for titanium blade and steel blade for straight lined pattern. While fig. 4.38 and fig. 4.39 reflects pressure variations for titanium blade and steel blade for zigzag lined pattern respectively. Pressure is uniformly distributed on planes shows the pressure inside the tube is highly varying it results in increase the temperature. This

causes less stability of the blade strength and easy to creep. Pressure in first tube is lower than the last tube indicating more heat is absorbed at trailing edge in second design of zigzag pattern. More pressure variation can be seen across the blade in second design that is effectiveness of turbine blade have increased slightly. Outside fluid pressure is lower than inside fluid pressure and therefore, there will not be any chocking of fluid. Hence, all designs are seems to do well in that case.

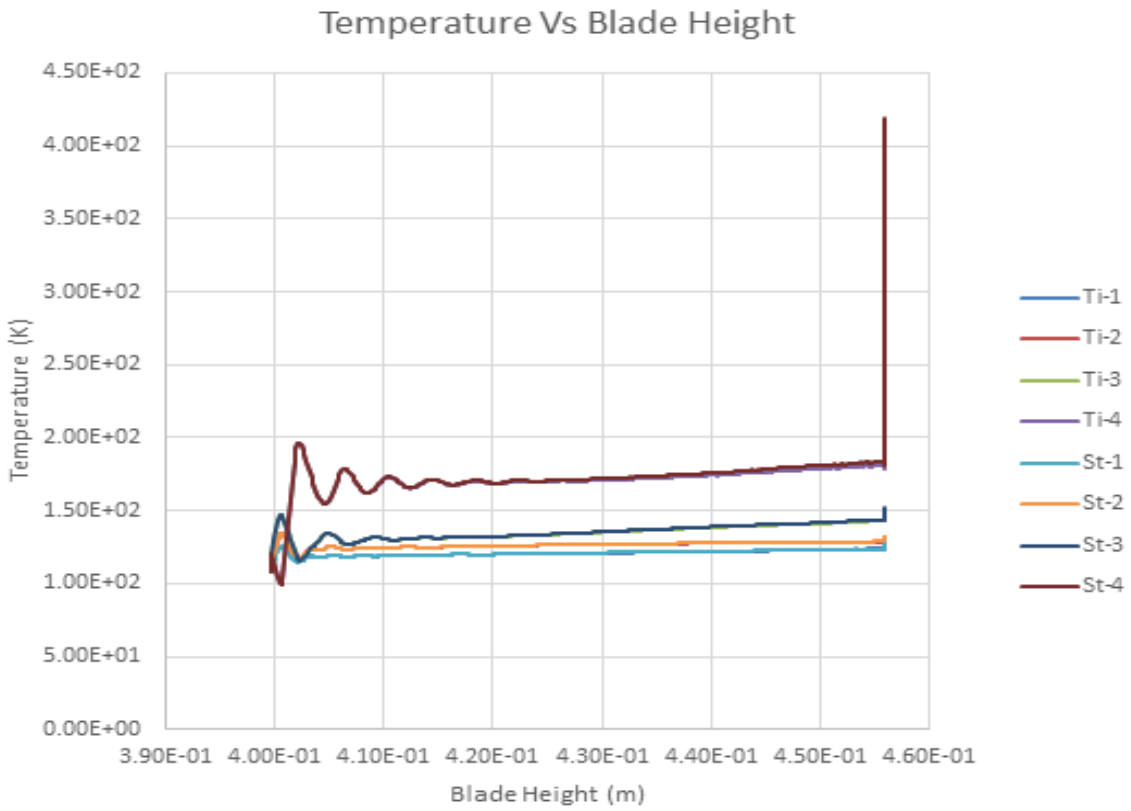

Fig. 4.41 Temperature variation with blade height for straight lined pattern blade

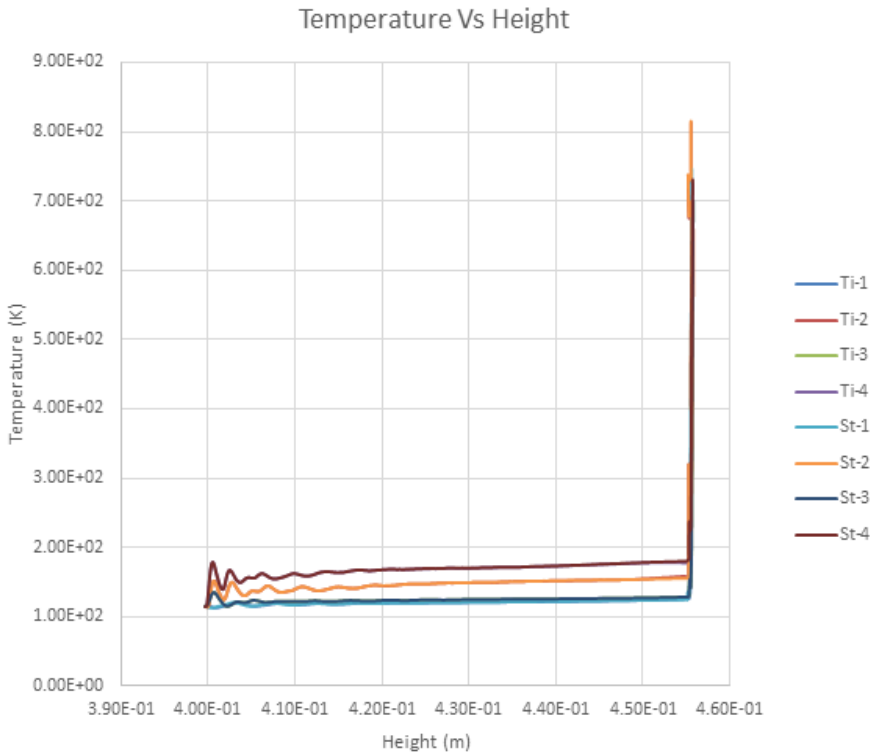

Fig. 4.42 Temperature variation with blade height for zigzag lined pattern blade

Fig. 4.40 and fig. 4.41 represents the comparison for straight lined pattern blade for zigzag lined pattern blade respectively. Above graphical plot showing, in all designs for particular one blade all cooling tubes are having same temperature variation among them. First design, with steel blade cooling fluid is getting heated gradually then it is staying constant for some distance and when it is very near to blade upper opening once again it is heated, after coming out from upper opening it is mixed with primary flowing fluid. This sudden very change in temperature may cause development of thermal stress; other characteristics are almost same excepting heating rate of the cooling fluid.

For second design, change in temperature is uniform in all tubes; irrespective of material the rate of increase in temperature is constant for particular tube. In zigzag design very little change is we are getting for titanium and steel, there is possibility it is because of high mass flow rate we can reduce the internal mass flow rate and size of the holes. It is important that if we are using blade material as steel with zigzag pattern cooling will be highly efficient so, design will be more economical. Averaged Wall heat transfer coefficient for zigzag design is 847 W/m^2-K with both the materials.

4.4 Results for 30 Pressure Ratio for inlet temperature 1400 K

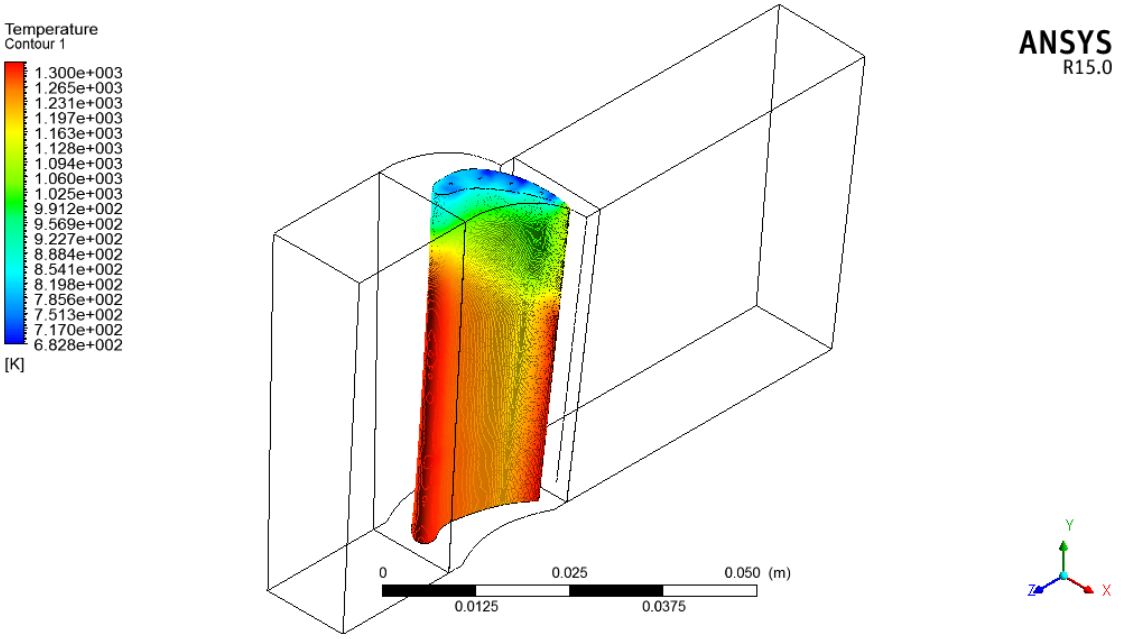

Fig. 4.43 Temperature of blade for Titanium blade (straight lined pattern)

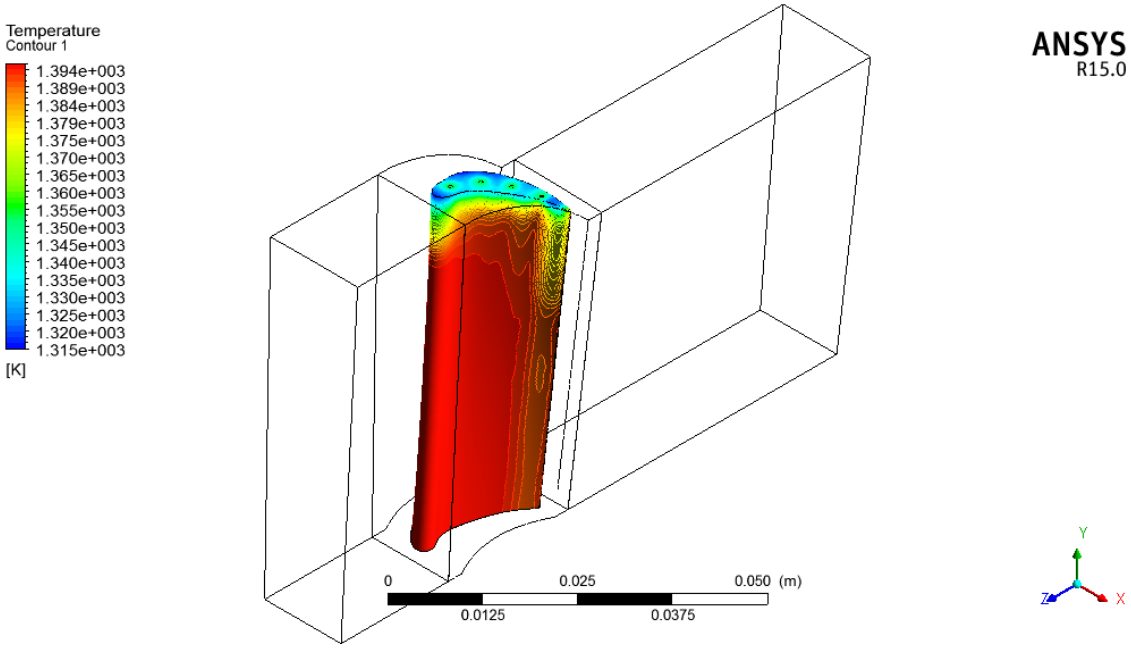

Fig. 4.44 Temperature of blade for Steel blade (straight lined pattern)

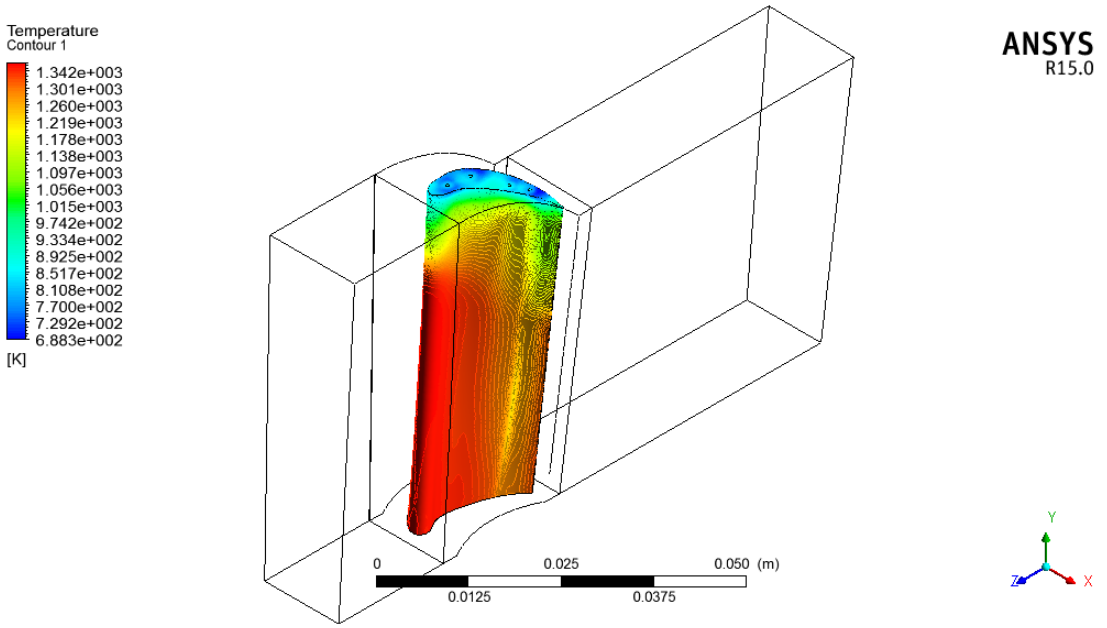

Fig. 4.45 Temperature of blade for Titanium blade (zigzag lined pattern)

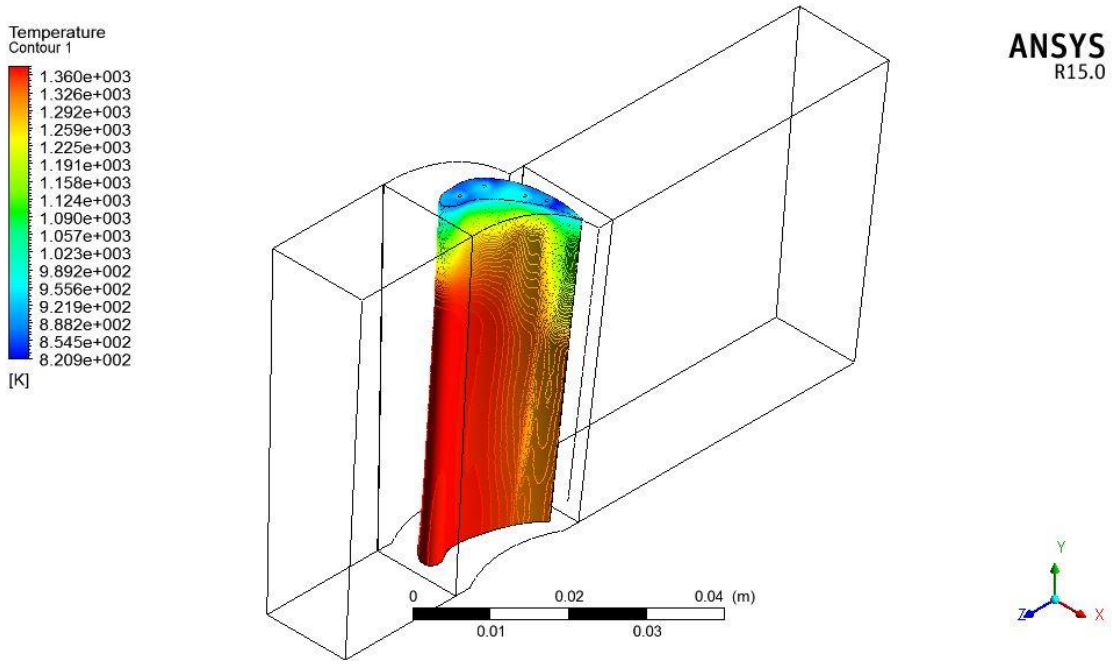

Fig. 4.46 Temperature of blade for Steel blade (zigzag lined pattern)

Fig. 4.41 and fig. 4.42 show the temperature variation of internal hole for titanium blade steel blade for straight lined pattern. By keeping the pressure and temperature of secondary air inlet

constant it has been found that there is an increase in velocity of secondary fluid causing lower heat transfer coefficient. There are two reasons for that one is blade height is lesser than blade height present in design for pressure ratio 30 ultimately surface are got decrease which was in contact previously. Here, contour plots are almost same for each design and maximum temperature present in both designs is also almost same approximately 17-22^{0}C difference is there. Volume average temperature in zigzag pattern for titanium blade is 1258.98K. Leading edge is exposed to higher temperature always there is no chance of making any kind of perforation because aerodynamics of blade will be poor. Hence, the contour plots are same temperature difference is very high and careful check is needed for plots. Fig. 4.43 and fig. 4.44 show the temperature of blade for titanium blade and steel blade for zigzag lined pattern.

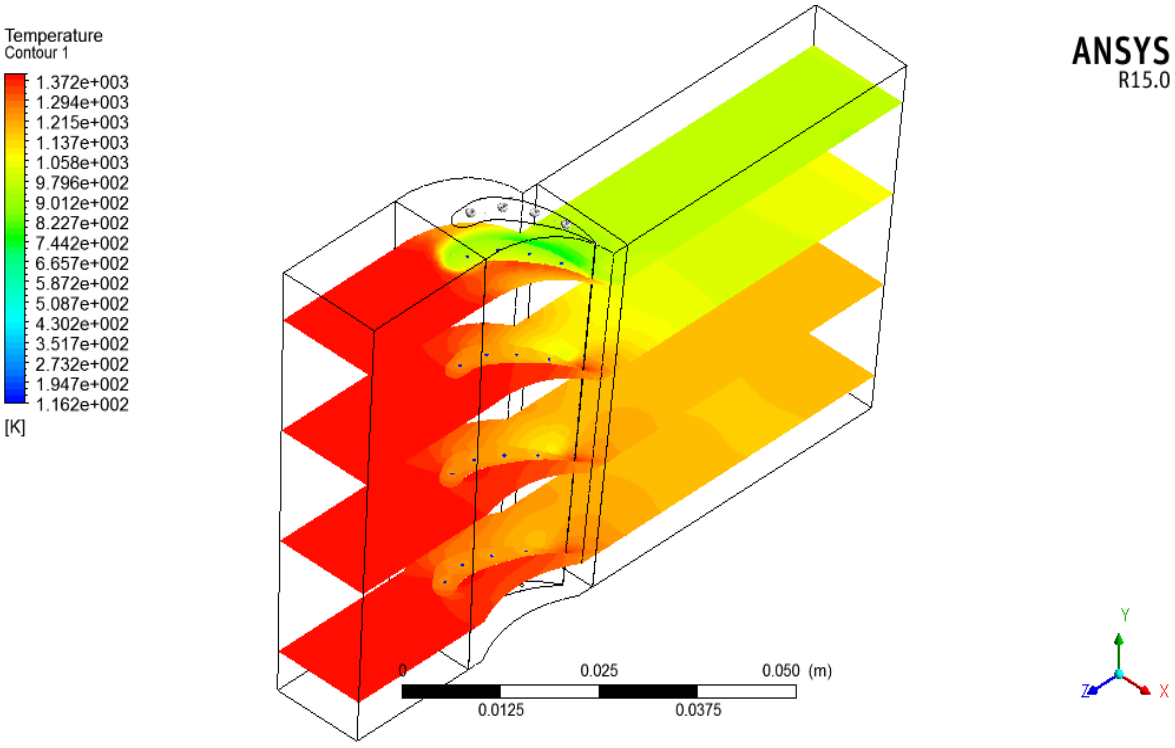

Fig. 4.47 Temperature plot on planes for Titanium blade (Straight lined pattern)

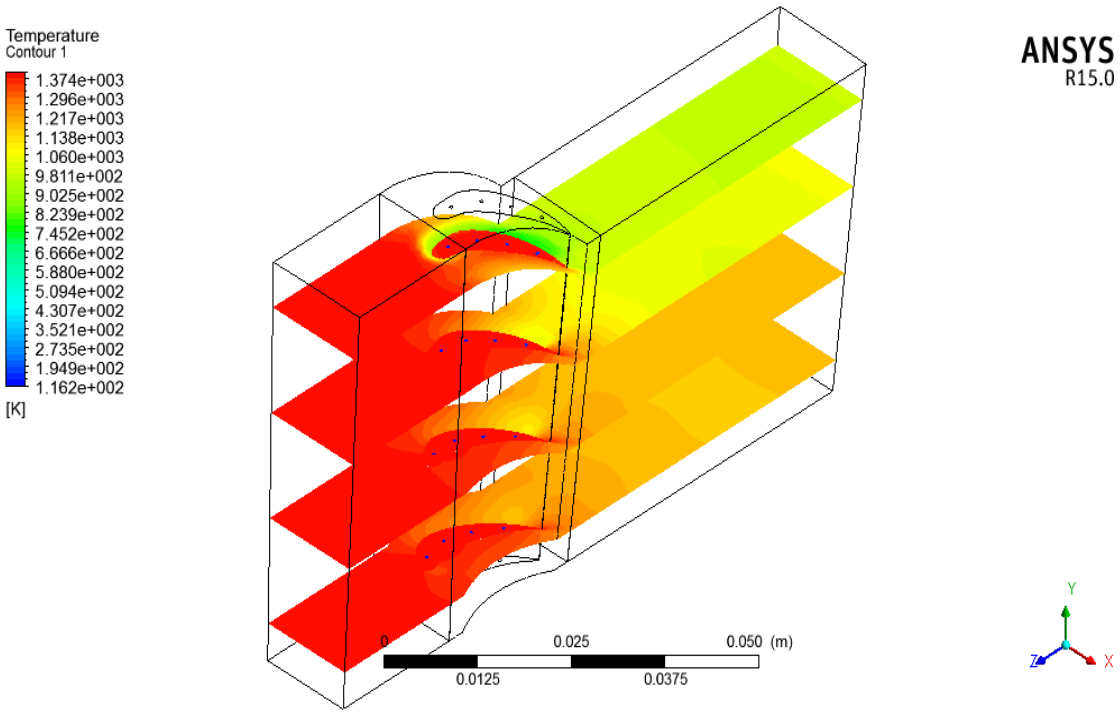

Fig. 4.48 Temperature plot on planes for steel blade (Straight lined pattern)

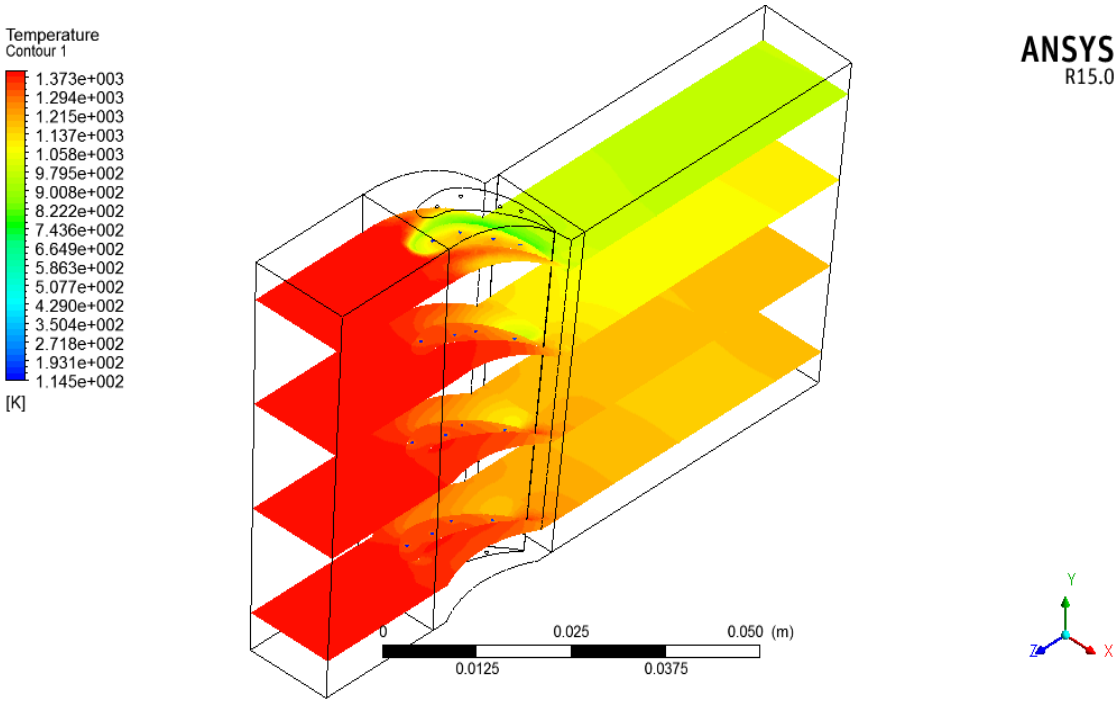

Fig. 4.49 Temperature plot on planes for Titanium blade (Zigzag lined pattern)

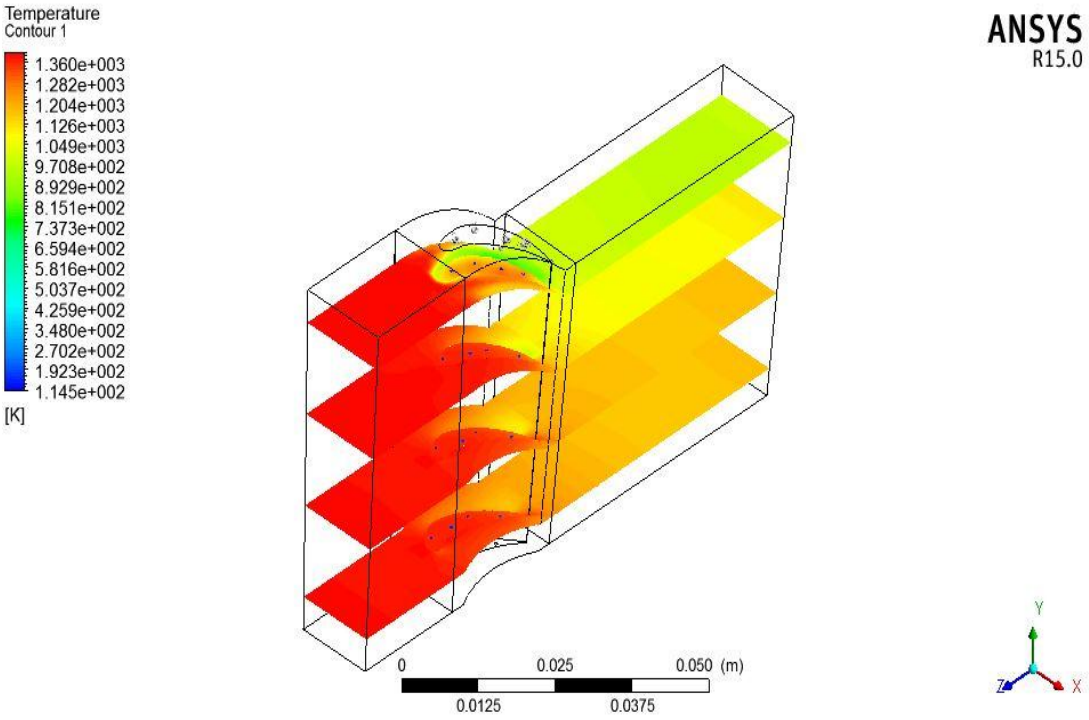

Fig. 4.50 Temperature plot on planes for steel blade (Zigzag lined pattern)

Fig. 4.45 and fig. 4.46 show the temperature plot on planes for titanium blade and steel blade for straight lined pattern. These figures are plotted for the cooling of holes rather than entire blade surface. Here, on temperature plot it seems to have almost same distribution. Above temperature plot showing control volume temperature for all domain temperature goes on decreasing towards the bottom side. Exit temperature for all designs is same while the blade temperature is 20^0C less for zigzag design as compared to straight lined design. Temperature of secondary fluid while exiting from steel blade is very high that means it is reached to highest capacity to absorb the heat. Titanium is having much higher temperature rise. This plot is actually intended to resolve core temperature of blade and temperature at interface of blade and fluid domain. Fluid coming out from cooling tubes impacting on top blade surface making high turbulence area and this velocity far lower than velocity got in design pressure ratio 30. With zigzag and with straight lined holes difference is only 20 m/s. that means irrespective of tube pattern the velocity is affecting on upper most surface of blade only that is shown in above plots.

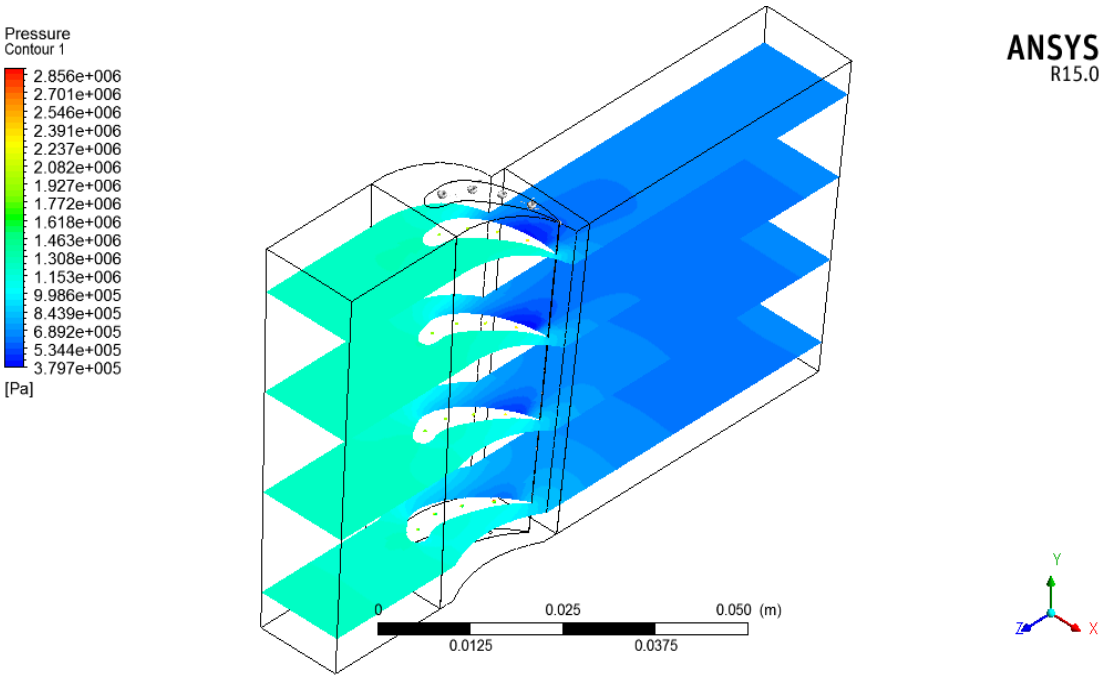

Fig. 4.51 Pressure plot on planes for titanium blade (Straight lined pattern)

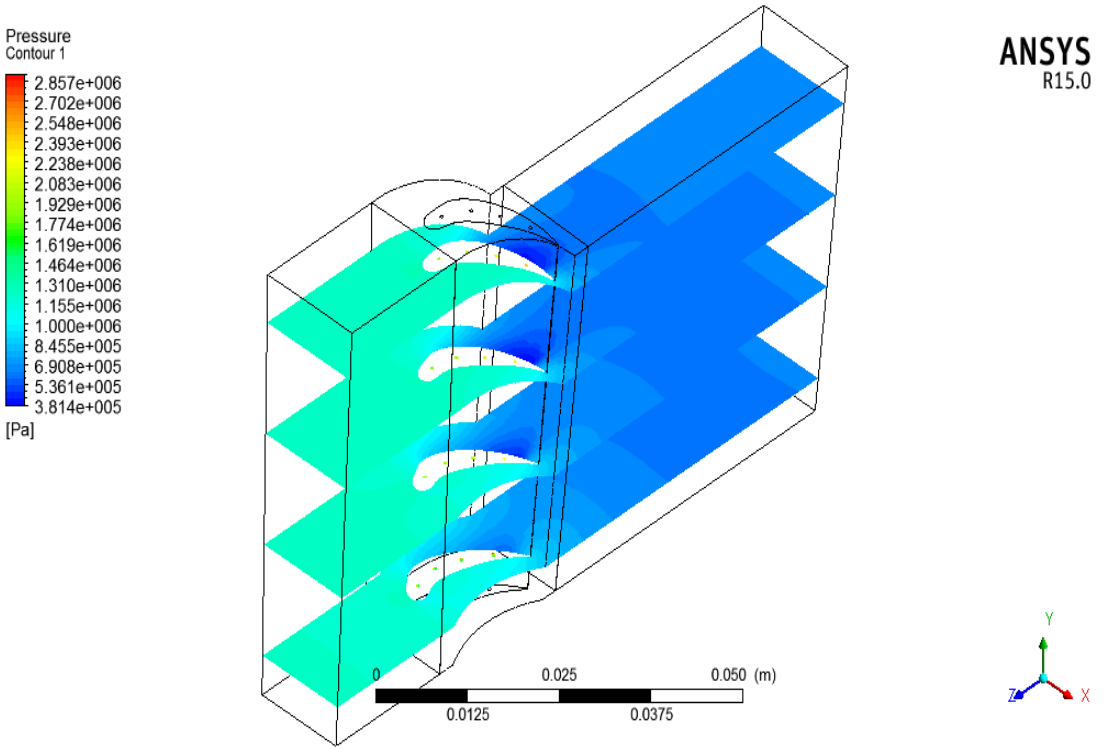

Fig. 4.52 Pressure plot on planes for steel blade (Straight lined pattern)

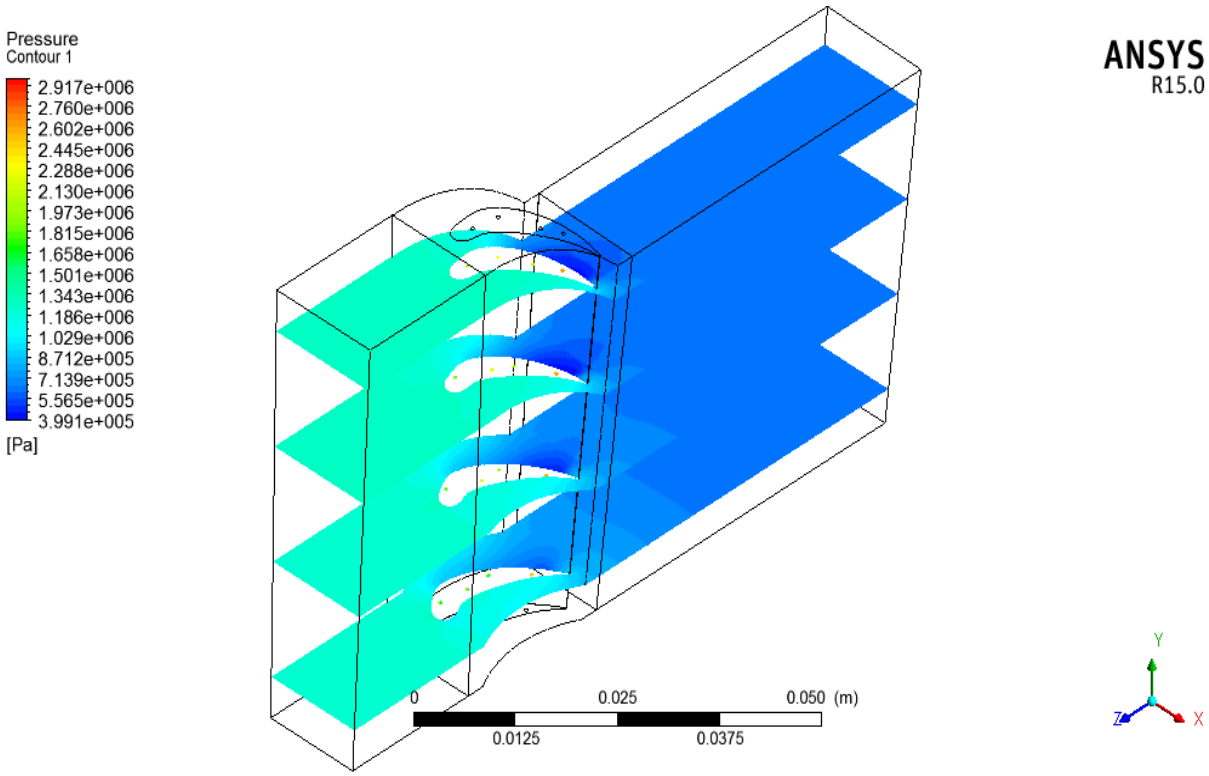

Fig. 4.53 Pressure plot on planes for Titanium blade (Zigzag lined pattern)

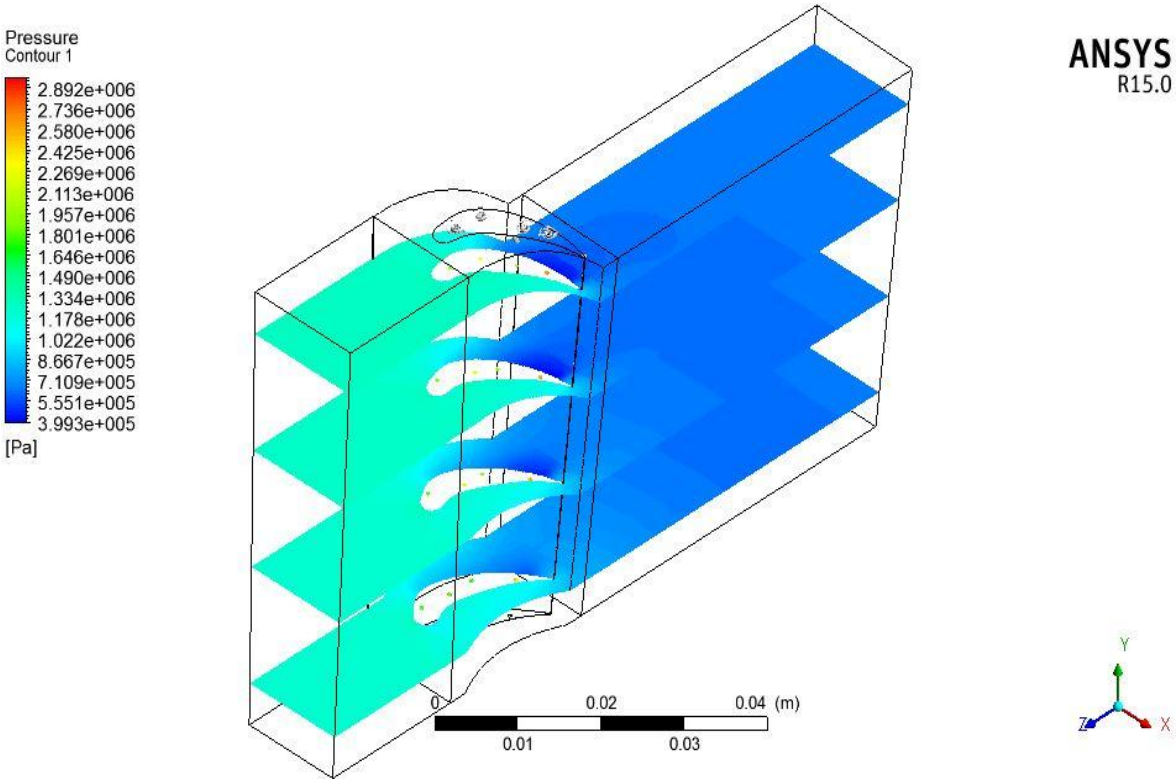

Fig. 4.54 Pressure plot on planes for steel blade (Zigzag lined pattern)

Fig. 4.49 through fig. 4.52 represents the pressure plot on planes for titanium blade and steel blade for straight lined pattern and zigzag lined pattern respectively. Pressure is uniformly distributed on planes shows the pressure inside the tube is highly varying. Due to this reason, temperature could also be high, causing less stability of the blade strength easy to subject for creep. Pressure in first tube is lower than the last tube indicating more heat is absorbed at trailing edge in second design of zigzag pattern. More pressure variation can be seen across the blade in second design that is effectiveness of turbine have increased slightly. Outside fluid pressure is lower than inside fluid so there will not be any chocking of fluid so all designs are seems to do well in that case.

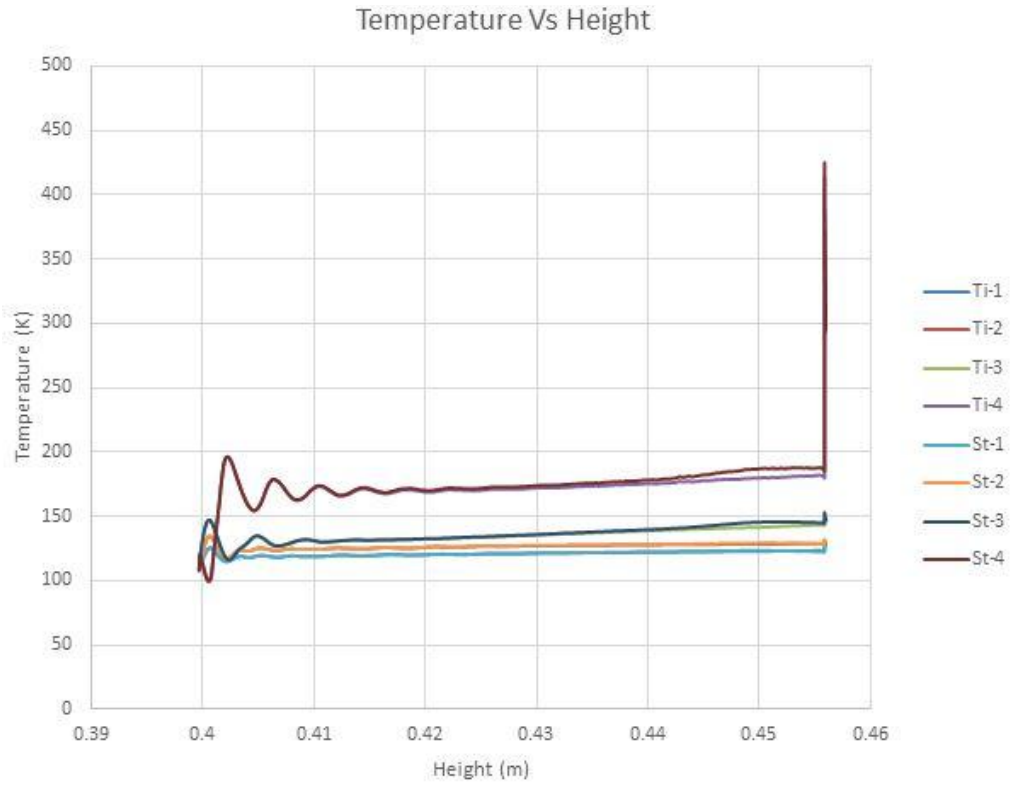

Fig. 4.55 Temperature variation with height of blade for straight lined pattern blade

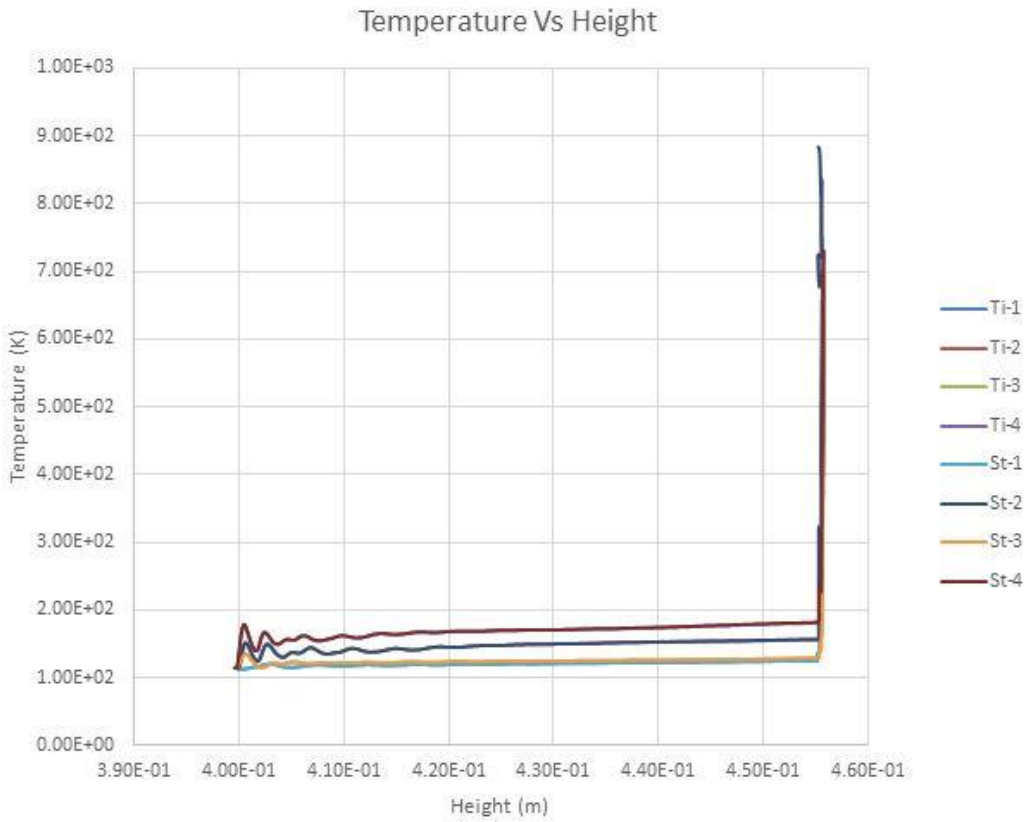

Fig. 4.56 Temperature variation with height of blade for zigzag lined pattern Blade

Fig. 4.53 and fig. 4.54 represents the variation of temperature inside the hole with blade height for straight line pattern and zigzag lined pattern blade. Above graphical plot showing, in all designs for particular one blade all cooling tubes are having same temperature variation among them. First design, with steel blade cooling fluid is getting heated gradually then it is constant for some distance and when it is very near to blade upper opening once again it is heated, after coming out from upper opening it is mixed with primary flowing fluid. This sudden change in temperature may cause development of thermal stress; other characteristics are almost same except heating rate of the cooling fluid. For second design, change in temperature is uniform in all tubes; irrespective of material the rate of increase in temperature is constant for particular tube. In zigzag design very little change appears for titanium and steel. There is possibility of high mass flow rate and can be reduced the internal mass flow rate and size of the holes. It is important that if using blade material as steel with zigzag pattern cooling will be highly efficient so, design will be more economical. Averaged Wall heat transfer coefficient for zigzag design is 847 W/m^2-K with both the materials.

SUMMARY AND CONCLUSIONS

Conclusions of the present work have been taken in the following paragraphs.

5.1 Conclusions drawn from the present analysis

In this Computational fluid dynamic simulation study, an attempt has been made to design and examine high pressure turbine for two different temperatures (1200K and 1400K) at the inlet of turbine with two different pressure ratio (20 and 30) of compressor. The aim was to determine the effect of two different holes patterns (straight lined and zigzag lined) for cooling system of turbine blades made up of two different materials (alloy steel and titanium alloy). For the present analysis, mass flow rate has been assumed 2.75% of primary mass flow rate for both pressure ratio and other parameters (pressure and temperature) also kept constant.

For pressure ratio 20, it has been observed that zigzag pattern is working fine and the results are in good agreement with the published data. Volume averaged temperature of blade is lower for zigzag lined pattern design for every given inlet temperature. After that, alloy steel material with zigzag pattern is working satisfactorily. That means, for 20 pressure ratio zigzag pattern design of holes for cooling is better as compared with straight line design irrespective of thermodynamic properties of blade material . Also, pressure plot shows aerodynamic behavior of designed blade at very high pressure. The average heat transfer coefficient is found for four cooling tube for both patterned design. For straight lined design it is 1281.09 W/m^2 and for zigzag lined pattern it is 687.146 W/m^2. Temperature distribution inside cooling tubes is found uniform.

Conversely for pressure ratio 30, it has been observed that straight lined pattern is working good enough. Volume averaged temperature of blade is lower for straight lined design for every given inlet temperature which is having titanium as a blade material. After that alloy (Titanium alloy) material with straight lined pattern is working better therefore for 30 pressure ratio, straight lined pattern design of holes for cooling is good design as irrespective of thermodynamics properties of blade material. Also, pressure plot given in previous chapter is showing the aerodynamic behavior of designed blade at very high pressure. Average heat transfer coefficient is found for four cooling tube for both patterned design; is 725.27 W/m^2K and 847.28 W/m^2K for straight lined design and zigzag lined

pattern respectively. Temperature distribution inside cooling tubes is found decreasing from tube near to leading edge to tube near to trailing edge.

For pressure ratio 20, secondary mass flow is 2.75% of primary flow and it was predicted well. For pressure ratio 30, it would have been better if mass flow rate less than 2.75% of primary flow for zigzag pattern. Improved performance of cooling is found if it is working in design of pressure ratio 20. For pressure ratio 30, straight lined pattern is performing better. Here, the blade cooling by zigzag holes pattern is thermodynamically adopted if suitable secondary mass flow rate has been chosen.

Table 5.1 Outcomes of the Turbine Blade Analysis for pressure ratio (20 bar at 1200K)

20 bar		wall averaged Temperature (K)				Avg.
Straight lined						
1200K	volume averaged temperature of blade	Tube-1	Tube-2	Tube-3	Tube-4	
Titanium	1185.59	1183.36	1182.29	1183.17	1182.25	1182.768
Steel	1194.01	1194.62	1194.51	1194.62	1194.49	1194.56
Zigzag lined						
1200K	volume averaged temperature of blade	Tube-1	Tube-2	Tube-3	Tube-4	
Titanium	1184.29	1171.48	1168.74	1164.63	1165.34	1167.548
Steel	1192.71	1187.37	1186.5	1185.08	1185.56	1186.128

Table 5.2 Outcomes of the Turbine Blade Analysis for pressure ratio (20 bar at 1400K)

20 bar		wall averaged Temperature (K)				Avg.
Straight lined						
1400K	volume averaged temperature of blade	Tube-1	Tube-2	Tube-3	Tube-4	
Titanium	1386.7	1386.1	1385.53	1385.82	1385.02	1385.618
Steel	1392.19	1392.71	1392.57	1392.7	1392.52	1392.625
Zigzag lined						
1400K	volume averaged temperature of blade	Tube-1	Tube-2	Tube-3	Tube-4	
Titanium	1204.02	1178.3	1176.46	1174.36	1177.78	1176.725
Steel	1387.6	1380.96	1379.03	1376.61	1376.88	1378.37

Table 5.3 Outcomes of the Turbine Blade Analysis for pressure ratio (30 bar at 1200K)

30 bar		Wall averaged Temperature (K)				Avg.
Straight lined						
1200K	volume averaged temperature of blade	Tube-1	Tube-2	Tube-3	Tube-4	
Titanium	1081.37	1087.26	1076.07	1057.24	1027.67	1062.06
Steel	1191.21	1193.07	1192.51	1191.64	1189.34	1191.64
Zigzag lined						
1200K	volume averaged temperature of blade	Tube-1	Tube-2	Tube-3	Tube-4	
Titanium	1115.43	1110.2	1112.27	1109.02	1079.08	1102.643
Steel	1140.09	1143.49	1145.32	1143.92	1123.29	1139.005

Table 5.4 Outcomes of the Turbine Blade Analysis for pressure ratio (30 bar at 1400K)

30 bar		Wall averaged Temperature (K)				Avg.
Straight lined						
1400K	volume averaged temperature of blade	Tube-1	Tube-2	Tube-3	Tube-4	
Titanium	1170.02	1176.98	1146.58	1120.18	1096.82	1135.14
Steel	1390.82	1392.54	1392.59	1392.4	1391.31	1392.21
Zigzag lined						
1400K	volume averaged temperature of blade	Tube-1	Tube-2	Tube-3	Tube-4	
Titanium	1257.98	1252.52	1251.44	1245.38	1198.14	1236.87
Steel	1309.4	1315.43	1316.74	1315.32	1284.61	1308.025

Recommendations for the future work

Cooling in gas turbines is one of the key technologies for any future improvement in engine performance. By developing highly sophisticated concepts, engineers have pushed today's cooling efficiencies to levels that were considered to be out of reach only a decade ago. Despite considerable progress in blade metallurgy, increase of gas temperature can only be afforded when the blade can be cooled effectively. Nowadays, with the continuous advancement in computational fluid dynamics field, this design and analysis tools not only lead to reduction of design cycle time and product development costs, but also improved test models.

In order to improve the cooling techniques, various studies still needs to be investigated which are discussed below:

1. Besides convective heat transfer phenomena, radiative heat transfer as well as heat conduction through the solid material have to be taken into account.
2. Meshing plays a key role in the accuracy reached by the computations. The meshes have to be defined in accordance with the solver capabilities.
3. Various composite materials should be employed in the design of turbine blades.
4. Future studies need to investigate how cooling effectiveness is influenced by increasing the number of impingement jets and film cooling holes, and optimizing the geometrical parameters (diameter, distance between them and their shape).
5. The blade-shaped coolant passages with high performance ribs. Also, with and without film cooling holes under realistic coolant flow, thermal and rotation conditions. The advanced CFD predictions would provide valuable information for designing effective cooled rotor blades for the new generation of gas turbines.
6. The performance related to the heat transfer coefficient is another prospective topic for future studies.

REFERENCES

1. **A. B. Moskalenko and A. I. Kozhevnikov (2016), "**Estimation of Gas Turbine Blades Cooling Efficiency", *International Conference on Industrial Engineering, Procedia Engineering, Vol. 150, pp: 61 – 67.*

2. **Amjed Ahmed Jasim AL-Luhaibi and Mohammad Tariq (2014), "**Thermal Analysis of cooling effect on Gas Turbine Blade", *International Journal of Research in Engineering and Technology, Vol. 3(3), pp: 603-610*.
3. **Beltran, A. M., Pepe, J. J., and Schilke, P. W. (1994),** "Advanced gas turbine materials and coatings", *GER-3569, General Electric*.
4. **Bladh, R., Castanier, M. P., and Pierre, C. (2001),** "Component-mode-based reduced order modeling techniques for mistuned bladed disks—part I: Theoretical models", *Journal of Engineering for Gas turbines and Power*, *123*(1), 89-99.
5. **Bunker, R. S., Bailey, J. C., and Ameri, A. A. (1999),** "Heat Transfer and Flow on the First Stage Blade Tip of a Power Generation Gas Turbine: Part 1—Experimental Results", In *ASME 1999 International Gas Turbine and Aeroengine Congress and Exhibition* (pp. V003T01A049-V003T01A049). American Society of Mechanical Engineers.

6. **Carlos A. and Estrada M. (2007),** "New Technology Used In Gas Turbine Blade Materials", Scientia et. TechnicaAño XIII, No 36, September 2007. Universidad Tecnológica de Pereira.

7. **C. H. S. Naga Prasad (2017)** Design and Finite Element Analysis of a Gas Turbine Blade, *International Journal of Innovative Technologies, Vol. 5(4), pp: 739-742*.

8. **Christophel, J. R. (2003)** *Comparison of the Thermal Performance of Several Tip Cooling Designs for a Turbine Blade* (Doctoral dissertation, Virginia Tech).

9. **Cowles, B. A. (1996)** High cycle fatigue in aircraft gas turbines - An industry perspective. *International Journal of Fracture*, *80*(2-3), 147-163.

10. **Dang, T., Damle, S., and Qiu, X. (2000),** "Euler-based inverse method for turbo machine blades", part 2: three-dimensional flows. *AIAA journal*, *38*(11), 2007-2013.

11. **Deepak Kumar Patel, Kamal Kumar Jain and R. K Dave (2016), "**Heat Transfer Enhancement of Gas Turbine Blade's Cooling Rectangular Channel with Internal Ribs of Different Rib Cross Sections Using CFD", *International Research Journal of Engineering and Technology, Vol. 3(5), pp: 1818-1824.*

12. **El-Masri, M. A. (1986),** "On the Thermodynamics of Gas Turbine Cycles-Part II: Model for Expansion in Cooled Turbines", ASME J. Eng. Gas Turbines Power, 108, pp 151-159.
13. **El-Masri, M.A. (1986),** "On Thermodynamics of Gas Turbine Cycles: Part III: Thermodynamic Potential and Limitations of Cooled Reheated-Gas-Turbine Combined Cycles", ASME Journal of Engineering for Gas Turbine and Power, Vol.108, pp 160-169.
14. **Fazeli, A. R. (2010),** "Statistical Modeling of Pin Gauge Dimensions of Root of Gas Turbine Blade in Creep Feed Grinding Process", *Engineering*, *2*(08), 635.

15. **G. Narendranath and S. Suresh (2012), "**Thermal Analysis Of A Gas Turbine Rotor Blade By Using Ansys", *International Journal of Engineering Research and Applications Vol. 2 (5), Sept.- Oct. 2012, pp: 2021-2027.*

16. **G.Muniyandi (2017)** "Review on Steady State Thermal & Structural Analysis of Gas Turbine Blade with Cooling System Using FEA", *International Research Journal of Engineering Sciences, Vol. 3 (2), pp: 25-33.*

17. **Gao, Z., Narzary, D. P., & Han, J. C. (2008),** "Film cooling on a gas turbine blade pressure side or suction side with axial shaped holes", *International Journal of Heat and Mass Transfer*, *51*(9-10), 2139-2152.

18. **Gao, Z., Narzary, D. P., & Han, J. C. (2009),** "Film-cooling on a gas turbine blade pressure side or suction side with compound angle shaped holes", *Journal of Turbomachinery*, *131*(1), 011019.

19. **Ghobadi, A., Javadi, S. M., &Rahimi, B. (2010, February),** "Cooling Turbine Blades using Exciting Boundary Layer", In *International conference on computational and mathematical engineering, Penang, Malaysia*.

20. **Gregory M. Laskowski and Frederic N. Felten (2010), "S**teady and unsteady CFD simulations of transonic turbine vane wakes with trailing edge cooling", *VthEuropean Conference on Computational Fluid Dynamics, Lisbon, Portugal, 14-17 June 2010*.

21. **Hale, F. J. (1984), "**Introduction to Aircraft Performance", *Selection and Design, Wiley, New York.*

22. **Harsha D A and Yogananda A (2017), "**CFD Analysis on Radial Cooling of Gas Turbine Blade", *International Journal of Innovations in Engineering Research and Technology, Vol. 4(6), pp: 47-51*.

23. **Hasanpour, A., Farhadi, M., &Ashorynejad, H. R. (2011),** "Hole configuration effect on turbine blade cooling", *World Academy of Science, Engineering and Technology*, *49*, 1-6.

24. **Hegde, S. S., Thamban, A., Ahmed, A., Upadhyay, M., &Mahalingam, A. (2016),** "Development of a Chassis Mounted Multi Stage Axial Flow Turbine for Wind Energy Harvesting on a Cruising Transport Vehicle: A CFD Based Approach", *ASME 2016 10th International Conference on Energy Sustainability collocated with the ASME 2016 Power Conference and the ASME 2016 14th International Conference on Fuel Cell Science, Engineering and Technology* (pp. V001T14A003-V001T14A003).

25. **Hildebrandt, T., Ettrich, J., Kluge, M., Swoboda, M., Keskin, A., Haselbach, F. and Schiffer, H. P (2006), "**Unsteady 3D Navier-stokes calculation of a film-cooled turbine stage with discrete cooling hole", *Springer Dordrecht, DOI : https://doi.org/10.1007/1-4020-4605-739, pp: 533-549.*

26. **Hohlfeld, E. M. (2003),** "*Film Cooling Predictions along the Tip and Platform of a Turbine Blade",* (Doctoral dissertation, Virginia Tech).

27. **Harsha D A and Yogananda A (2017), "**CFD Analysis on Radial Cooling of Gas Turbine Blade", *International Journal of Innovations in Engineering Research and Technology, Vol. 4(6), pp: 47-51.*

28. **Hou, J., Wicks, B. J., & Antoniou, R. A. (2002),** "An investigation of fatigue failures of turbine blades in a gas turbine engine by mechanical analysis", *Engineering Failure Analysis*, *9*(2), 201-211.

29. **John. V., and T. Ramakrishna (2012),** "The Design and Analysis of Gas Turbine Blade", *International Journal of Advanced Research and Studies, Vol. 2(1), Dec 2012.*

30. **Joseph L. Steger, William R. Van Dalsem, Argyris G. Panaras and K. V. Rao (1988), "**A Formulation for the Boundary-Layer Equations in General Coordinates", *Ames Research Center, Moffett Field, California.*

31. **Josin George and Titus R. (2014),** "The Design and Analysis of First Stage Gas Turbine Blade with a Modification on Cooling Passages Using ANSYS", *International Journal of Latest Trends in Engineering and Technology, Vol. 3(4), 2014, pp: 313-326.*

32. **Jovin Jose and V. V Prathibha Bharathi (2017),** "Advanced Cooling of Gas Turbine Blades with Sodium Liquid and Air", *International Journal of Advanced Engineering, Management and Science, Vol. 3(2), pp: 134-140.*

33. **K. Vijaya Krishna Varma and M.V BabuTanneru (2016), "**Film Cooling of Turbine Blade Surface with Extended Exit Holes", *International Journal of Design and Manufacturing Technology, Vol. 8(2), pp: 23-47.*

34. **Koff, B. L., &Koff, B. L. (2004),** "Gas Turbine technology evolution: a designer's perspective", *Journal of propulsion and power*, *20*(4), 577-595.

35. **L. Uma maheswara rao and K. Mallikarjuna rao (2014), "**Design and Analysis of Gas Turbine Blade using FEM", *International Journal of Latest Trends in Engineering and Technology, Vol.4 (4), pp: 19-24.*

36. **M. Mirzaei and R. Karimi (2001),** "Stress Analysis and Life assessment of a Gas Turbine Blade", *Oral Reference: ICF100312OR, Honolulu 2001.*

37. **M. Y. Jabbari, K. C. Marston, E. R. G. Eckert and R. J. Goldstein (1996)** Film cooling of the gas turbine discrete holes Endwall by Discrete- hole Injection, *Journal of Turbomachinery, Vol. 118 (2), pp: 278-284.*
38. **Majid Rezazadeh Reyhania, Mohammad Alizadehb, AlirezaFathic and HiwaKhaledid (2013)** Turbine Blade Temperature Calculation and Life Estimation-A sensitivity analysis, *Propulsion and Power Research, Vol. 2(2), 2013, pp: 148–161*.

39. **Mattingly, J. D., Heiser, W. H., and Pratt, D. T (*2002*)**, "*Aircraft Engine Design", second ed., AIAA Education Series, AIAA, Reston, VA.*
40. **Mehdi Tofighi Naeem, Seyed Ali Jazayeri and Nesa Rezamahdi (2008),** "Failure Analysis of Gas Turbine Blades", *Proceedings of the 2008 IAJC-IJME International Conference.*
41. **Mohapatra, A. K. (2018), "**Exergetic evaluation of gas-turbine based combined cycle system with vapor absorption inlet cooling", *Applied Thermal Engineering*, *136*, 431-443.

42. **Muktinutalapati, N. R. (2011),** "Materials for gas turbines–an overview", In *Advances in Gas Turbine Technology*.

43. **Nageswara Rao Muktinutalapati (2011),** "Materials for Gas Turbines - An Overview", *Advances in Gas Turbine Technology, pp: 293-314, ISBN: 978-953-307-611-9.*
44. **Nandakumar, N., and Moorthi, N. S. (2015),** "Performance Analysis of Gas Turbine Blade Cooling by CFD", *International Journal on Applications in Mechanical and Production Engineering*, *1*(4), 3-9.

45. ***P. Walsh, Paul Fletcher,*** *"Gas Turbine Performance", Second Edition Philip John Wiley & Sons, 2004*

46. **P. V. Krishnakanth, G. NarasaRaju, R. D. V. Prasad and R. Saisrinu (2013), "**Structural & Thermal Analysis of Gas Turbine Blade by Using F.E.M", *International Journal of Scientific Research Engineering & Technology, vol. 2(2), pp: 60-65.*

47. **Pedaprolu Venkata Vinod , T. Seshaiah and T. VictorBabu (2012), "**The Design and Analysis of Gas Turbine Blade" , *International Journal of Advanced Engineering Research and Studies, Vol. 2(1), Oct.-Dec. 2012, pp:136-138.*

48. **Prasad, B. N. (2013),** "Energy and exergy analysis of intercooled combustion-turbine based combined cycle power plant", *Energy*, *59*, 277-284.

49. **Pritchard, L. J. (1985),** "An eleven parameter axial turbine airfoil geometry model", *ASME 1985 International Gas Turbine Conference and Exhibit* (pp. V001T03A058-V001T03A058). American Society of Mechanical Engineers.

50. **Priyanka Singh and O. P. Shukla (2016),** "Heat Transfer Analysis of Gas Turbine Rotor Blade Through Staggered Holes Using CFD", *International Journal of Engineering Research and General Science Volume 4(2), pp: 538-545*.

51. **R. D. V. Prasad, G. Narasa Raju, M. S. S. Srinivasa Rao and N. Vasudeva Rao (2013), "**Steady State Thermal & Structural Analysis of Gas Turbine Blade Cooling System", *International Journal of Engineering and Research Technology, Vol.2(1), Dec. 2013, pp: 1-7.*

52. **R. C. Wilcock, J. B. Young and J. H. Horlock (2005), "**The effect of turbine blade cooling on the cycle efficiency of gas turbine power cycles", *J. Engineering for Gas Turbines and Power, 127, pp. 109-120.*

53. **R. Jones, S. Acharya1 and A. Harvey (2005), "**Improved turbulence modeling of film cooling flow and heat transfer", *WIT Transactions on state of the Art in Science and Engineering, Vol. 15, ISSN 1755-8336, USA.*

54. **R. S. Bunker (2007), "**Gas turbine heat transfer: Ten remaining hot gas path challenges", *J. Turbomachinery, 129, pp. 193-201.*

55. **R.C. Haubert, H.M. Maclin, M.E. Noe, E.S. Hsia, R.O. Brooks (1980),** "High pressure turbine blade life sensitivity", *AIAA- 80-1112, 1980.*

56. **Rao, R., and Pandey (2014),** "Simulation of gas turbine blade for enhancement of efficiency of gas turbine using ANSYS", *IJMER,* Vol. 4(9) *ISSN: 2249–6645.*

57. **Ravi Ranjan Kumar and Pandey, K. M (2017), "**Static structural and Modal analysis of a gas turbine blade", *IOP Conference Series: Materials Science and Engineering225*.

58. **Robert Yancey, Michael Dambach, J. S Rao and Marc Ratzel (2011),** "Optimizing Cooling Passages in Turbine Blades", *Altair Engineering, Inc.; David Corson, Acusim Software 20 June 2011.*

59. **Ronald S. Bunker and Jeremy C. Bailey (1999), "**Heat Transfer and flow on the First Stage Blade Tip of a Power Generation Gas Turbine Part 1: Experimental Results", 44th Gas Turbine and Aero-engine Congress, *Symposium sponsored by International Gas Turbine Institute of the American Society of Mechanical Engineers Indianapolis, Indiana, June 7-1.*

60. **Rottwinkel, B., Nölke, C., Kaierle, S., &Wesling, V. (2014),** "Crack repair of single crystal turbine blades using laser cladding technology", *Procedia Cirp, 22,* 263-267.

61. **S. Friedrichs, H. P. Hodson and W. N. Dawes (1997),** "Aerodynamics Aspect of End wall Film Cooling", *Journal of Turbomachinery, Vol. 119 (4), pp: 786-793.*

62. **S. Gowreesh, N. Sreenivasalu Reddy and N. V. Yogananda Murthy (2009), "**Convective Heat Transfer Analysis of a Aero Gas Turbine Blade Using ANSYS", *International journal of Mechanics of solids, vol. 4(1), March 2009, pp: 55-62.*

63. **Song, S. H., Castanier, M. P., & Pierre, C. (2007, January),** "System identification of multistage turbine engine rotors", *ASME Turbo Expo 2007: Power for Land, Sea, and Air* (pp. 569-582). American Society of Mechanical Engineers.

64. **V. Naga BhushanaRao, I. N. Niranjan Kumar and K. Bala Prasad (2014), "**Failure analysis of gas turbine blades in a gas turbine engine used for marine applications"**,** *International Journal of Engineering, Science and Technology Vol. 6(1), 2014, pp: 43-52*

65. **V. Veeraragavan (2012), "**Effect of Temperature Distribution in 10c4/60c50 Gas Turbine Blade Model Using Finite Element Analysis", *International Journal of Engineering and Research Technology, Vol. 1(10), pp: 1-6.*

66. **Wang Rongqiao, Jing Fulei and Hu Dianyin (2013),** "In-phase thermal–mechanical fatigue investigation on hollow single crystal turbine blades", *Chinese Journal of Aeronautics, Vol. 26(6), 2013, pp: 1409-1414.*

67. **Yepuri Giridhara Babu, Gururaj Lalgi, Ashok Babu Talanki Puttarangasetty, Jesuraj Felix, Sreenivas Rao V. Kenkere and Nanjundaiah Vinod Kumar (2013),**

“Experimental and Numerical Investigation of Effect of Blowing Ratio on Film Cooling Effectiveness and Heat Transfer Coefficient Over a Gas Turbine Blade Leading Edge Film Cooling Configurations”, *Proceedings of the ASME 2013 Gas Turbine India Conference GTINDIA2013 December 5-6, 2013, Bangalore, Karnataka, India*.

68. Yadav, R. (2007), “Steam & Gas Turbines and Power Plant Engineering” 5th Ed. Central publishing House, Allahabad.

69. Young, J. B. and Wilcock, R. C. (2002), “Modeling the Air-Cooled Gas Turbine: Part 1-General Thermodynamics”, Journal of Turbomachinery,Vol.124, pp. 207-213.

70. http://www.grc.nasa.gov/WWW/K-12/airplane/aturbj.html.

71. http://v3.espacenet.com/origdoc?DB=EPODOC&IDX=FR534801&F=0&QPN=FR534801sod1280.tmp